Competition between visual stimuli in the monkey parietal cortex

Annegret Lea Falkner

Submitted in partial fulfillment of the
requirements for the degree
of Doctor of Philosophy
under the Executive Committee
of the Graduate School of Arts and Sciences

COLUMBIA UNIVERSITY
2012

ABSTRACT

Competition between visual stimuli in the monkey parietal cortex
Annegret Falkner

We live in a complicated visual world where stimuli are constantly clamoring for our limited attentional resources. We use our eyes to explore the world and our brain must make moment-to-moment decisions about which points of space contain the most information or are associated with likely rewards. In our neural representation of the visual world, stimuli locked in a constant battle for spatial priority and a single winner must emerge each time an eye movement is to be made, though the mechanisms by which this winner emerges are unclear. In this thesis we explore how competition between visual stimuli in the parietal cortex may be implemented by changes in the activity and reliability of neural signals. The macaque lateral intraparietal area (LIP) is part of an oculomotor attentional network and its activity represents the relative priority of spatial locations. We demonstrate how neurons in LIP use surround suppressive mechanisms to resolve conflict between spatial locations and explore the role of shared variability in the priority map network. We manipulate the cognitive state of the monkey by changing his expected reward and show that the activity, reliability, and noise correlation are affected by the context of the monkeys' choice. Finally, we demonstrate how behavioral variables such as the monkeys' performance and saccade latency are modulated during competitive choice.

Table of Contents

Chapter 5. Conclusions

References

List of figures

Acknowledgements

I'd like to thank my advisor Mickey Goldberg and my collaborator Suresh Krishna for their guidance, and my all-star committee members, Daniel Salzman, Larry Abbott, Norma Graham, and Bob Wurtz for their invaluable help. Thank you to my labmates Sara Steenrod, Anna Ipata, Angela Gee, and Yixing Xu for their never ending support and for putting up with my round-the-clock whining. Thanks Yana Pavlova and Latoya Palmer for friendship and technical support. Thank you Mom, Dad, sisters, and all my friends in NYC. Finally, thanks Z: our house is falling apart beneath our feet, but we still have everything.

Dedication

I'd like to dedicate this thesis to my dear friend Neil who was killed in a hit-and-run in Brooklyn exactly one year ago this April. You were an amazing writer, artist, and confidant. At Oberlin and in NYC, you influenced me in profound ways I'm sure you never knew. You are missed.

How many miles to Babylon?

Three score and ten--

Can I get there by candlelight?

Yes, and back again --

If your feet are nimble and light

You can get there by candlelight.

Chapter 1: Introduction

1.1 How does the winner win?

We live in a visually complex world where a myriad of stimuli are constantly clamoring for our attention. Since our neural resources are limited and some stimuli are more informative than others, the brain must select which stimuli are the most relevant and then prepare appropriate behaviors in a flexible manor. In most situations, such as deciding which email to open first or which person to attend to at a noisy party, the consequences for these moment-to-moment choices are trivial. However in other situations these processes can be vital to survival. For example, if when crossing a busy street you become suddenly transfixed by a shiny silver dollar on the ground, you run the risk of being run over by a speeding car. Since salient stimuli can cause shifts in attention and undesired eye movements (Egeth and Yantis, 1997), ignoring the silver dollar is imperative so that focus can be appropriately allocated to the steady stream of traffic. But how does the brain decide to prioritize the traffic over the silver dollar?

To sort out the wheat from the chaff of the visual scene, the brain is equipped with a network dedicated to visual processing and attentional allocation. In many primates including humans, this network includes areas in the frontal and parietal cortices as well as subcortical structures such as the superior colliculus. Since we use our eyes to scan the visual scene for information and we often look at what we attend to, these areas also have a known role in the production of rapid "saccadic" eye movements (Kustov and Robinson, 1996; Corbetta et al., 1998; Moore and Fallah, 2001; Ignashchenkova et al., 2004).

Within this network, how does the brain flexibly decide where to attend to and where to direct the next saccade? In order for this to occur, several variables must be kept track of in the brain. First, the brain must monitor the spatial locations of potentially interesting events. Next, the brain must assign a relative value or importance to each object. And last, the neural representations of these important and unimportant spatial locations must compete with each other in a common neural currency such that there can be a "winning" spatial location.

Several current models suggest that the representations of visual stimuli compete in a priority map, a topographical 2D network where the activity of cells in the map represents the priority or salience of a given spatial location (Koch and Ullman, 1985; Wang, 1999; Itti and Koch, 2000). In these models, salient features of the visual world are combined with top-down influences into a general measure of priority as represented by a "peak" on a spatial map. Attention is then allocated dynamically based on a moment-to-moment determination of highest peak of the map. Physiological evidence for priority maps has been described from several different primate brain areas including the lateral intraparietal (Bisley and Goldberg, 2003a), the superior colliculus (McPeek and Keller, 2002), the frontal eye fields (Thompson and Bichot, 2005), and the pulvinar nucleus of the thalamus (Morris et al., 1997). According to these models, attentional or saccadic selection occurs on the basis of moment-to-moment "winner-take-all" competition between dynamically changing peaks on this map. Additionally, lateral suppression between different locations on this map plays a critical role for resolving competition between stimuli, though there is little physiological support for this mechanism as of yet.

Historically, the parietal cortex has a known role in attentional allocation and saccade selection and is a likely candidate to mediate competition between visual stimuli. In humans, patients with unilateral right parietal lobe damage have trouble attending to visual stimuli in the left side of their visual field. Termed "hemi-neglect" syndrome, patients with these attentional deficits had no appreciable deficits in visual processing (see Adair and Barrett, 2008 for review). Additionally, bilateral lesions of the parietal cortex in humans have been linked with the inability to filter distracting stimuli from targets, even when stimuli were widely spaced apart (Friedman-Hill et al., 2003), though fascinatingly, the patients in this study had no trouble identifying the target when it was presented without distractions. These deficits demonstrate that while the parietal cortex may not be necessary for basic visual processing, it likely is involved in prioritizing spatial information when multiple visual stimuli are in competition.

To explore whether the parietal cortex plays a role in spatial competition, the animal model we will use is the awake behaving rhesus macaque (*maccaca mulatta*). Monkeys are the ideal neuro-ethological system to probe complex questions, especially those pertaining to visual processing and eye movements, because their visual system parallels the human visual system in many critical ways. Monkeys can be trained to sit still and perform complex tasks in exchange for liquid rewards, and they will perform thousands of identical "trials" so that we can generate accurate estimates of the underlying processes. Using a magnetic eye coil in tandem with standard neurophysiological techniques, we can simultaneously monitor both the monkeys' saccadic behavior and the activity of single (or multiple) neurons. On each trial, the eye movement offers us a unique window into the cognitive processes that underlie the decision that

the monkey makes, and we can rigorously quantify the relationship between the neural activity and the monkeys' behavior across changing task demands.

In this thesis, I will examine how neural activity in the monkey lateral intraparietal area (LIP) represents ongoing competition between visual stimuli during a planned saccade task and a saccadic choice task. Monkey LIP receives "bottom-up" visual input from sensory areas and "top-down" input from fronto-cortical areas including the frontal eye fields (FEF). LIP also sends a direct input to the superior colliculus (SC), an area known to be involved in saccade generation. Previous studies have suggested that LIP firing rates encode information that represents the upcoming decision, and thus may represent a final stop on the cortical path to the motor/saccade command. Saccades also an ideal behavioral readout with which to study competitive processes in LIP. Saccades are ballistic all-or-none events such that there is a "winning" spatial location each time an eye movement is made. Unlike head orienting or reach mechanisms, the details of how the muscle commands that generate saccades are well understood, leaving us free to concentrate on the functions of more upstream neural structures. Additionally, current recording techniques allow us to precisely measure several important saccade metrics, including latencies, amplitudes, and endpoints. Trials where the monkeys make saccades that are not correctly timed or targeted are counted as errors and give us additional insight into the cognitive processes that underlie saccade generation and attentional allocation. In the next section I will outline several neural signals that may reflect competitive processes in LIP.

1.2 Mechanisms of competition

In brain areas that encode a map of the visual world in retinotopic space, each point on the map is determined by the relative firing rates of the neurons that encode the representation of that particular spatial location. For competition to occur in the brain, the magnitude of this signal and its reliability are of the utmost importance. The magnitude of the signal contributes to the encoded priority of the spatial location, and the amount of spatial accuracy is determined by the fidelity of this representation over repeated trials. To examine how spatial locations compete in LIP, we must also consider how the representations of these locations interact dynamically. In this body of work I will quantitatively explore three separate mechanisms that contribute to competitive processes in monkey LIP: 1) changes in the firing rate of LIP neurons, 2) changes in the across-trial variability of single LIP neurons, and 3) changes in the shared variability or "noise" correlation between pairs of simultaneously recorded neurons. Within each of these three mechanisms I will explore how changes are reflected in the monkeys' saccadic behavior, including saccade latency, errors, and endpoint accuracy.

1.21 Changes in firing rates

How do changes in the magnitude of the neural response aid in the filtering of distracting information? To return to our example of the traffic and the silver dollar, we see that the car and the silver dollar are actively competing for your attention and your upcoming eye movements. Since you can't saccade to both the silver dollar and the car at the same time, one way to solve this problem would be to make the response to the car so much higher than the silver dollar so that it effectively "wins" the competition. Another solution would be to make the response to the

silver dollar so small that it "loses." But which is it? One optimal neural strategy would be to implement both processes simultaneously. Here I will explore how surround suppressive mechanisms work in tandem with top-down enhancement mechanisms to filter irrelevant visual information.

1.22 Changes in across-trial variability

The across-trial variability of neural responses is a potential nuisance to competitive mechanisms. If the silver dollar one day causes a low neural response on the priority map, but the next day a high response, the signal is unreliable and may result in detrimental behaviors. For example, few extra spikes at a non-target location could potentially confuse a downstream decoding mechanism and cause erroneous saccades. Here I will examine the relationship of saccadic behavior to the across-trial reliability of neural responses in LIP. I propose that surround suppressive mechanisms in LIP (in addition to suppressing irrelevant spatial information) can also increase the precision of LIP's responses by improving the variability at non-target locations.

1.23 Changes in the shared variability between LIP neurons.

How do neurons in LIP interact with each other during a saccadic decision? Thus far, I have only considered the responses of single neurons. But are these neurons acting independently, or do the firing rates depend on each other? For a complete description of how neurons might compete with each other, we can examine whether neural noise is correlated in an ongoing decision. In this study I record the precise responses to 2 competing options and

examine how the correlations between these neurons encoding the competing spatial locations change as the decision emerges in time. Since correlations are indicative of shared variability between neurons, I propose a mechanism by which shared variability is reduced during an ongoing decision.

In this introduction, I will begin by giving a brief account of the anatomy and connectivity of area LIP, followed by a description of previous work that demonstrates how LIP encodes several types of cognitive and motor related information. I will also briefly describe several current models that describe activity in LIP, and summarize the current findings that are related to competitive processing in cortex.

1.3 The Lateral Intraparietal Area

1.31 Anatomy

LIP is part of a macaque fronto-parietal network dedicated to attentional allocation and saccade generation. An intuition of the diverse anatomical connectivity of LIP is a necessary precursor to understanding of the signals known to be encoded by LIP neurons. LIP is located in the lateral bank of the intraparietal sulcus (the human analog to LIP is the intraparietal sulcus), and is uniquely situated to have convergent connections with visual, frontal, and oculomotor structures (Figure 1.1). Structures linked to visual processing have historically been grouped into a either the ventral stream, which is responsible for recognition and object identification (the so-called "what" pathway), and the dorsal stream which is responsible for using visual information to direct action (the "where" stream). LIP (along with other parietal areas) is

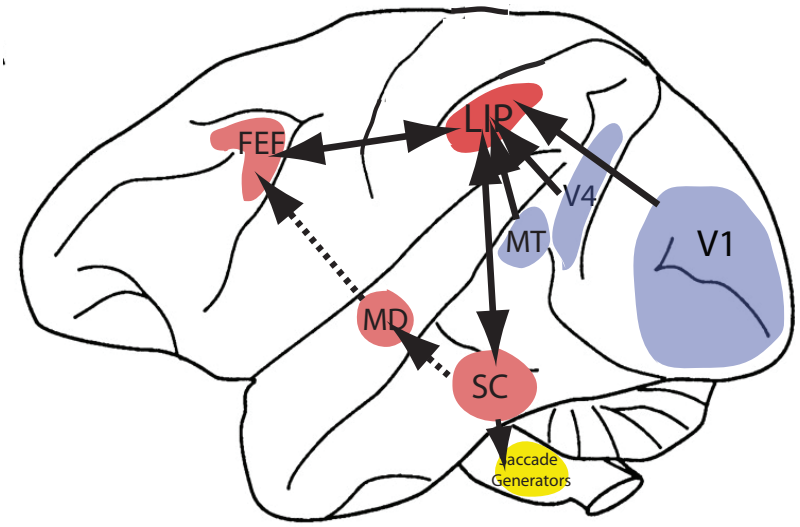

Figure 1.1
Anatomical projections of LIP. Connections of macaque LIP from visual areas (blue), with oculomotor areas, and through corollary discharge pathway (pink). LIP influences saccade generation through brainstem saccadic nuclei via a projection through the SC.

classically thought to be part of the dorsal stream, though this segregation of pathways is largely a descriptive convenience since there is massive overlap of connectivity between the structures (Van Essen, 2005).

The intraparietal sulcus is separated into several anatomical areas that have unique functional domains. Areas in the anterior IPS are known to have largely tactile motor and somatic sensation functions, while areas in the posterior IPS are more related to visuomotor processing (Grefkes and Fink, 2005). The ventral intraparietal area (VIP) responds to multimodal and especially tactile stimuli (Duhamel et al., 1998; Avillac et al., 2005), vestibular, (Bremmer et al., 2002), and body surface information (Schlack et al., 2002). The medial intraparietal area (also known as the parietal reach region, PRR) has been shown to be specific for arm reaching (Andersen, 1997; Snyder et al., 1997). In contrast, areas 7a and LIP receive direct projections from several visual areas including V1, V3, V3a, V4, and MT/MST (Blatt et al., 1990; Baizer et al., 1991; Colby and Goldberg, 1999). The specificity of these inputs endows LIP with the capacity to selectively respond to salient information in the visual field such as

motion in the case of MT, and color or object in the case of V4. LIP receptive fields (RFs) can vary quite considerably. Stereotypical LIP RFs subtend ~10 visual degrees and while the majority of LIP RFs are located contralaterally to the recoded hemisphere, RFs can be located foveally and to a lesser degree ipsilaterally (Ben Hamed et al., 2001).

LIP receives direct input from several structures related to top-down control and memory. It is reciprocally connected to the frontal eye fields (FEF), a structure known to play a role in top-down attention and saccade generation, and also receives input from the prefrontal cortex (PFC), a structure with large, often bilateral RFs which is known to flexibly encode information based on task demands (Schwartz and Goldman-Rakic, 1984; Andersen et al., 1985). LIP also receives input from structures known to encode memory information, including the perirhinal and parahippocampal cortex, and the posterior cingulate (Blatt et al., 1990; Lewis and Van Essen, 2000).

LIP is also well situated to provide information to saccade generation structures. LIP has a direct input to the SC, an oculomotor structure with a strict retinotopic topography (Asanuma et al., 1985; Lynch et al., 1985). Microstimulation of the SC evokes saccades to particular regions of the visual field (for review see (Gandhi and Katnani, 2010). The SC also sends a projection back up to the FEF via the medial dorsal nucleus of the thalamus (Sommer and Wurtz, 2006). This signal is thought to provide an efference copy of motor commands made by the colliculus, in essence, reporting back to the oculomotor-attentional network what eye movement has just been programmed. This recurrent feedback effectively closes the loop between sensory and motor commands and provides a potential pathway for online adjustment of eye movements.

1.32 The components of the LIP signal

The wealth of connections to and from LIP endows it with the capability to encode both sensory and cognitive signals. Though LIP contains cells with a variety of response properties, the canonical LIP cell has several properties that I will describe in detail in the following section. First, it responds to an abrupt visual stimulus with a very stereotyped neural latency. Second, it has a saccade-related signal that rises in preparation prior to the eye movement. And lastly, it has a relatively unique firing property: the activity generated by a visual stimulus persists even in the absence of the stimulus itself (Figure 1.2).

Visual onset

LIP cells receive input from visual cortex and have RFs that are coded in retinotopic coordinates. Neurons in LIP respond to abrupt visual stimuli with a short stereotyped neural latency, ~42ms, which suggests that this information is travelling only a few synapses before reaching LIP (Bisley et al., 2004). This short-latency response can be thought of a rapid orienting response to events that are new and salient. This view is further reinforced by experiments performed by Gottlieb et al in which monkeys brought a stable stimulus into the RF with a saccade (Gottlieb et al., 1998). In contrast to an abrupt transient response to a flashed stimulus, the stable stimulus evoked very little response, suggesting that it is not simply the appearance of a stimulus in the RF that evokes the response, but the novelty of the response itself. However LIP neurons still have vigorous responses to distracting stimuli have no information relevant to the task (Robinson and Goldberg, 1978; Powell and Goldberg, 2000;

Balan and Gottlieb, 2006), though neurons responded more to stimuli that required a response than to stimuli that were ignored (Bushnell et al., 1981).

LIP neurons also respond to visual stimuli that will appear in the RF after a saccade and are thought to perform a function akin to spatial updating. When monkeys were required to make a saccade across the visual field, neurons responded to a flashed stimulus that will appear in the RF after the saccade several hundred ms prior to the initiation of the saccade itself (Kusunoki and Goldberg, 2003).

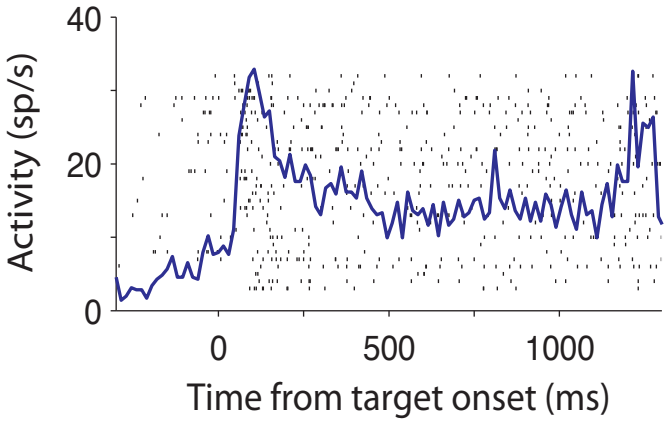

Figure 1.2 Response of an LIP neuron during a memory guided saccade. Raster and PSTH of neuron exhibiting the hallmarks of the LIP neuron: the visual transient aligned to the target onset, the elevated activity during the delay period relative to the activity prior to the target, and the ramp-up activity following the saccade go-cue (at 1000ms).

Furthermore, the visual onset responses of LIP neurons carry information about the stimuli contained within them. When tested on a variety of visual search tasks where monkeys were required to discriminate a target stimulus from a number of distracting stimuli, neurons reliably encode the location of the target (relative to a distractor response) within 100ms (Ipata et al., 2006a). LIP neurons respond rapidly to a "pop-out" singleton stimulus though this response can disappear with training if the stimulus contains no information relevant to the task (Ipata et al., 2006b).

Saccade generation

LIP also has strong ties to the oculomotor network and can signal an upcoming saccade plan. Response rates in LIP are modulated by the orbital position of the eye (Andersen et al., 1990) and prior to the onset of a saccade, neurons "ramp up" in preparation to make an eye movement to a target in the RF center (Gnadt and Andersen, 1988), leading some to speculate that LIP exclusively signaled the so-called "intention" of the saccade plan, a view that has become extremely controversial. As a counter to this, when monkeys were cued to make saccades to an untagged location opposite the visual target (an "antisaccade"), rather than explicitly coding for the saccade target location most neurons in LIP responded vigorously to the target, but not to the goal of the upcoming saccade (Gottlieb and Goldberg, 1999). Additionally, LIP still shows responses when required to respond to a target with a manual response rather than a saccade (Andersen et al., 1998; Oristaglio et al., 2006).

Additionally, though low microstimulation of both the FEF and the SC can evoke short latency saccades with highly stereotyped endpoints (Robinson and Fuchs, 1969; Robinson, 1972; Bruce et al., 1985), the same is not always true for LIP. Only at relatively high current can saccades be evoked (Thier and Andersen, 1998; Constantin et al., 2007; Constantin et al., 2009), leading some to suggest that stimulation in LIP is generating saccades by activating the FEF, or that LIP's (relatively) loose spatial topography is to blame. In sum, though LIP has strong ties to the saccade generation system and in many cases exhibits saccade-related activity, it is evident that the structure cannot clearly be defined as a motor output structure.

Persistent activity

Another hallmark of the LIP neuron is the elevated responses to a remembered target location. This is tested using the "memory guided delayed saccade" paradigm (Hikosaka and Wurtz, 1983) in which monkeys make saccades to a disappeared saccade target after a fixed delay. In this paradigm, the activity is increased during this delay period relative to the pre-target activity and is thought to presumably represent that memory of the target's spatial location (Colby et al., 1996). This property is shared with fronto-cortical areas including the FEF and PFC and is a known characteristic of neural networks with recurrent connectivity (Wang, 2001; Brunel, 2003).

1.4 Modulation of LIP neurons by cognitive signals

In addition to encoding visual and saccade related activity, LIP's responses can be strongly modulated by the demands of the task. Here I will describe how cognitive signals related to attention, reward, and decision making are explicitly encoded in LIP.

1.41 LIP and attention

Nearly 40 years ago, neural signals related to visiual attention were discovered in the monkey SC (Goldberg and Wurtz, 1972), and since then, evidence for attentional modulation has been found in several cortical and subcortical structures including the pulvinar nucleus of the thalamus, the frontal eye fields (FEF), lateral intraparietal area (LIP), and several areas in the visual cortex. Although their contributions to visual attention are clearly different and not well understood, it is believed that these areas form a distributed network, cooperatively dedicated to

the maintenance and allocation of attention. It has also been suggested that attention represents the local selective transfer of information between these brain areas (Assad, 2003).

Attention is typically thought to have a "bottom-up" and a "top-down" component. "Bottom-up" exogenous visual attention represents image properties and the intrinsic salience of visual objects. Spotting the one banana in a big bowl full of red apples is easy because the banana effectively "pops" out of the visual field due to its salient color and shape relative to the surrounding apples. The salience of color, orientation, luminance, and motion are stimulus properties that may be represented by exogenous attentional processes. In contrast, "top-down" endogenous processes encode signals related to task relevance and goal-driven processes. "Top-down" signals like attention or motivation can act by enhancing the neural responses to visual stimuli (see Kastner and Ungerleider, 2000 for review).

Single cell recordings in monkeys trained to covertly attend to stimuli in or out of the cell's receptive field have shown attentional effects in a range of visual areas including V4 (Spitzer et al., 1988; McAdams and Maunsell, 1999; Reynolds et al., 2000), MT (Treue and Maunsell, 1999; Cook and Maunsell, 2004), and even V1 (McAdams and Reid, 2005). These effects manifest themselves as an increase in the gain of the neural activity across some relevant feature space (for example motion in MT, or orientation in V1). The hallmark of gain modulation is that neurons change the amplitude of their response properties (i.e. the height of the feature tuning curve) without changing their tuning (the width of the tuning curve). Tuning curves that have suppression in the flanks of the tuning curve might be expected to have increased gain on the suppression. Behaviorally, attentional allocation can be probed identifying the contrast sensitivity at the spatial locus of attention, which should be enhanced at the when

spatial attention is deployed (and often this is often accompanied with a decrease of sensitivity at non-attended locations).

LIP does not typically respond to a particular feature (though see LIP and non-spatial modulation), so instead the parameter of interest for attention is retinotopic space. Since LIP responds to the targets of upcoming saccades, studies that probe attention must decouple the locus of attention from the endpoint of a saccade. When this is achieved, LIP firing rates track the locus of covert spatial attention in a perceptually demanding task where they required monkeys to monitor a cued spatial location for a small change and responded manually to that change (Bisley and Goldberg, 2003a). When monkeys were distracted from this goal by a salient flashed distractor with no informational value, their performance on this task declined precipitously when the distractor flashed occurred around the time of the target change. This suggested that attention was covertly shifted from the cued location to the distractor location for the brief epoch of distraction. At the time when the distractor response was at its highest, the monkeys' performance was lowest, demonstrating that the lower success rates at detecting the change were correlated with reduced firing rates at the location of the target.

Though attention can be operationally described as a "spotlight" (Posner et al., 1982), a "zoom lens" (Eriksen and St James, 1986) or effectively modeled as an increase in response gain, it must be remembered that attention itself is a psychophysical construct, not an explanation therein. Studies that describe the effects of attention lack a complete description of the implementation of the processes that allow for attentional modulation. Current models of attention such as "divisive normalization" (Reynolds and Heeger, 2009) suggest that this happens

through interactions between a stimulus drive and suppressive surround that require interactions between spatial locations, but these details have not been explored physiologically.

1.42 LIP and reward

Monkeys are sensitive to changes in their expected reward and will typically modify their behavior to reflect these changing sensitivities. For example, trials where monkeys expect high rewards relative to low rewards are associated with faster reaction times, increased accuracy, and increased frequency of choice to the high reward targets (Lauwereyns et al., 2002; Watanabe et al., 2003a, b). In addition to these behavioral changes, LIP responses can reflect relevant information about reward states, including reward magnitude, reward probability, and information about previous rewards.

In a now classic experiment, Platt and Glimcher (1999) first discovered the link between LIP and reward when they had monkeys make saccadic choices between potential saccade targets while adjusting either the magnitude of the reward or the probability of the reward. They found that LIP neuronal responses are correlated with both the magnitude and probability of the reward for a given target and speculated that LIP encodes the expected value of a given visual stimulus. They speculated that LIP, an area that lies on the border between sensory and motor responses, is instrumental in mapping the *value* of an action onto the cells that encode the spatial location for that action. Following this landmark paper an explosion of work in the booming field of "neuroeconomics" attempted to clarify the role of LIP in encoding reward related decision variables.

In addition to encoding information about upcoming rewards, neurons in LIP can also encode information about past rewards. Using a modified foraging task where monkeys could optimally harvest rewards by keeping track of their past choices, Sugrue et al. (2004) found that neurons in LIP could reliably track the expected reward or local income associated with a particular choice. In this task, monkeys made free choices between targets with varying relative reward probabilities that were each baited with the "flip" of an independent coin. In this task the monkeys allocated their choices to the targets with the same frequency of their relative reward probability of the chosen target (Hernstein, 1961). Astonishingly, they found that LIP neurons encoded a measure of the reward history that could predict these upcoming choices. When monkeys planned saccades into the RF of the recorded neuron, the firing rates of LIP neurons significantly regressed with a weighted average of the past history of choices to that particular target (a "leaky" integration of past rewards). Neurons did not track the expected income during a single target saccade task, suggesting that information about past choices is most relevant when it is necessary to inform the upcoming choice.

But can reward information still modulate LIP responses even if the motor outcome is stereotyped? This was explicitly tested by pairing a delayed saccade with information about the upcoming reward for that saccade (Peck et al., 2009). In this task, monkeys were instructed by a randomly located cue whether the upcoming saccade would be rewarded or not, and following the reward cue, a second cue instructed the monkey the required endpoint location of the upcoming saccade. Even though monkeys could not change the saccade for each trial and the reward cue only gave them advance notice about the upcoming reward (and monkeys could not skip unrewarded trials), both the firing rates and the monkey's saccadic accuracy were severely

affected by this advance information about the upcoming reward. Firing rates were suppressed by information that indicated no upcoming reward, and these changes were correlated with deficits in the monkey's saccadic behavior.

These experiments clearly demonstrate how firing rates in LIP are sensitive to changes in reward, but a complete framework for these changes influence the monkeys' decisions is lacking. For example, LIP neurons may encode the subjective desirability of a particular action (Dorris and Glimcher, 2004), and this information may be used to map the likelihood of a particular choice onto neurons that encode the specific action for that choice (i.e. a saccade to a particular spatial location, Gottlieb and Balan, 2010). However, like spatial attentional processes, it is unclear how these interactions are implemented. What is the relationship between the spatial locations that encode desirable actions and spatial locations that encode undesirable actions? When the values of competing actions are equal, are the representations of them independent? How do changing reward expectations affect the reliability of the neural signal?

1.43 LIP and decision making

LIP, which receives direct visual input from several visual sensory areas, has been shown to be involved in sensory-based decision-making. The classic paradigm used to explore this relationship is the "random dot motion" task, in which the monkey views a patch of randomly moving dots (where a certain percentage of them are moving coherently) and must use this information to make a decision, which is then indicated with an eye movement. When the patch

of dots has a high coherence, the decision is easy, but if the coherence is low, the decision is more difficult, decisions take longer and are less accurate.

Shadlen and Newsome first demonstrated that firing rates in LIP explicitly encoded a signal related to the upcoming saccadic choice: as monkeys viewed the informative stimulus, LIP neurons, which directly receive motion information from MT, signal a measure of how much evidence has been amassed in favor for a particular decision, and this information is integrated over the time window of stimulus viewing (Shadlen and Newsome, 1996, 2001). These data suggest that evidence accumulates to a fixed bound at which point a decision is be made and a saccade is generated to the target. For trials where the coherence of the random dots was high, evidence was integrated quickly and response rates were high, and for trials where the coherence was low and the trial was difficult, evidence was integrated more slowly and response rates were slower (Roitman and Shadlen, 2002). Further experiments demonstrated that both microstimulation of LIP during this task (Hanks et al., 2006) and perturbing the amount of sensory evidence observed by the monkey (Huk and Shadlen, 2005) biased the monkeys' choices in favor of the stimulated alternative, and effectively contributed to the amount of integrated sensory evidence (Mazurek et al., 2003).

Some models of decision-making in LIP suggest that competing decisions race to the threshold independently (Hanes and Schall, 1996; Ratcliff and Rouder, 2000; Smith and Ratcliff, 2004; Palmer et al., 2005), while others implement the decision process by assuming that LIP has wide-ranging mutual inhibition between spatial locations such that when one option is favored, it automatically suppresses competing responses (Constantinidis and Wang, 2004; Wong et al., 2007). However these predictions have not been tested experimentally. LIP firing rates have

also been shown to be lowered when monkeys chose between 4 competing targets rather than 2 (Churchland et al., 2008). On these trials, the response rates during the target onset epoch were reduced, which the authors interpreted as a lowered starting point for the evidence accumulation process. A possible mechanism for the reduction of these responses would be mutual suppression by the competing targets, but this also remains to be shown.

1.44 Spatial vs. non-spatial information

There appear to be many commonalities between responses that encode spatial attention, reward signals, and sensory evidence during decision-making. All three types of information modulate neural response properties of target and non-target stimuli in a spatially selective manner, and then this activity is then mapped on to a corresponding saccade generator. One unifying framework for comparing across these differing conditions would be to suggest that LIP is representing the priority of spatial locations on an ongoing basis.

Though it is tempting to speculate that LIP exclusively encodes information in the spatial domain, many previous studies have demonstrated that LIP responses can respond to information that is not tied to a particular spatial location. Properties such as elapsed time (Janssen and Shadlen, 2005), effector specificity (Oristaglio et al., 2006), categorical membership (Freedman and Assad, 2006), and shape selectivity (Sereno and Maunsell, 1998) can modulate LIP responses and seem at first glance difficult to reconcile with a framework of spatially specific responses.

Through its diffuse connectivity LIP can combine both sensory information from the visual system and "top-down" information from the frontal cortex into a unified representation.

This representation can then be flexibly mapped to a particular visuomotor response. As experimenters, we can vary the task parameters (both sensory and cognitive) such that the animal learns to prioritize a particular set of associations. LIP neurons may then encode the priority of these associations across a particular set of task demands.

The question then still remains one of competition for priority: on each trial, how does that monkey chose one option (a single peak of the priority map) at the expense of all other options and its associated motor output? In the next section I will review some general strategies used by the visual cortex that demonstrate that neuronal responses are modulated by adjusting the firing rates and the variability associated with competing options and that this processes lead to both advantages in perception and action selection.

1.5 Mechanisms of competition in visual cortex

1.51 Surround suppression

Surround suppression is the mechanism by which a stimulus outside the "classical" excitatory response field can modulate the response in the RF. Surround suppression is a ubiquitous neural strategy, and decades of research have shown evidence of suppression at many levels of the visual processing stream including retinal ganglion cells (Kuffler, 1953), the lateral geniculate nucleus (Alitto and Usrey, 2008), area V1 (Angelucci and Bressloff, 2006), MT, MST (Allman et al., 1985a; Eifuku and Wurtz, 1998; Orban, 2008) and V4 (Desimone et al., 1985; Desimone et al., 1993). Prior to this study, surround suppression had not been explored in

LIP and its very existence in this area has been somewhat controversial (Churchland et al., 2008).

Across areas of the visual cortex, surround suppression has been supposed to play a diverse set of roles in visual processing. In V1, suppression is seen in nearly all cells (>94%), is found in all cortical layers (Jones et al., 2001) and has been proposed to be involved in several computations including contrast normalization and divisive normalization (see Graham, 2011 for review). Though "surround" suppression is typically thought of as being symmetrical around a cell's RF, suppression in V1 can be evoked by both annular and point stimuli, so the term "surround" suppression is actually a bit of a misnomer. Since V1 neurons respond preferentially to oriented bars and there is a slight bias for suppression to be maximal at the ends of these bars, it has been proposed that suppression might help encode "end stoppage." In contrast, surround suppression in MT, an area selective for motion processing, has been shown to be maximal when the motion of the surround suppressing stimuli is opposite the preferred motion of the RF and this difference is presumed to play a role in computing figure ground segmentation. Though these are just a few examples of the roles of surround suppression, these differences highlight the fact that despite having generic similarities at different levels of the visual processing stream, the influence of suppression may serve wildly different functions at separate levels of the visual cortex.

Thus far we have only considered the influence of suppression evoked by a visual stimulus, but in many cases the magnitude of surround suppression can be modulated by "top-down" cognitive processes. In V4, an area known to be modulated by spatial attention, the magnitude of the response to a stimulus in the RF is modulated by the locus of spatial attention

(Sundberg et al., 2009). In this task, monkeys were trained to covertly track a moving stimulus without making an eye movement. In some cases, the attended stimulus flanked the RF, and in others, an unattended stimulus was the flanker. The surround suppression was maximal if the flanking stimulus was the attended one, though in both cases, the brain received identical visual stimulation from the outside world. Additionally, this study found that suppressive modulation was reduced when attended stimuli were farther from the RF, suggesting a possible center-surround mechanism for attentional deployment.

Similarly, in FEF, visual stimuli appearing within the RF during a visual search task have been shown to be filtered by surround suppressive mechanisms. When target stimuli appeared in locations adjacent to the RF, the response to flanking non-target stimuli were significantly reduced (Schall et al., 2004). Interestingly, this reduction was modulated by the difficulty of the task: target stimuli that shared more features with the distractor stimuli elicited a greater suppressive response. These interactions can be fit with a difference of Gaussians model (a narrow distribution of excitation and a wider distribution of inhibition) which is strongly suggestive of the combined influence of local excitation and long range inhibition. Indeed many psychophysics studies have confirmed that the attentional field exhibits a center surround shape (Steinman et al., 1995; Caputo and Guerra, 1998; Muller et al., 2005).

In another fronto-cortical area, the PFC, task irrelevant distractors were filtered by surround suppressive mechanisms when animals performed a simplified version of the RSVP task. Monkeys were required to respond to a particular visual stimulus and ignore all others after being cued to attend to a cued spatial location (DeSouza and Everling, 2004). Task irrelevant stimuli that appeared contralateral to the cued spatial location were suppressed relative to the

responses during uncued trials of the task, suggesting that suppressive attentional fields in the PFC are large and bilateral. Interestingly, the onset for suppressive influences in the PFC appears at longer latencies than in other areas, making it unlikely that the PFC is the origin of the top-down suppressive response in other visual cortical areas.

Surround suppressive mechanisms can also have behavioral consequences for upcoming eye movements. Within the oculomotor network, in addition to the FEF, several studies have provided evidence for suppression in the SC (Munoz and Istvan, 1998; Li and Basso, 2005; Lee and Hall, 2006). In experiments designed to elucidate the spatial relationship between a target and a distractor representations in the SC, a flashed distractor caused more saccadic errors when it was flashed close to the target locations, and experimenters observed a significant suppression when the target was flashed at a distant location (Dorris et al., 2007). Microstimuluation adjusted the distribution of saccadic errors towards the site of stimulation, but since it was not done concurrently with recording, it is unclear whether these effects were accompanied by suppression.

It is important to remember that in these experiments, suppression is acting via the presence of a visual stimulus. Though attentional mechanisms may act to enhance or reduce the visually-evoked response to particular stimuli, the interactions are being mediated by the response to the stimulus itself. It remains an open question whether the visual stream can generate suppression by the mechanistic implementation of attention without the corresponding stimulus.

1.52 Lateral inhibition vs. feedback inhibition

Since by definition, the effects of surround suppression extend well beyond the classic receptive field center, a brain area that implements surround suppressive effects must have an architecture that supports these interactions. Surround suppression can be implemented by a network that has local excitation and long-range inhibition (and is sensitive to feed-forward excitation) though some aspects of suppression can be modulated by inhibitory feedback (Ozeki et al., 2009). Visual areas such as V1 and MT have anatomically robust inhibitory and excitatory connections, making it likely that some aspects of suppressive computations are performed locally (Allman et al., 1985b, a). However the SC, an area shown to have suppression mediated by distantly appearing stimuli, appears to lack this architecture (Lee and Hall, 2006). Using photostimulation and whole patch recording, they found that IPSC's were evoked most often from a distance of 200um (and occasionally from 500um). Since the SC has a very strict topography, this data suggests that suppressive interactions are not being implemented across long distances within the SC and instead are being generated elsewhere. In contrast, LIP, with its relatively loose topography would not require inhibitory connections to be as far ranging to derive such responses. Iontophoresisng bicuculline, a GABA antagonist, into LIP, widens the spatial extent of LIP RFs (Zhang et al. unpublished data), demonstrating that LIP has the necessary inhibitory connections, and that they may in fact play a role in determining the spatial selectivity of a particular neuron.

Within the oculomotor network, several studies have attempted to clarify the roles of FEF, LIP, and the SC by pharmacologically manipulating these structures to perform loss of function studies. While chronic lesions of the FEF cause only minor deficits in saccade

generation, inactivating with muscimol, a $GABA_A$ agonist, impaired saccade latency and accuracy to saccades directed into the contralateral hemisphere (Dias and Segraves, 1999). Ablation of the SC using this technique abolishes only very short latency "express" saccades (Schiller and Tehovnik, 2003, 2005). However, injecting muscimol into LIP affected the goal and latency of saccades only if they were surrounded by distractors, suggesting that inhibition in LIP modulates how representation of space compete with each other (Wardak et al., 2002). Inactivation on LIP also caused deficits in target selection during a visual search task that scaled with task difficult, further reinforcing its role in attentional selection and spatial priority (Wardak et al., 2004). FEF inactivation during search showed similar deficits, though they were unaffected by task difficulty (Wardak et al., 2006).

Surround suppressive mechanisms may play a role in attention and attentional filtering in LIP. Regardless of where in the oculomotor network suppression is implemented, the net effect is dependent on the type of downstream decoding mechanism reading the LIP responses. Suppression may work in tandem with excitation, suppressing the responses to irrelevant stimuli while concurrently increasing the responses to relevant ones. If, as in signal detection theory, stimuli are discriminated by the differences in the distributions of their responses, suppression will act to push the means of the distributions farther apart and increase discriminability (Green and Swets, 1966).

Lateral inhibition also plays a key role in "winner-take-all" models of neural competition. In these models (which most often employ a layer of recurrent excitatory cells and a second layer of broadly connected inhibitory cells), the strength of the inhibition is critical for determining the stability of the network (Xie et al., 2002; Moldakarimov et al., 2005; Mao and Massaquoi, 2007).

1.53 Across-trial variability in visual cortex

Surround suppression can act to change the relative firing rates of stimuli in the visual processing stream, but a secondary concern is the reliability of these signals. If signals are highly variable, they might have significant behavioral consequences. For example, imagine a basketball player poised to make a series of throws. For each shot to be successful, he must have an accurate representation of the stimuli relevant to his action. On some shots, the net may be represented by a high response rate, and on others by a low response rate. If we simply are looking at the average response to the net over many successive throws, it may appear that the athlete has a highly accurate representation of the world. But on each shot the response to the net might actually affect the outcome of his shot. Therefore a complete description of the neural variables that contribute to motor outcome will include an analysis of neural reliability.

Neural variability might also play a role in spatial competition. For the basketball player, it is vitally important for him to ignore irrelevant information while he is focused on his free throw. The response to a cheering fan might be a distraction and it would be advantageous for the player to be able to reliably reduce his neural representation of these potential distractors. But how does the brain do this?

One way to quantify the reliability of neural signals is to examine the across-trial variability: the amount of variance in a neural signal to an identical stimulus presentation. A decrease in the amount of across-trial variability can result in an increase in the precision of neural responses and potentially improve discriminability (Paradiso, 1988; Vogels, 1990). The amount of variability can be quantified in a neural signal by using the Fano factor (the ratio of

the variance of the spike count divided by the mean of the spike count). A high Fano factor is indicative of a high amount of variability in the signal whereas a low Fano factor demonstrates a more precise response. Changes in across-trial variability have been found in premotor cortex, where neurons have been found to have decreased variability prior to an arm movement (Churchland et al., 2006b). The firing rates of these neurons did not initiate a movement at a fixed threshold, but instead converged upon a particular mean firing rate, the "optimal subspace" for the neuron.

Though many sensory modalities likely require a precise and reliable neural response for perception (for example in audition, see DeWeese et al., 2005), in this introduction I will focus on variability in visual processing. There is some precedent for this as this has been explicitly compared across aggregated physiological data from 7 different monkey visual areas, including LIP (Churchland et al., 2010). The authors examined the across-trial variability when visual stimuli appeared and found that across all brain areas, the onset of the visual stimulus evoked a sustained decrease in the across-trial variability (as measured by the Fano factor) for the duration of the stimulus presentation. This decrease was true across stimulus conditions, for anesthetized as well as the awake behaving monkey, indicating that the variability reduction is a property of the cortical network, not the cognitive state of the monkey. Importantly, they demonstrated that this increase in neural reliability could occur without concurrent changes in the spike rate (a potential confound since an increase in Fano factors can result from either an increase in spike count variance or a decrease in mean spike count). By rigorously mean matching and recalculated Fano factors for trials in which the average spike counts were unchanged by the stimulus presentation, they confirmed this result for a static neural response.

The authors propose that the onset of the stimulus stabilizes the activity in cortex by reducing the amount of noise in the ongoing spontaneous activity. This suggestion is consistent with theoretical work showing that in a dynamical system, inputs can move networks out of chaotic regimes (Rajan et al., 2010).

In addition to sensory input, changes in the cognitive state of the monkey can also affect levels of across-trial variability. Top-down processes such as attention or reward expectation could have effects on neural variability that would be then associated with improved behavioral outcomes. Changes in the variability were found in the responses of V4 neurons while monkeys performed an attentionally demanding task (Mitchell et al., 2007, 2009). The authors found that when monkeys attended stimuli located at the RF center, the response to the stimuli exhibited a modest increase in firing rate, but a large decrease in across-trial variability, suggesting that a secondary role of attention is to increase the reliability of the attended stimulus. Changes in across-trial variability in V4 were also associated with improved behavioral performance in a saccade targeting task (Steinmetz and Moore, 2010). When monkeys were required to make saccades to targets at the RF center, monkeys made faster saccades when variability was more reduced.

Changes in the neural variability in visual cortex provide a unique signature for understanding cognitive processes such that examining the across-trial variability can give clues to the underlying neural processes. For example, several models have been suggested to underlie the rise in firing rate during a sensory evidence decision-making task. The models make identical predictions about the firing rates, but have different predictions about what the dynamics of the variability will be across the decision. For example, a “variable rate of rise

model" (Carpenter and Williams, 1995; Hanes and Schall, 1996) predicts that variability should be correlated across the trial, while drift diffusion models (Ratcliff and McKoon, 2008) propose that this co-variation will decrease for time epochs that are widely separated. Using the law of total variance which is derived by subtracting the amount of variability due to spiking from the total measured variance, an analysis of LIP data during a decision making task supports the evidence accumulation hypothesis (Churchland et al., 2011).

What is the relationship between neural variability and attentional priority? Previous experiments have sufficiently demonstrated that variability can be reduced in a visual cortical area at the location of the target, but in a brain area such as LIP that represents locations of events in retinotopic space, does this benefit extend to non-target locations? Additionally, how do the different locations on the map interact with each other to produce a stable representation of the visual world and how does the brain use these representations do generate spatially accurate eye movements? We can examine these interactions and also explore the relationship between changes in neural variability and the monkeys' saccadic behavior, particularly in cases where the demands of the task are variable.

1.54 Changes in shared variability in visual cortical areas

Since the state of the LIP map represents an ongoing competition between spatial locations in the visual field, studying the responses of single neurons has obvious limitations. If interactions between neurons play a role in the competition process, we are missing this aspect of the story by recording neurons one at a time. A description of the correlations between neurons recorded simultaneously gives us an estimate of the shared variability between those neurons: a

significant correlation suggests that 2 neurons share input and the sign of the correlation gives us information about the nature of the interaction (Moore et al., 1970; Lytton and Sejnowski, 1991). Positive correlations suggest that neurons share a common input, negative correlations suggest a negative input such as mutual inhibition, and a lack of correlation suggests that spatial representations in LIP are independent. When neurons share spatial RFs or have similar tuning properties, correlations can be due to changes in the visual stimulation, but if neurons share variability independent of the stimulus, these correlations are thought to be a function of shared fluctuations in firing rates (so-called "noise" correlations).

Low levels of correlations have been found between neurons in V1 in both the spontaneous and stimulus driven activity (Smith and Kohn, 2008; Kohn et al., 2009). Unsurprisingly, these correlations are strongest for neurons that share tuning properties and for neurons that are physically closest in cortex. The magnitude of the correlation decreases as a function of distance between neurons, but remains significantly higher than 0 for distances as much as 10 mm cortical separation indicating that neurons share variability through wide swaths of cortex. In the parietal cortex, the amount of noise is correlated with the amount of signal in a reaching task, though primarily for close inter-neuronal distances (Lee et al., 1998).

If neurons in cortex have independent amounts of variability, averaging across a population of neurons will eliminate the downstream effects of that variability. However if neurons share variability, that noise can never be averaged out. In MT, neurons have been found to have very fine behavioral sensitivity such that correlations between neurons could impose limits to the amount of information that a population of neurons can encode (Zohary et al., 1994; Shadlen and Newsome, 1998). However, the exact implications of correlations are unknown will

depend on downstream decoding mechanisms (Abbott and Dayan, 1999; Averbeck et al., 2006). The relevant timescale to look for these correlations is hundreds of milliseconds: correlations are maximal at increasing bin size until they plateau (Mitchell et al., 2009), though correlations on shorter timescales (<5 ms) which primarily quantify the number of synchronous spikes in an epoch may have other behavioral relevance (Fries et al., 2001).

Several studies have shown that correlations in cortex can change as a function of the cognitive demands of the task. In a random dot motion decision task, neurons in MT that represent the motion stimulus have higher correlations when the direction to be discriminated required that information from the neurons be pooled than if the discriminated motion direction is orthogonal to the preferred directions of the cells (Cohen and Newsome, 2008). This indicates that functional connectivity between neurons representing visual information is not static and can change trial-to-trial depending on the demands of the decision.

Noise correlations can also be modulated by attentional allocation. In V4, when spatial attention was deployed to a particular spatial location, the attended location is associated with a small increase in firing rate, a small decrease in across-trial variability, and correlations between attended and unattended targets are significantly decreased (Mitchell et al., 2009). Indeed when the effects of attention were quantified on a trial-by-trial basis, the contributions of correlation reduction far outstripped the benefits of both increases in firing rate and reduction in across-trial variability (Cohen and Maunsell, 2009).

Changes in the magnitude of correlations across time may give us clues to the competitive processes in a brain region. During a visual search task, correlations are maximally positive when the target to be discriminated lies in the receptive field of both neurons, and less

when the target excites neither RF (Cohen et al., 2010). It is completely unknown however, how neurons in the oculomotor network who do not share RFs interact during a competitive saccadic decision. If, as in V4, attention is allocated to a particular choice target, we may expect to see a similar reduction in correlation during the choice. Alternatively, if neurons in LIP behave independently as would be predicted by an independent race to threshold model, we should see no change in the correlation over the course of the trial. Furthermore, it is unknown whether correlations are affected by top-down information in LIP that could encode information that is vital to the upcoming choice.

In this thesis I will explore how oculomotor competition in LIP is implemented in three distinct ways: 1) Neurons compete by suppressing the firing rates of irrelevant information. 2) Neurons increase their coding precision through decreases in the across-trial variability, and 3) Populations of neurons in LIP decorrelate during a saccadic competition. In all three of these cases I will explore how top-down variables such as the expectation of reward affects these competitive processes and I will discuss how these processes are intimately linked to the actions of the monkey, including his saccadic behavior.

Chapter 2: Surround suppression sharpens the priority map in the lateral intraparietal area.

2.1 Abstract

In the visual world, stimuli compete with each other for allocation of the brain's limited processing resources. Computational models routinely invoke wide-ranging mutually suppressive interactions in spatial priority maps to implement active competition for attentional and saccadic allocation, but such suppressive interactions have not been physiologically described and their existence is controversial. Much evidence implicates the lateral intraparietal area as a candidate priority map in the macaque (*Macaca mulatta*). Here, we demonstrate that the responses of neurons in LIP to a task-irrelevant distractor are strongly suppressed when the monkey plans saccades to locations outside their receptive fields. Suppression can be evoked both by flashed visual stimuli and by a memorized saccade plan. The suppressive surrounds of LIP neurons are spatially tuned and wide-ranging. Increasing the monkey's motivation enhances target-distractor discriminability by enhancing both distractor suppression and the saccade goal representation; these changes are accompanied by correlated improvements in behavioral performance.

2.2 Introduction

In the visual world, stimuli are in constant competition for allocation of the brain's limited processing resources. Salient stimuli are often not relevant to the task at hand, but can nevertheless transiently capture attention and result in disadvantageous behaviors (Egeth and Yantis, 1997; Bisley and Goldberg, 2003b; Peck et al., 2009). For example, a jungle predator may have difficulty monitoring his elusive prey when there is a distracting insect flying in his field of view. It would be disadvantageous for this predator to lose focus on the location of the prey, either through an eye movement or a shift of attention to the location of the insect. Human subjects can reduce the capture of attention by an abruptly appearing, task-irrelevant stimulus by attending to a different, task-relevant location before the distractor appears (Egeth and Yantis, 1997). This reduction in attentional capture could be achieved in the brain by enhancing the neural activity encoding the location of the task-relevant stimulus or by suppressing the neural activity associated with the location of the task-irrelevant stimulus. In principle, an efficient neural strategy might incorporate both mechanisms simultaneously, though how such interactions occur is not yet understood.

Many models of attentional and saccadic processing posit that the allocation of visual attention and the selection of saccade targets are both based on the dynamically evolving peak of activity in a map-like representation of spatial priority (Schall, 1995; Gold and Shadlen, 2000; Itti and Koch, 2000; Fecteau and Munoz, 2006; Goldberg et al., 2006; Serences and Yantis, 2007; Armstrong et al., 2009). Current evidence suggests that such priority-map representations exist in

several interconnected brain regions including the lateral intraparietal area (LIP), the frontal eye fields (FEF) and the superior colliculus (SC) (Keller and McPeek, 2002; Thompson and Bichot, 2005; Goldberg et al., 2006). It is commonly theorized that different spatial locations on this map mutually suppress each other over large distances in order to facilitate the evolution of a clear peak of activity which can serve as the focus of visual attention and select the target for saccadic eye movements (Koch and Ullman, 1985; Itti and Koch, 2001; Deco et al., 2002; Constantinidis and Wang, 2004). Such mutual suppression is also considered crucial for maintaining a localized and persistent focus of attention that is resistant to abruptly appearing distractors (Constantinidis and Wang, 2004; Wong et al., 2007), and for the programming of sequential saccades (Xing and Andersen, 2000). Long-ranging interactions across the priority map may also be necessary for the global computations of relative reward value that are known to affect the priority map in LIP (Dorris and Glimcher, 2004; Sugrue et al., 2004).

Despite this theoretical interest, suppression has never been explicitly studied in LIP (or any other priority map area), and its very existence is controversial. Surround suppression has been postulated to explain the decrease in activity with increasing set size in a visual search task (Balan et al., 2008), but it has also been recently argued that LIP has no surround suppression (Churchland et al., 2008). In this study we demonstrate that the priority map in LIP is, in fact, powerfully influenced by surround suppression. Surround suppression in LIP possesses novel properties that have not been demonstrated before in other visual areas.

2.3 Materials and Methods

We used three male rhesus monkeys (*Macaca mulatta*) weighing 8–12 kg in this experiment. All experimental protocols were approved by the Animal Care and Use Committees at Columbia University and the New York State Psychiatric Institute, and complied with the guidelines established by the Public Health Service Guide for the Care and Use of Laboratory Animals. We located the intraparietal sulcus in each monkey using a T1 volume scan obtained on a GE Signa 1.5 T magnet. Using standard sterile surgical techniques and endotracheal isofluorane general anesthesia we made a 2 cm trephine hole over the intraparietal sulcus and implanted 12-16 titanium screws in the monkey's skull and used them to anchor an acrylic cap in which we placed a head holding device, the recording chamber, and the plug for subconjunctival search coils for eye position recording. We used three recording cylinders: (Monkey D, left hemisphere, Monkey I, right hemisphere, Monkey Z, right hemisphere).

2.31 Data collection and task design

We used the REX/MEX/VEX system developed at the National Eye Institute's Laboratory for Sensorimotor Research for behavioral control, visual stimulus display and data collection using Dell Optiplex PC's running QNX (REX and MEX) and Windows 2000 (VEX). The monkeys sat in a dimly illuminated room with their head fixed and viewed a screen that stood 75 cm away. Visual stimuli were back-projected onto the screen using a LCD projector (Hitachi CP-X275) with a refresh rate of 75 Hz. We used a photodiode to register the actual times for stimulus onsets and offsets. Fixation point and saccade target stimuli were 0.3 degree

wide colored squares and distractors were 1.5 degree wide white squares. We introduced the electrodes through a guide tube positioned in a 1 mm grid (Crist Instruments). We recorded single units from area LIP with glass-insulated tungsten electrodes (Alpha Omega Engineering, Nazareth, Israel). while the monkeys performed a passive fixation task as white spots flashed sequentially at different locations in the visual field. We amplified, filtered and discriminated action potentials using an amplitude window discriminator (MEX software). Only well-isolated single neurons were studied.

We considered neurons to be in LIP if they showed consistent visual, delay-period and/or saccade related response during the memory-guided saccade task or were located between such neurons in that electrode penetration. 52/98 (53.06%) neurons tested responded significantly more during the delay period of a memory-guided delayed saccade task (t-test, one-tailed $p<0.05$, average of 49.84 trials per neuron) during the delay period compared to baseline. Every neuron responded to the abrupt onset of a visual stimulus in its RF.

2.32 Task details

For each neuron we isolated, we identified the center of the RF using flashed spots at 400ms intervals (4 per trial, located on a 40 x 40 degree grid with 5 degree spacing, less than 50 ms duration) during passive fixation (Figure 2.1C). We defined the center of the RF as the spatial location of the flashed spot that elicited the maximum activity. We then ran a No-Saccade control, where the monkeys fixated a central red fixation spot for 2050 ms. 1000 ms after the monkey achieved fixation, a brief white spot flashed for less than 50 ms (2-3 video frames in 90

% of trials; 1 video frame on the remaining trials) in the center of the RF. The duration of the distractor was independent of all other task parameters including stimulus locations, timing and reward size. The No-Saccade control was identical to the Target Mapping Task (below), except that no saccade target appeared and the monkey had to maintain fixation throughout the trial to get his reward. After about 50 trials of the No-Saccade control task, we had the monkey perform several variants of the delayed saccade paradigm. We ran each task only on a subset of neurons, depending on the neuron's isolation quality and the monkey's satiety.

The Target Mapping Task began with the appearance of a central red fixation spot; 500 ms after the monkey fixated the central spot, a saccade target appeared at a location randomly chosen from 80 possibilities (on a 40 x 40 degree grid with 5 degree spacing). Occasionally, for some neurons, we sampled from a slightly different set of locations, varying either the sampling or the spatial extent of the grid in order to more closely sample particular regions of space or to ensure sufficient data collection within the limited recording time available. A distractor flashed briefly for less than 50 ms (two or three video frames in about 90% of trials) at the center of the RF 500 ms after the saccade target appeared. When the center of the RF coincided with one of the 80 target locations, the distractor flashed on top of the (much smaller) saccade target. The fixation spot disappeared 550 ms after distractor onset; this was the cue for the monkey to make the saccade (go-cue). Monkeys had to keep their eyes within a 3x3 degree window until the cue to make the saccade appeared. The mean standard-deviation of eye-position during the fixation period was less than 0.25 degrees for all sessions. Monkeys had 400 ms after the go-cue to make a saccade to a 4.5x4.5 degree window around the saccade goal. If the monkey's eye was in the

window for 100 ms from 400 ms to 500 ms after the go-cue, he received a drop of water or juice as reward. In less than 5 % of randomly interleaved trials on this task, no saccade target appeared and the monkey was rewarded for maintaining fixation throughout the trial (interleaved No-Saccade control). The Distractor Mapping Task was similar to the Target Mapping Task, except that the saccade target location was fixed at the RF center while the distractor location was varied over a 40x40 degree grid. In another task variant of the Target Mapping Task, we also had the monkey make a memory-guided saccade to an effective location in the suppressive surround, while the distractor appeared at the RF center (approximately 75 trials). We typically used this task after about 500 trials on the Target Mapping Task, after which an effective location could be identified. Finally, we measured neuronal properties on the Cued Reward Task, where we cued either a large or a small reward randomly on each trial by the saccade target color. For most neurons, we first ran a control task where the saccade target could be one of two different colors, but each was associated with the same reward (approximately 50 trials with distractor at RF center and saccade to suppressive surround, and approximately 50 trials with saccade to RF center and distractor in the suppressive surround). Next, the monkeys performed the Cued Reward Task, where the two chosen saccade target colors was associated with different reward sizes. In the first block, the distractor appeared at the RF center and the saccade was made to the suppressive surround (approximately 200 trials) and in the second block, the saccade was made to the RF center and the distractor appeared in the suppressive surround (approximately 50 trials). Actual reward magnitudes were chosen daily based on the monkey's satiety level and his behavioral sensitivity to the difference in reward sizes. The reward ratio between small and large rewards was approximately 1:6 on average, and ranged from 1:3 to 1:10 for all but 2 neurons (for

which we used higher ratios of 1:20 and 1:50 respectively). The apparently large range of reward ratios is explained by the fact that ratios are very sensitive to changes in the denominator when the denominator is small.

On a given trial, the monkey's eye had to remain within a 4.5x4.5 degree window around the saccade goal from 400 ms to 500 ms after the go-cue for reward delivery. The monkey's eye usually entered this window with the first saccade after the go-cue: for example, in the Cued Reward Task, in 96.5 % of trials, the first saccade after the go-cue landed within this window. Counting only saccades at least 1.5 degrees in amplitude, the monkeys usually made only one (92.9 %) or two (6.8 %) saccades during the period between the go-cue and the reward.

2.33 Data analysis

All data analysis programs were written in MATLAB (Mathworks Inc, Natick, MA). For the Target Mapping Task we verified that a given saccade target location lay outside the RF by comparing the response to the onset of the saccade target to the pre-target response (response 30 to 230 ms after target onset compared to response -170 to 30 ms relative to target onset; t-test, one-tailed $P<0.05$). This insured that the suppression of the distractor response as a result of the saccade plan could not be simply attributed to response adaptation as the result of an excitatory response to the target. We computed population-averaged PSTHs by first obtaining PSTHs from each neuron and then finding the mean of these PSTHs. We used ANOVAs to quantify the spatial properties of the surround. In order to have a sufficient number of trials for these analyses we first pooled the saccade target locations into 9 10x10 degree clusters before performing the ANOVA. When we computed the S_{max} (defined as the 10x10 degree cluster of saccade targets

associated with the minimum distractor response), we found that in 2/72 neurons there were two such clusters that were associated with the minimum distractor response. In these two ambiguous cases, we picked one cluster at random as the S_{max}. In the remaining 70 neurons, our algorithm identified a unique S_{max} and there was no ambiguity. We defined the angular position of the target with respect to the RF as the angle between a line connecting the saccade target to the RF center and a horizontal line passing through the RF center. We used t-tests wherever applicable rather than alternatives like the Wilcoxon signed-rank test or the rank sum test because we consistently observed that whenever there was an occasional discrepancy between the t-test and the alternatives (which do assume that the underlying distribution is symmetrical), it was the t-test that agreed with the results of permutation tests based on repeated simulations. For the analyses of proportions and latencies, the underlying distributions were very skewed and we therefore used a permutation test that compared the z-statistic for the paired difference between large and small-reward trials with the null distribution for the paired difference obtained by 10,000 random shuffles of the two distributions being compared.

2.34 Error Classification

On error trials, the monkeys usually made one (70.5 %) or two (20.8 %) or three (5.7 %) saccades from a time beginning 350 ms after distractor appearance. For categorizing error trials, we first classified saccades in these trials as either a) target-directed (if its endpoint lay within 5 degrees of the saccade goal) b) distractor-directed (if its endpoint lay within 5 degrees of the distractor goal) or c) elsewhere-directed, if it was neither target-directed nor distractor-directed. We then used the following scheme to categorize a given error trial: If there were no target-

directed or distractor-directed saccades, it was classified as an elsewhere-directed error trial. If only target-directed saccades were present, it was a target-directed error trial and similarly, if only distractor-directed saccades were present, it was a distractor-directed error trial. If both target-directed and distractor-directed saccades were present, then we classified the trial as target or distractor-directed depending on which saccade was earlier.

In 24.5 % of error trials, REX truncated data collection of the eye position signal before the end of the final saccade and so the saccade endpoint could not be determined directly; in these cases, we classified saccades whose mean direction was within 0.35 radians (20 degrees) of the line joining the fixation point to the saccade target as target-directed saccades, and saccades that were not target-directed and whose mean direction was within 0.35 radians of the line joining the fixation point to the distractor location as distractor-directed saccades.

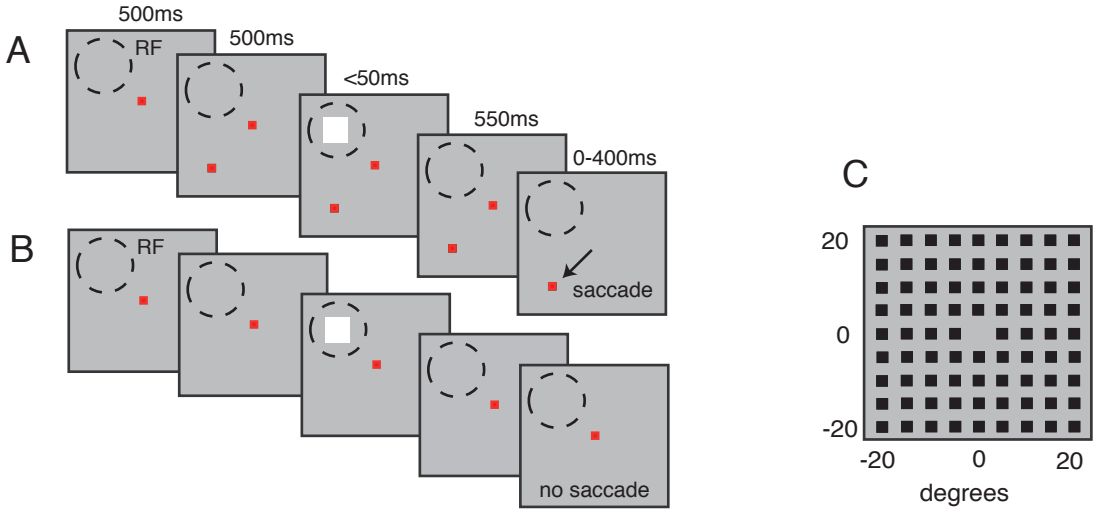

Figure 2.1 Task design.
A) Target Mapping Task: monkeys fixated for 500 ms, after which a target appeared at a location randomly chosen from a 40x40 degree grid of locations in the visual field, with 5 degree spacing in most cases (1C). After 500 ms, a distractor was flashed briefly (<50ms) at the RF center. After a 550ms delay, the fixation spot was turned off, and the monkey made a saccade to the target to obtain the reward. B) The No-Saccade control task was otherwise identical, except that the fixation spot was never turned off, and monkeys maintained fixation throughout the trial to obtain the reward. C) Grid of potential target locations.

2.4 Results

We studied the effect of surround suppression on the visual responses of a total of 105 LIP neurons LIP in 3 monkeys (43 in monkey Z, 26 in monkey D, 36 in monkey I). Our dataset consists of LIP neurons with systematically mapped receptive fields (RFs) based on their clear visual response to a briefly flashed spot (Methods). We considered neurons to be in LIP if they showed consistent visual, delay-period and/or saccade-related responses during the memory-guided saccade task or were located between such neurons in that electrode penetration.

2.41 LIP neurons show clear surround suppression by a planned saccade.

We looked for evidence of surround suppression of LIP neural responses by systematically mapping the effect of a visually guided delayed saccade plan on the response to a task-irrelevant distractor in a subset of 72 neurons. In this task (the Target Mapping Task, Figure 2.1A), the monkey fixated the central fixation point and a small red target appeared at a location chosen randomly on each trial from the grid (Figure 2.1C). 500 ms later, a large, white, salient but task-irrelevant distractor flashed in the center of the RF for less than 50 ms The fixation point disappeared 550 ms later, which served as a cue for the monkey to make a saccade to the target within 400 ms to earn a reward. We compared the neuronal response in the Target Mapping Task to the response in a control task (the No-Saccade control Task, Figure 2.1B) run in a separate block, in which the monkey was rewarded for maintaining fixation and no saccade target appeared. The No-Saccade control task was otherwise identical to the Target Mapping Task. We also ran a small proportion of No-Saccade control trials interleaved within the Target Mapping Task: the distractor response in this condition was not significantly different from that in the blocked version (mean difference ± SEM = 1.16 ± 1.73 spikes/second, t-test p=0.5027, n=72 neurons, Figure 2.2).

In the Target Mapping Task, a saccade plan to locations in the visual field outside the RF suppressed the response to the distractor flashed at the RF center relative to the distractor response in the No-Saccade control Task (Figure 2.3). Suppression could be evoked from a range of spatial locations. The degree of suppression varied markedly as a function of saccade target location (example response map in Figure 2.3). To quantify the maximal amount of suppression

for each neuron, we identified a 10°x10° region outside the RF (S_{max}, red square in Figure 2.3A) from which the saccade plan maximally suppressed the distractor response. We used a randomly selected two-thirds of trials to define the location of the S_{max} for each neuron. Locations were considered to be outside the RF if the appearance of the saccade target did not elicit a significant response from the neuron (Methods). We then cross-validated, using the remaining one-third of trials to estimate the magnitude of the suppression evoked by the saccade plan to locations within S_{max}. When the monkey planned a saccade to regions within S_{max}, the distractor response was reduced compared to the No-Saccade control (see example neuron, Figure 2.3B). This reduction was strongly present in our LIP population: in 66 of 72 neurons (91.7%), planning a saccade to locations within S_{max} reduced the neuron's response to the distractor relative to the No-Saccade control (Figure 2B; two-sample t-test, one-tailed $p<0.05$, n=number of trials in the session). Across the population, the distractor response was strongly reduced compared to the No-Saccade control task when planning a saccade to locations within S_{max} (mean reduction ± SEM = 14.14 ± 1.46 spikes/second, $p<0.0001$, n=72 neurons). In addition, the net distractor response (calculated by subtracting the pre-distractor firing rate 240 ms before to 30 ms after distractor onset) was also significantly suppressed when the monkey planned a saccade to locations within S_{max} compared to the No-Saccade control task (mean reduction ± SEM = 8.27 ± 1.19 spikes/second, $p<0.0001$, n=72 neurons).

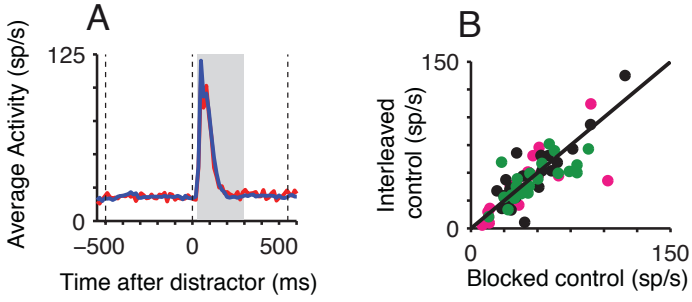

Figure 2.2 No saccade control
A,B) No-Saccade Control response is similar whether run in a separate block (blue PSTH in A, abscissa in B) or interleaved with Target Mapping trials (red PSTH in A, ordinate in B) Mean difference between blocked and interleaved control responses = 1.16 ±1.73 sp/s, p=0.5027, n=72 neurons.

Suppression emerged in the background activity even before the distractor appeared, beginning 100 ms after the appearance of the saccade target, and continuing through the trial until the go-cue (Figure 2.4A, n=72 neurons). The pre-distractor baseline response (-500 to 30 ms around distractor onset) when the monkey planned a saccade to locations within S_{max} was significantly reduced compared to the No-Saccade control task (mean reduction ± SEM = 3.43 ± 1.15 spikes/second; p=0.0037, n=72 neurons). When we recalculated the S_{max} based on the pre-distractor baseline response itself, rather than basing it on the distractor response, an even larger effect on the pre-distractor baseline response was visible (mean reduction ± SEM = 7.09 ± 1.07 spikes/second, p<0.0001, n=72 neurons).

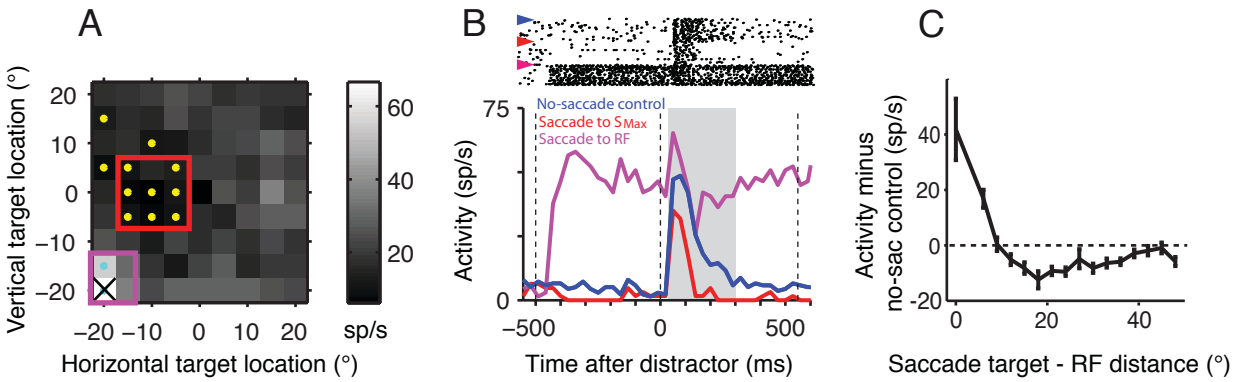

Figure 2.3 Single cell response during target mapping task.
A) Suppression of example LIP neuron by a saccade plan to the surround. Grayscale map of response to the distractor (average firing rate from 30-300 ms after distractor onset) as a function of saccade target location with respect to the central fixation point. Target locations with yellow/cyan dots are significantly suppressed (yellow) or enhanced (cyan) relative to the No-Saccade Control (p<0.05, t-test with Bonferroni correction for 80 simultaneous comparisons). Boxed locations indicate saccade target locations defined as the RF (magenta) and Smax (red) for the rasters and PSTHs in E. X at -20,20 indicates distractor location. B) PSTHs and rasters from the example neuron, aligned to distractor onset: saccade plan to the Smax leads to a reduced distractor response (red) compared to both the No-Saccade control response (blue) and to response when saccade is planned to the RF (magenta). Rasters are sorted by trial type. Dashed vertical lines indicate time of saccade target onset (left), distractor onset (middle) and time of saccade go-cue (right). C) Distractor response varies with distance of saccade target from the RF center. Example neuron's distractor response during the Target Mapping Task (minus the response during the No-Saccade control, horizontal dashed line at 0) plotted as a function of the distance between the saccade target and the RF center. Error bars show SEMs (n=number of locations contributing to each data point).

2.42 Surround suppression is long-ranging and radially symmetric in the population.

Suppressive surrounds from individual neurons in LIP had a wide variety of shapes, similar to reports of surround suppression from lower visual areas (Orban 2008). The amount of suppression elicited by a saccade target varied significantly with its spatial location in 57/72 neurons (Kruskal-Wallis ANOVA, $p<0.05$). Surround suppression extends over long distances: the farthest location from which significant suppression could be elicited lay greater than 21.2 degrees from the excitatory receptive field center in all 66 neurons that showed significant surround suppression. The mean farthest location was 35 degrees. S_{max} lay further than 10 degrees from the RF center in 65/72 neurons (90.3 %).

Although individual neurons showed diverse surround shapes, surround suppression averaged across the population was radially symmetric and showed a systematic dependence upon the distance of the saccade target from the RF center (Figure 2.4). For each neuron, we plotted the average activity from the Target Mapping Task for each target location (minus the activity in the No-Saccade control task) as a function of the distance between the distractor and target locations (example neuron in Figure 2.3). On average, suppression reached a maximum between 12° and 35° from the RF center, and remained significant up to 40 degrees away from the RF center. A similar distance dependence was seen for the baseline response (Figure 2.5). To evaluate the radial symmetry of the surround around the excitatory receptive field center, we plotted the average activity from the Target Mapping Task at each location outside the RF (minus the activity in the No-Saccade control task) as a function of the angular locations of the target

with respect to the RF center (Figure 2.4D, black). The population-averaged surround was

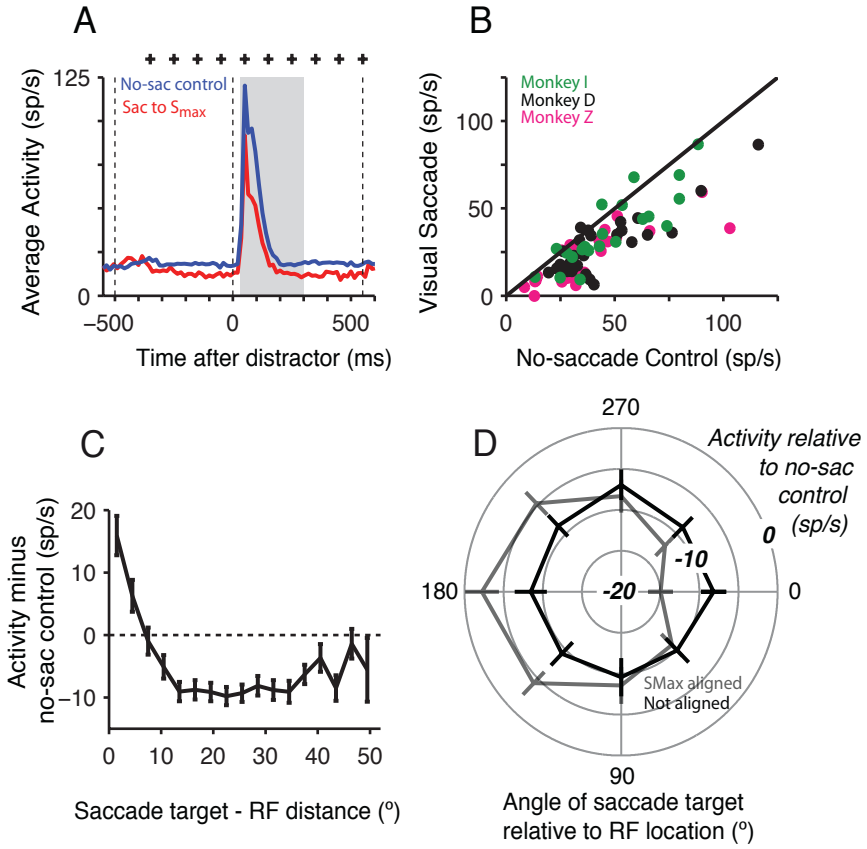

Figure 2.4 Population responses during target mapping task.
A) Population average PSTH reveals significant suppression of both baseline and distractor response when a saccade is planned to the Smax (red) compared to the No-Saccade control (blue). Only the 1/3rd of trials that were not used to calculate the Smax contribute to the response in red. Black crosses mark the centers of non-overlapping 100 ms time bins with a significant difference between responses (paired t-test, $p<0.05$, n=72 neurons). B) Scatter plot of each neuron's response to the distractor (30-300 ms after distractor onset, grey bar 2C) during the No-Saccade control (abscissa) and the saccade plan to Smax condition (ordinate). Paired t-test: $p<0.0001$, n=72. Green, black and magenta circles indicate neurons from monkeys I, D and Z respectively. C) Distractor response varies with distance of saccade target from the RF center. Population averaged distractor response during the Target Mapping Task (minus the response during the No-Saccade control, horizontal dashed line at 0) plotted as a function of the distance between the saccade target and the RF center. Averaged tuning curves were first calculated for each neuron and then averaged together to produce the population average. Error bars show SEMs. (n=number of neurons contributing to each data point.) D) Population-averaged suppression extends in all directions from the RF. Polar plot showing average level of suppression in 8 binned angular directions (bin size=45 degrees) around the RF center. Polar tuning plots were first computed for each neuron and then averaged together. Error bars as in C. The magnitude of suppression (spikes/s) is plotted as a function of absolute direction around the RF center (black), and after rotating all target angles so that the center of Smax lies at 0 degrees (grey). The 4 circles in the polar plot lie at -15, -10, -5 and 0 spikes/s.

radially symmetric around the RF center, and showed no significant dependence upon the angular location of the saccade target with respect to the RF center (Kruskal-Wallis ANOVA, p= 0.8732).

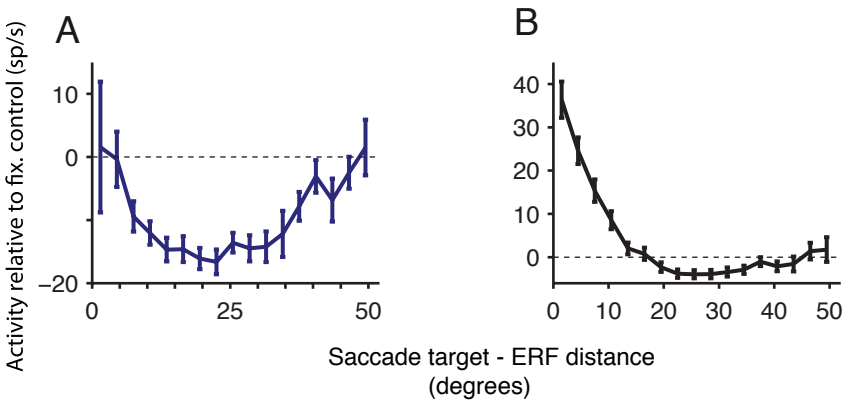

Figure 2.5 Spatial tuning of baseline response.
A) Since suppression is not radially symmetric (Figure 2D), we re-evaluated the dependence of the degree of suppression upon the distance of the saccade target from the RF center. Identical to Figure 2C, except that instead of averaging data from all saccade target locations, we averaged data from saccade targets that were outside the RF and lay within 10 degrees of a line running from the RF center to the Smax. Suppression is clearly visible and dependent on the distance of the saccade target from the RF center. B) Identical to Figure 2C, except that the baseline response is used instead of the distractor response. The baseline response (-500 to 30 ms following distractor onset) also shows a clear dependence upon the distance of the saccade target from the RF center.

Individual neurons, however, did not in general have circularly symmetric surrounds. When we re-plotted the data in the blue trace in Figure 2.4D after rotating the location of S_{max} so that it always lay at 0°, thereby aligning the locations with the maximum amount of suppression, the average response showed a clear dependence upon angular location of the saccade target with respect to the excitatory receptive field center (grey trace, Kruskal-Wallis ANOVA, $p<0.0001$). In accordance with this result, the degree of suppression in individual neurons along a ring passing through S_{max} (with the RF as center) depended significantly upon the angular location of

the saccade target in 33/72 neurons (45.8 %, Kruskal-Wallis ANOVA, $p<0.05$). Finally, though the RF centers were all in the contralateral visual field or along the midline, the locations of the S_{max} for each cell showed only a small tendency to lie in the contralateral hemifield: 18/25 neurons (72.0 %) in monkey Z and 15/22 neurons (68.2 %) in monkey D lay in the contralateral hemifield ($p=0.0455$ and $p=0.1356$ respectively, test of proportions), but only 9/19 (47.4 %) neurons in monkey I did ($p\sim1$, test of proportions).

2.43 Suppression can be maintained without the presence of the visual target.

LIP neurons show enhanced activity throughout the delay period of the memory-guided delayed saccade task (Gnadt and Andersen, 1988). We tested whether this was also true for surround suppression in a subset of 48 neurons by modifying the Target Mapping Task. Instead of a visually-guided delayed saccade, we asked the monkey to make a memory-guided delayed saccade to a saccade target which flashed briefly for 50 ms at a single location within the suppressive surround. The task was otherwise identical to the Target Mapping Task (Figure 2.1A). We briefly flashed a distractor in the RF center 500 ms after the saccade target appeared. The fixation point disappeared 550 ms after the distractor disappeared, and the monkey was rewarded for making a saccade to the spatial location of the vanished stimulus. For 40 of the 48 neurons the neuronal response to the distractor that appeared during the delay period was significantly suppressed relative to the No-Saccade control (83.3 %; two-sample t-test, one-tailed $p<0.05$; Figure 2.6B). Suppression was strongly significant across the population of sampled neurons (mean reduction ± SEM = 16.09 ± 2.33 spikes/second, $p<0.0001$, n=48 neurons, Figure

2.6C). Suppression by a memory-guided saccade, like suppression by a visually-guided saccade, began 100 ms after the saccade target appeared and continued until the go-cue (Figure 2.6B, n=48 neurons).

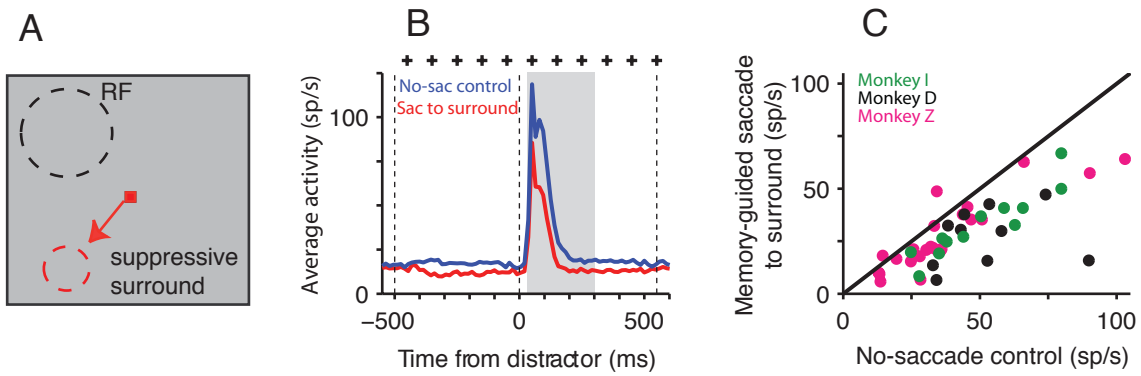

Figure 2.6 Suppression can be maintained without the presence of the saccade target.
A) Task design: Identical to the Target Mapping Task, except that monkeys planned a memory-guided saccade to a single fixed location within the surround. The distractor was flashed at the RF center. B) Population average PSTH reveals significant suppression of both baseline and distractor response when a memory-guided saccade is planned to the surround (red) compared to the No-Saccade control (blue). Binwidth=15 ms. C) Scatter plot of each neuron's response to the distractor (grey bar: 3B) during the No-Saccade control (abscissa) compared to the saccade plan to the surround (ordinate). One point (control response =131.70, saccade plan=59.64) omitted for visibility. Paired t-test: $p<0.0001$, n=48. Figure format for B and C otherwise identical to Figs. 2.4A and 2.4B respectively.

2.44 A distractor in the surround transiently suppresses the response to the saccade target.

In a subset of neurons (n=37), we looked to see whether a flashed distractor in the surround would have a suppressive effect on the maintained activity during a planned saccade to the excitatory receptive field (Figure 2.7A). In this task (the Distractor Mapping Task), a variant of the Target Mapping Task, the saccade target always appeared at the RF center while the spatial location of the distractor (rather than the saccade target) was randomized. The Distractor

Mapping Task was otherwise identical to the Target Mapping Task. As a control, during a small number of interleaved trials, no distractor appeared during the delay period (the No-Distractor Control). Again we used half the trials to determine the 10x10 degree region where the distractor evoked maximal suppression (DS_{max}) and then used the remaining trials to estimate the effect of a distractor flashed within DS_{max}.

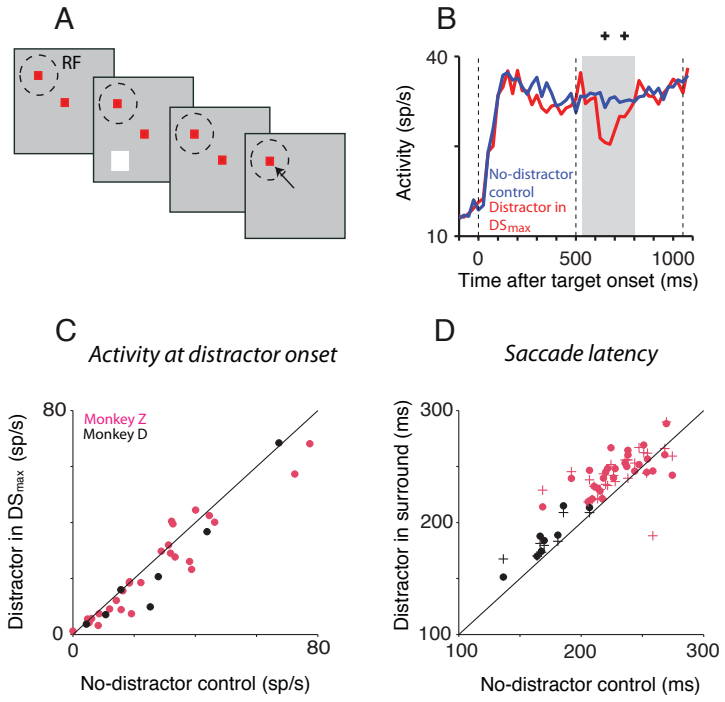

Figure 2.7 A flashed distractor elicits suppression.
A) Distractor Mapping Task: Identical to the Target Mapping Task (Fig. 1A), except that the saccade target location was fixed at the RF center, and the distractor location was chosen randomly on each trial from the 40x40 degree grid of locations (Fig 1C). In interleaved No-Distractor Controls, the distractor was not flashed. B) Distractor-onset in the surround evokes transient suppression. Population average PSTHs show the No-Distractor Control (blue) and the population average response when the distractor was flashed within DSmax calculated from the bottom-up response map (red). Trials used to calculate DSmax not included in the PSTH. PSTHs aligned to saccade target onset. Black crosses as in Fig.2A. Binwidth=25 ms. C) Scatter plot of each neuron's response to the distractor during the No-Distractor Control (abscissa) compared to the response with the distractor within DSmax (ordinate). Paired t-test: p=0.007, n=37. Two points at (control response =176.02, 134.35 and saccade plan=189.92, 123.28) omitted for visibility. D) Distractor appearance leads to slowed saccadic latencies: scatter plot of mean saccadic latency during the No-Distractor Control (abscissa) vs. the mean saccadic latency with the distractor flashed either within DSmax (ordinate, filled circles) or anywhere in the visual field (ordinate, plus signs). Each point represents data from the recording of one neuron. Paired t-tests for both comparisons: p<0.0001, n=37. Figure format for B and C otherwise identical to Figs. 2A and 2B respectively.

A distractor flashed within DS_{max} caused a significant transient suppression of the maintained delay-period response of the neuron. This effect was significant for two consecutive 100 ms bins following distractor onset (Figure 2.7B for the population average; n=37 neurons). The response 30-300 ms following the distractor flashed within S_{max} was significantly lower than the response in the same period in the No-Distractor Control (Figure 2.7C, mean decrease ± SEM = 3.00 ± 1.07 spikes/second, p=0.0075, n=37). In addition, the saccadic latency on these trials (where distractor appeared within DS_{max}) was significantly longer compared to the interleaved No-Distractor Control trials, despite the fact that the distractor appeared 550 ms before the go signal (Figure 2.7D, mean increase ± SEM = 13.07 ± 2.85 ms, p<0.0001, n=37), confirming that the distractor had a disrupting effect on the monkey's saccade plan. Saccade latencies are also longer when averaged across all possible distractor locations (not just the DS_{max}: Figure 2.7D, mean increase ± SEM = 12.35 ± 3.42 ms, p<0.0001, n=37).

2.45 Increasing expected reward increases the response to the target and decreases the response to the distractor.

We studied the effect of motivation on surround suppression on a subset of neurons in LIP (n=48) using a variant of the Target Mapping Task. We cued the monkey to expect a large or a small reward using the color of the saccade target to indicate the upcoming reward (Cued Reward Task). We used two specific spatial configurations (always in separate blocks): to measure the distractor response, we presented the distractor at the RF center (and the saccade target at a fixed location in the suppressive surround), and to measure the target response, we

presented the saccade target at the RF center (and the distractor at a fixed location within the suppressive surround). The Cued Reward Task was otherwise identical to the Target Mapping Task. We randomly assigned color pairings with large and small rewards during each recording session. Large and small reward targets were interleaved within each block of trials. The monkeys learned the reward contingencies associated with the color of the saccade target within a few trials, as indicated by significantly faster saccade latencies and significantly fewer distractor-directed saccades on the large-reward trials compared to the small-reward trials (Roesch and Olson, 2003; Hikosaka et al., 2006).

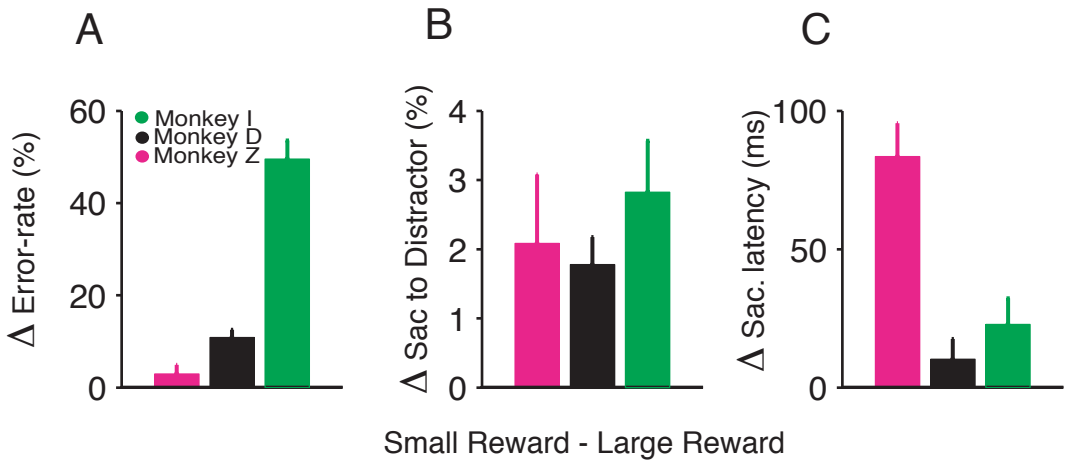

Figure 2.8 Behavior during cued reward task.
A, B and C shows the difference in 3 psychophysical measures between small and large-reward trials for the 3 monkeys. Error-bars are SEMs (21, 19 and 8 sessions for monkeys I, D and Z respectively). 1, 2, 3 and 4 asterisks indicate significance at the 0.05, 0.01, 0.001 and 0.0001 levels respectively using a permutation test based on the z-statistic. A) Monkeys made proportionally more errors during small-reward trials than during large-reward trials. B) Monkeys made proportionally more erroneous distractor-directed saccades during small-reward trials. C) Monkeys made slower saccades to the target during small-reward trials compared to large-reward trials.

On large-reward trials, the three monkeys never made an error-saccade directed towards the distractor. However, on small-reward trials, all three monkeys made a very small, but significant proportion of error-saccades directed towards the distractor (permutation $p<0.0001$ in

each monkey, mean proportion ± SEM in monkey: Z, 2.08 ± 1.07 %, n=8; D, 1.77 ± 0.41 %, n=19; I, 2.82 ± 0.76 %, n=21). Monkeys Z and I also made significantly shorter latency saccades to the saccade targets associated with the large reward than to those associated with the small reward (Mean decrease ± SEM in monkey: Z, 83.46 ± 12.86 ms, p=0.0002, n=8; D, 10.21 ± 7.54 ms, p=0.1813, n=19; I, 22.80 ± 9.70 ms, p=0.0258, n=21). These results indicate that the monkeys could assess the reward value of the trial based on the saccade target color and were more highly motivated during large-reward trials (Figure 2.8).

The relative magnitude of the cued reward affected the responses to both the distractor (when the monkey planned a saccade to the surround and the distractor appeared at the RF center) and the target (when the target and distractor locations were reversed). The neuronal response to the distractor flashed at the RF center on large-reward trials was significantly lower than the response on small-reward trials in three consecutive 100 ms periods following distractor onset (Figure 2.9A, n=46 neurons). This reduction was significant in 31 of the 46 neurons taken individually (67.4 %; two-sample t test, one-tailed $p<0.05$). In the population, the reduced distractor response on large-reward trials was highly significant (Figure 2.9B, mean decrease ± SEM = 10.36 ± 1.83 spikes/second, $p<0.0001$, n=46 neurons).

The neuronal response to the saccade target appearing at the RF center was greater when the monkey expected a large reward instead of a small reward. In the population, the enhanced target response (400 ms before distractor onset to 30 ms after distractor onset) on large-reward trials was highly significant (Figure 2.9C, mean increase ± SEM = 11.15 ± 2.27 spikes/second, $p<0.0001$, n=38 neurons). The target response was significantly higher on large-reward trials in 22 of the 38 neurons taken individually (57.9 %; two-sample t test, one-tailed $p<0.05$). The

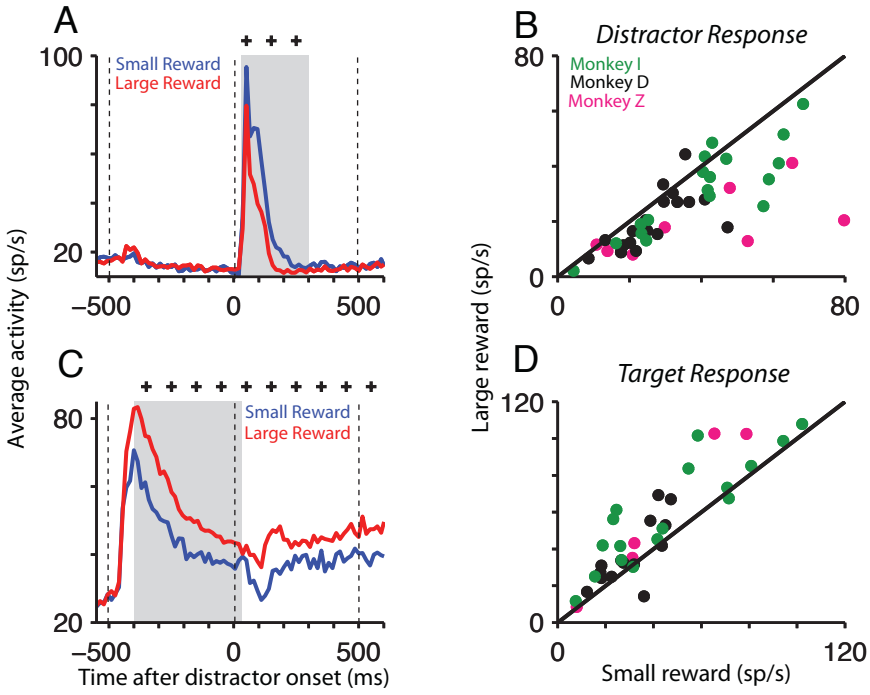

Figure 2.9 Increasing motivation enhances suppression.
A) Distractor response is lower during large-reward trials: With distractor in RF and target in the suppressive surround, population average PSTH shows reduced distractor response in large-reward trials (red), compared to small-reward trials (blue). Black crosses as in Fig.2A. B) Scatter plot of each neuron's response to the distractor during small-reward (abscissa) and large-reward (ordinate) trials. Paired t-test: $p<0.0001$, $n=46$. One point (small-reward: 105.63, large-reward: 79.00) omitted for visibility. C) Target response is larger during large-reward trials: With target in RF and distractor in the suppressive surround, population average PSTH shows enhanced target response in large-reward trials (red), compared to small-reward trials (blue). Black crosses as in Fig.2A. D) Scatter plot of each neuron's response to the target (-400 to 30 ms after distractor onset, grey bar 5C) during small-reward (abscissa) and large-reward (ordinate) trials. Paired t-test: $p<0.0001$, $n=38$. PSTH binwidths: 15 ms. Two points (small-reward: 150.26 and 153.30, large-reward: 184.38, 149.44) omitted for visibility. Figure format for PSTHs and scatter plots as in Fig.2.4.

enhanced target response, averaged across monkeys, was significant throughout the trial from 100 ms after saccade target onset until the go-cue (Figure 2.9D, n=38 neurons). The duration of the enhanced target response was variable across monkeys. Monkey D showed an enhanced

target response only during the early part of the trial, while the other two monkeys showed an enhanced response throughout the trial until the go-cue (Figure 2.10).

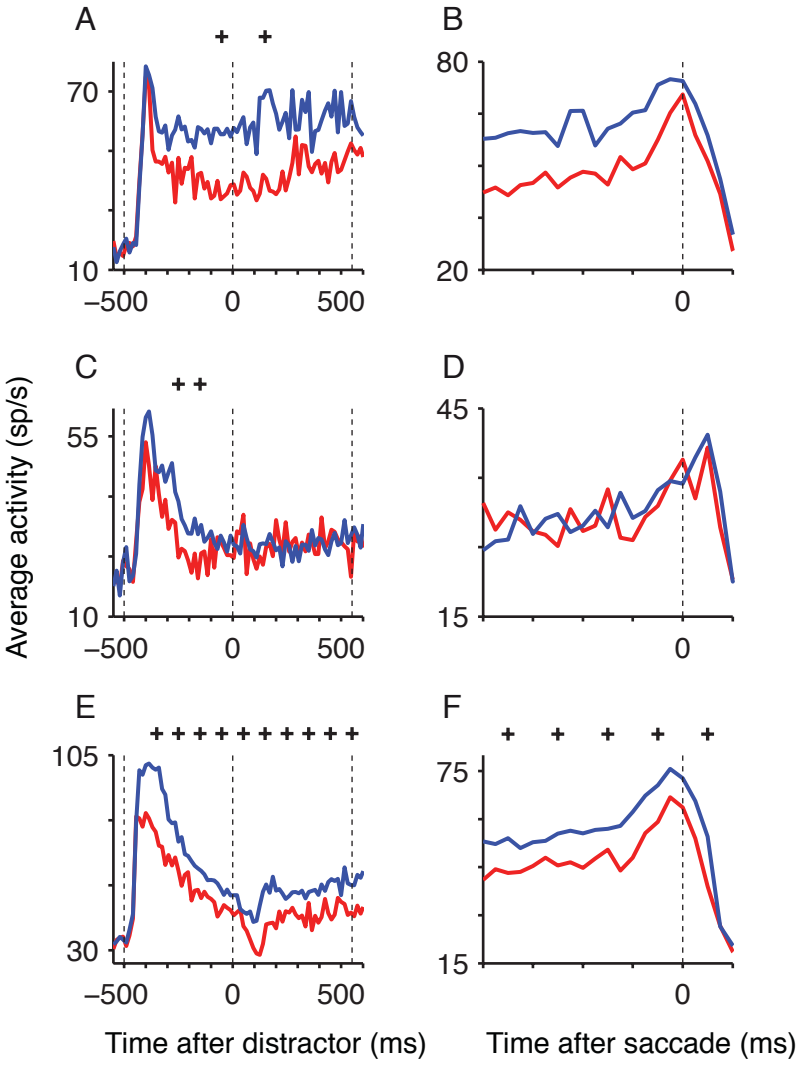

Figure 2.10 Cued reward task for all monkeys.
Same data and format as in Figure 2.9C, but separately for the 3 monkeys Z (in A), D (in C) and I (in E). All 3 monkeys show greater responses to the target in large-reward trials during the early part of the trial. However, from about 100 ms before distractor onset, monkey D no longer shows an enhanced target response. B,D,F) Same format as in A,C and E, except the PSTH is aligned to saccade onset. The difference between monkeys in the effect of absolute reward on the late delay response is visible. The absence of statisticalsignifcance for the effects in monkey Z is likely due to the small number of neurons recorded from this monkey (N=8).

To ensure that the effects of varying expected reward were not due simply to a systematic (though unlikely) overlap of the chosen reward associations with LIP color selectivity, we performed a control experiment in a subset of the neurons recorded in the Cued Reward Task (Figure 2.11). Before associating different reward sizes with different colors, we recorded the responses of LIP neurons with both target colors associated with the same reward size, sampling

both spatial configurations (distractor at RF center and target in suppressive surround in one block and target at RF center and distractor in suppressive surround in another block). We found no significant behavioral differences (n=38 neurons) between trials with the two saccade target colors in the total percentage of errors (mean difference ± SEM = 0.37 ± 0.67 %, p=0.58), the percentage of distractor-directed error saccades (mean difference ± SEM = 0.036 ± 0.060 %, p=0.50), and in saccadic latency (mean difference ± SEM = 1.44 ± 2.24 ms, p=0.53). Prior to reward association, we also found no significant differences between the two colors in either the distractor response (mean difference ± SEM = 0.22 ± 0.67 spikes/second, p=0.74, n=35), or the target response (mean difference ± SEM = 2.12 ± 2.32 spikes/second, p=0.36, n=31).

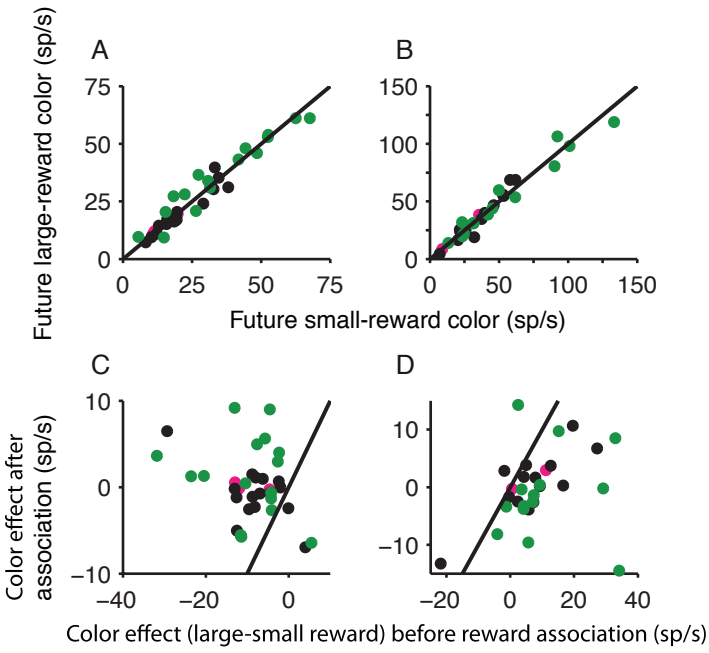

Figure 2.11 Effects of saccade target color are not significant before reward association.
Both the distractor response (A, distractor at RF center) and the target response (B, target at RF center) are not significantly different when the saccade target has the future small-reward color (abscissa) or large reward color (ordinate). A: mean difference ± SEM = 0.22 ± 0.67 sp/s, p=0.7423, n=35 neurons. B: mean difference ± SEM = 2.12 ± 2.32 sp/s, p=0.36, n=31 neurons. The effects of saccade color were not explicitly measured prior to reward association in the remaining neurons. One point in B at (small-reward color response = 155.57, large-reward color response = 94.09) omitted for visibility.

2.46 Distractor and saccade target responses are correlated with saccade latency.

We looked for correlations between the neuronal response and the monkeys' saccade latency in the Cued Reward Task. For small-reward trials, the distractor response was positively

correlated with saccade latency on a trial-by-trial basis: increased distractor responses were associated with longer-latency saccades when the distractor was flashed at the RF center. The average correlation coefficient (Spearman's rho) between trial-by-trial neuronal activity 30 to 300 ms after distractor onset and saccadic latency was significantly greater than zero (Figure 2.12, mean ± SEM =0.088 ± 0.024, p=0.0006, n=46). Conversely, the target response was negatively correlated with saccade latency on a trial-by-trial basis: increased target responses were associated with shorter-latency saccades when the target appeared at the RF center. The average correlation coefficient between trial-by-trial neuronal activity 300 to 500 ms after distractor response and saccadic latency was significantly negative (mean ± SEM = -0.14 ± 0.04 ms/Hz, p=0.0005, n=38).

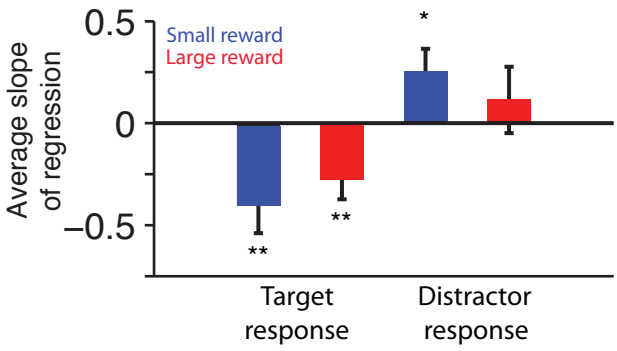

Figure 2.12 Correlates of LIP neurons with saccadic behavior in the cued-reward task: Larger LIP neuronal responses are associated with faster saccades to the RF and slower saccades to the surround. In the small-reward condition (blue bars), correlation coefficients were significantly negative (Paired t-test: p=0.0005, n=38) with target in RF and distractor in the surround, while slopes were significantly positive with distractor in RF and target in the surround (Paired t-test: p=0.0006, n=46). Effect-sizes were smaller in the large-reward condition (red bars) and only significant with the target in RF (Paired t-test: p=0.0132, n=38) and not with the distractor in the RF (Paired t-test: p=0.2266, n=46).

In large-reward trials, there was a similar negative correlation coefficient when the target lay at the RF center (mean ± SEM = -0.069 ± 0.027 ms/Hz, p=0.0132, n=38), but not when the distractor was flashed at the RF center (mean ± SEM = 0.033 ± 0.027 ms/Hz, p=0.2266, n=46). Since the reduced distractor response on large-reward trials is accompanied by a reduced

variance (mean ± SEM = 8.59 ± 2.43 Hz^2, p=0.0002, n=46), we interpret this result as reflecting that once distractor responses are highly suppressed (as in the large-reward trials), their reduced residual trial-by-trial variability contributes less to the overall variation in saccadic latency

2.47 The distractor response in LIP predicts erroneous saccades.

The monkeys had an error-rate of only 5.0 % on average during large-reward trials. But because they usually made far more errors on small-reward trials (mean error-rate=31.5%), we were able to use the small-reward trials to test whether there was any correlation between the distractor response in LIP and the monkey's saccadic behavior. To eliminate any contamination of the distractor response (30 to 300 ms following distractor onset) from saccade-related signals, we included only error trials where the monkey made an erroneous saccade after 350 ms following the distractor onset. We divided error trials into three types depending on whether the erroneous saccade was directed towards the distractor (distractor-directed error trials), preemptively towards the target (target-directed error trials) or towards neither the distractor nor the target (elsewhere-directed error trials). The distractor response in LIP was significantly enhanced on distractor-directed error trials compared to correct trials (Figure 2.13C, mean increase ± SEM = 15.80 ± 3.54 spikes/second, p=0.0003, n=18 neurons). The population average PSTH on distractor-directed error trials (Figure 2.13: red PSTH) was significantly different from the PSTH on correct trials (Figure 6B: blue PSTH) from 100 to 300 ms following distractor onset (n=18 neurons). The enhancement of the distractor response was specific to distractor-directed error trials and was not present for the other two types of error trials. There was no significant

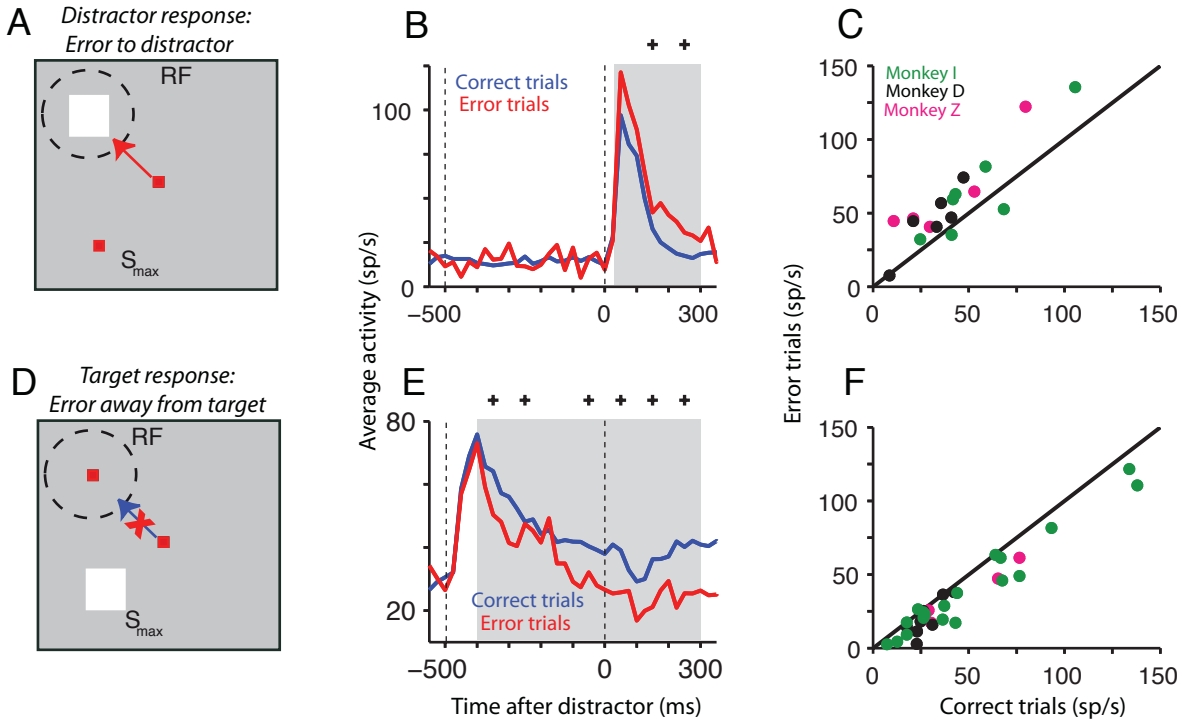

Figure 2.13 Target and distractor responses predict saccadic targeting during small-reward error trials.
A lower target response predicts saccades away from the target. A higher distractor response on such trials predicts a distractor-directed saccade. A) Schematic depicting distractor-directed error trials. B) Population average PSTH shows larger distractor responses on distractor-directed error trials (red) compared to correct trials (blue). C) Scatter plot of each neuron's response to the distractor during correct trials (abscissa) and distractor-directed error trials (ordinate). Paired t-test: p=0.0003, n=18 neurons. D) Schematic depicting small-reward error trials where monkey saccades away from the target. E) Population average PSTH shows reduced target responses on these error trials (red) compared to correct trials (blue). Black crosses as in Fig. 2A. F) Scatter plot of each neuron's response to the target (-400 to 300 ms relative to distractor onset, grey bar 6E) during correct trials (abscissa) and error trials (ordinate). Paired t-test: p<0.0001, n=31 neurons. PSTH binwidths=25 ms. Only errors made at least 350 ms after distractor onset included. Figure format for PSTHs and scatter plots as in Fig.2.

difference between the distractor response on elsewhere-directed error trials and correct trials (mean difference ± SEM = 2.75 ± 1.99 spikes/second, p=0.1691, n=35 neurons). Similarly, the distractor response on target-directed error trials was actually significantly lower than that on correct trials (mean decrease ± SEM = 4.60 ± 2.48 spikes/second, p=0.0270, n=35 neurons). The

enhanced distractor response therefore predicted the impending erroneous saccade towards the distractor.

There was no significant difference in the target response (from 400 ms before to 300 ms after distractor onset) between distractor-directed error trials and elsewhere-directed error trials (mean difference ± SEM = 2.29 ± 3.81 spikes/second, p=0.5405, n=9 neurons); we therefore pooled these two types of trials together as error trials with saccades directed away from the target. The target response on these trials (Figure 2.13E: red PSTH) was significantly higher than that on correct trials (Figure 2.13E: blue PSTH; mean increase ± SEM = 10.03 ± 1.55 spikes/second, $p<0.0001$, n=31 neurons, Figure 2.13F). Thus, a lower target response predicts error trials where the monkey saccades away from the target. On these error trials, a higher distractor response predicts a distractor-directed saccade.

2.5 Discussion

Our results show, for the first time, that LIP neurons have strong suppressive surrounds that influence and sharpen the LIP priority map. By systematically characterizing these effects, we find that suppression of LIP responses is wide-ranging and can therefore link the representations of stimuli that are distant from each other in physical space.

2.51 Surround suppression in LIP is affected by cognitive influences.

Surround suppression evoked by visual stimuli is a ubiquitous neural strategy and has been reported in many visual areas including the retina, lateral geniculate nucleus (Alitto and Usrey,

2008), area V1 (Angelucci and Bressloff, 2006), MT, MST (Allman et al., 1985a; Eifuku and Wurtz, 1998; Orban, 2008) and V4 (Desimone et al., 1985; Desimone et al., 1993). However the surround suppression we report here in LIP has several unique properties not seen in other visual areas. Most importantly, surround suppression observed in LIP is affected by cognitive processes that are not dependent upon the presence of a particular visual stimulus. We demonstrated this in two ways: first, suppression of LIP responses can be maintained by the memory of a visual stimulus which will guide a future saccade, whereas the surround suppression demonstrated in lower visual areas was evoked and maintained by a visual stimulus itself. Second, suppression of LIP responses is enhanced when the monkey expects a larger reward as a result of a learned association with a visual stimulus. Increased motivation enhanced the representation of the saccade goal and suppressed the representation of the distractor. The enhancement of the target response in our single-target task conflicts with prior claims based on data from game-based choice tasks (Dorris and Glimcher, 2004), but is entirely consistent with reports from various other parts of the brain including the dorsolateral prefrontal cortex, frontal and supplementary eye fields, the basal ganglia and the SC (Ikeda and Hikosaka, 2003; McCoy and Platt, 2005; Hikosaka et al., 2006; Watanabe, 2007).

Spatial attention has been shown to suppress distractor responses through center-surround interactions in the near-surround of V4 neurons (Sundberg et al., 2009) and from locations far outside the RF in V1 neurons, especially at higher task difficulties (Chen et al., 2008). We suggest based on our results that the center-surround interactions measured in V1 reflect long-range suppressive effects established in another cortical area like LIP, especially if enhancement

of surround suppression by higher task difficulty is based on the same circuitry as the enhancement of surround suppression by higher reward expectation (Maunsell, 2004).

2.52 Surround suppression in priority maps

Given the ubiquity of surround suppression in the visual system, it is surprising that the existence of surround suppression in LIP has been controversial (Churchland et al., 2008). Data from other putative priority map areas in the brain has also been inconclusive. Data from FEF during a visual search task indicate only spatially local suppressive effects in less than a third of neurons that extend on average up to four to six degrees outside the RF at ten degrees eccentricity (Schall et al., 1995; Schall et al., 2004). In the SC, distractors flashed at locations distant from the excitatory RF evoke short-latency suppression of pre-target activity in a gap-saccade task in some neurons (Dorris et al., 2007). In DLPFC, a memory-guided saccade plan has been shown to slightly suppress baseline neuronal responses opposite to the saccade goal (Constantinidis et al., 2002). Our characterization of surround suppression goes well beyond these prior descriptions by unequivocally demonstrating the spatially wide-ranging, strong and ubiquitous influence of surround suppression of LIP responses and by illustrating several important and novel properties that have not been previously reported from other areas (using tasks that were not explicitly designed to study surround suppression).

The suppressive effects we have measured in LIP may not necessarily be mediated by direct suppressive effects upon LIP neurons, and could instead reflect suppressive interactions in

other areas that are then relayed to LIP. This is of course also true for every other response property measured from LIP neurons to date: there is not a single known response property of LIP neurons that is known to be definitively established within LIP itself. However, we do know that inhibitory inputs exert a strong influence on LIP neurons, since the majority of LIP neurons respond with dramatically increased firing after iontophoretic injection of bicucculine hydrochloride, a GABA-A receptor antagonist and decreased responses after injection of GABA (Zhang, Wang, and Goldberg, 2007). Because LIP surround suppression can be maintained by a memory-guided saccade plan, it is likely to emerge from one or more "priority-map" brain areas active during the delay period of the memory-guided saccade task like LIP itself (Sereno and Amador, 2006) FEF, DLPFC, and SC. These areas also contain neurons whose activity is enhanced when a larger reward is expected following a saccade into the neuron's RF (Watanabe, 2007), in turn leading to enhanced suppression of neurons representing competing locations. The reward-cue signal that mediates the effects of motivation on surround suppression could emerge from a range of areas including the amgydala, striatum and the perirhinal, entorhinal, orbitofrontal and insular cortices (Salzman et al., 2005; Simmons et al., 2007).

2.53 Implications of LIP surround suppression for behavior

LIP represents a priority map whose peak can be used by the visual system for the allocation of visual attention (Bisley and Goldberg, 2003a) and the oculomotor system for the generation of saccades when saccades are appropriate (Ipata et al., 2006a). Network models of priority maps often posit that global inhibitory interactions enable the emergence of a peak of

activity on the priority map (Koch and Ullman, 1985; Itti and Koch, 2001) and are critical for the maintenance of stable, localized persistent activity that is resistant to perturbation from external distractors (Constantinidis and Wang, 2004). Mutually suppressive push-pull interactions in LIP have also been postulated to be critical for the programming of sequential saccades (Xing and Andersen, 2000).

Studies of perceptual decision making in LIP often model the decision process as a race to a threshold between competing alternatives (Gold and Shadlen, 2007). Our data supports models of perceptual decision making that incorporate mutual inhibition between competing choices (Usher and McClelland, 2001) and argues against models of the decision process as independent random walks towards a threshold. Specifically, our finding that surround suppression can strongly suppress visually-driven LIP responses suggests that surround suppression could explain the recently reported large reductions in LIP responses to stimulus onset in a four-choice task compared to a two-choice task (Churchland et al., 2008). Surround suppression of LIP responses also provides a mechanism for the baseline-resetting that is part of models for evidence accumulation towards a saccadic decision in LIP (Seung et al., 2000; Roitman and Shadlen, 2002; Churchland et al., 2008)). The reward-modulation of surround suppression immediately provides a possible mechanism for the global computations of normalized reward value that have been hypothesized to underlie saccadic choice decisions in LIP (Sugrue et al., 2004).

Converging physiological evidence indicates that the firing-rate of neurons in priority maps in FEF, LIP and SC are tightly linked to attentional allocation (Bisley and Goldberg, 2003b; Armstrong et al., 2009). Our findings provide a mechanism by which spatial locations can compete with each other for attentional priority: the higher firing-rates associated with LIP neurons representing a particular location (in this case, the saccade goal) lead to lower firing rates in neurons representing other competing locations. Consistent with the tight linkage between LIP activity and spatial attention, this mechanism correlates with a reduction of attentional allocation to the RF when the RF location competes with the saccade goal outside the RF for attentional priority.

It could be argued that attention is the *cause* of the reduced responses to the distractor in LIP in the presence of the saccade plan to a competing spatial location. This argument posits that the distractor response is lower in the presence of a saccade plan because the distractor is less likely to capture attention compared to the distractor in No-saccade control condition. However, attention is a psychophysical construct and cannot cause neural effects. Instead, it is the neural implementation of attention that must cause the measured effects in LIP, not attention itself. Therefore, this argument is identical to one discussed above where the suppressive effects measured in LIP reflect suppressive interactions in other areas that are then relayed to LIP. The surround suppression we measure in LIP, whether it is implemented in LIP or elsewhere, provides a mechanism that could underlie the ability of focused attention to modulate attentional capture by an abruptly appearing irrelevant stimulus in human subjects (Egeth and Yantis, 1997). In keeping with the broad extent of the suppressive surrounds we find in LIP, a human patient

with bilateral parietal lesions had difficulty filtering distractors even over large distances (Friedman-Hill et al., 2003). The increased suppression of distractor responses in LIP when a higher reward is cued provides a physiological basis for possible improvements in attentional focusing and distractor suppression as a function of the cognitive demands of the task.

Chapter 3: Surround suppression improves across trial variability in LIP.

3.1 Abstract

The receptive fields (RFs) of most macaque LIP neurons possess extensive suppressive surrounds (Falkner, Krishna and Goldberg, 2010). Neuronal responses to a distractor are substantially reduced when monkeys plan saccades to targets outside the excitatory RF in their suppressive "surround." Here, we show that saccades to the surround also induce systematic and strong variations in the across-trial variability of LIP neurons during the pre-distractor epoch, as quantified by the Fano factor. For saccade targets outside the RF that do not evoke excitatory responses, lower neuronal firing-rates are accompanied by lower Fano factors. This relationship between mean firing-rate and Fano factor becomes stronger as the distance of the saccade target from the RF center increases. Thus, the reduction of firing-rate of distractors by surround suppression in LIP is accompanied by reduced across-trial variability. Changes in across-trial variability can be modulated by the cognitive demands of the task. When the monkey's motivation is increased (by increasing reward expectation), the neural variability of both target and distractor responses is reduced, irrespective of the fact that this modulation causes opposite effects on the firing rates of the 2 responses (i.e. increasing the target response and decreasing the distractor response). We also find significant differences in across-trial variability when saccades are sorted by the accuracy of the saccadic endpoint. When saccades were prepared to remembered locations in a neuron's surround, the variability of the response in the pre-saccadic epoch was reduced if saccadic endpoints were more accurate. The effect of surround stimulation

on variability can potentially further improve the precision of the LIP priority map, working in concert with the improvement induced by the suppressive effects on mean firing-rate (Paradiso, 1988). These duel processes may have implications for saccadic and attentional selection mechanisms.

3.2 Introduction

Kicking a goal in soccer presents a problem for both the visual and motor systems. Not only does the kick itself require a high degree of athletic skill, the kicker must have an accurate representation of the spatial location of the goalposts in his brain in order to correctly target the kick. Distracting events in his environment, or a representation of the world that is not static could threaten his focus on the goal and the kick could end up wide of its intended target. On top of it all, the kicker must do this repeatedly in every game, throughout the duration of his career. In a situation where a repeated motor command depends on a high degree of spatial accuracy, even small amounts of variability in the representation of the intended goal could be the difference between a score and a zero. How then, does the kicker reduce the amount of variability in his internal representation of the world?

One of primary jobs of the visual system is to select relevant information and ignore unnecessary or distracting stimuli. In the visual system, areas in an occulomotor-attentional network (including the frontal eye fields, the lateral intraparietal area, and the superior colliculus) receive incoming sensory information and represent that information in spatially accurate coordinates. The monkey lateral intraparietal area (LIP) encodes the priority

of spatial locations and the activity of LIP neurons can predict the locus of attention (Bisley and Goldberg, 2003a, 2006) or the target of an upcoming saccade if a saccade is appropriate (Ipata et al., 2006a). Changes in the mean spike rate of LIP neurons can affect the relative salience of peaks on LIP's priority map and a "winning" spatial location can be determined on a moment-by-moment basis.

We have recently demonstrated that LIP neurons also have extensive spatially tuned suppressive surrounds, such that a planned saccade to a spatial location outside the neuron's excitatory receptive field can suppress both the spontaneous activity and the responses to visual stimuli appearing at the receptive field center (Falkner et al., 2010). These interactions can be modulated by cognitive variables such as reward expectation which links the representations of competing stimuli at distant locations by adjusting their firing rates in opposite directions.

In addition to changes in the mean activity, the precision of a neural representation can be improved by reducing the variability of its neuronal responses (Paradiso, 1988; Vogels, 1990), though the mechanism for reducing this variability is unclear. It is now well established that the onset of visual and non-visual stimuli can cause a cortex-wide (including area LIP) reduction in the amount of across trial variability as measured by the Fano factor, a ratio of the spike count variance divided by the spike count mean (Churchland et al., 2010). This reduction can take place even without a concurrent increase in the mean firing rate evoked by the stimulus in the receptive field. This is an important consideration since the Fano factor will decrease if the variance is dropping, or if the mean firing rate is rising and cannot disambiguate between these cases.

A reduction in the variability of the representation of a visual stimulus amounts to an increase in the signal-to-noise ratio of a particular pattern of spikes and could increase the behavioral sensitivity to a sensory stimulus (Scobey and Gabor, 1989; Zohary et al., 1994; Bair et al., 2001). Changes in the variability of the spontaneous rates in visual areas have been attributed to changes in the cortical state, rather than in changes in the stimulus itself (Arieli et al., 1996; Kenet et al., 2003) which suggests direct links between neural variability and behavior.

Several converging lines of evidence suggest that variability reduction in visual cortex may have important links to perception and saccadic behavior. In V4, a visual area known to be involved in attentional allocation (Moran and Desimone, 1985; Spitzer et al., 1988; Reynolds et al., 2000), a reduction of across-trial variability was associated with spatial attention (Mitchell et al., 2007, 2009) and correlated with saccade latency to a target presented in the RF of a V4 neuron (Steinmetz and Moore, 2010). The reduction of across trial variability has been proposed to represent a cortex-wide "stabilization" due to sensory input, though it is unclear how this would be implemented across brain areas or even within a single brain area.

Surround suppressive mechanisms, which link neurons with widely separated RFs could play a potential role in the reduction of variability and could result in an increase in the precision of signals that carry information about spatial priority. It is known that variability is reduced at the locus of the visual stimulus itself, even when that stimulus is not the preferred stimulus to drive the cell, but it is unclear how these effects are modulated in the spatial domain. Spatial locations that have a physiological link to the target location due to surround suppressive effects may be equally affected by mechanisms that reduce variability.

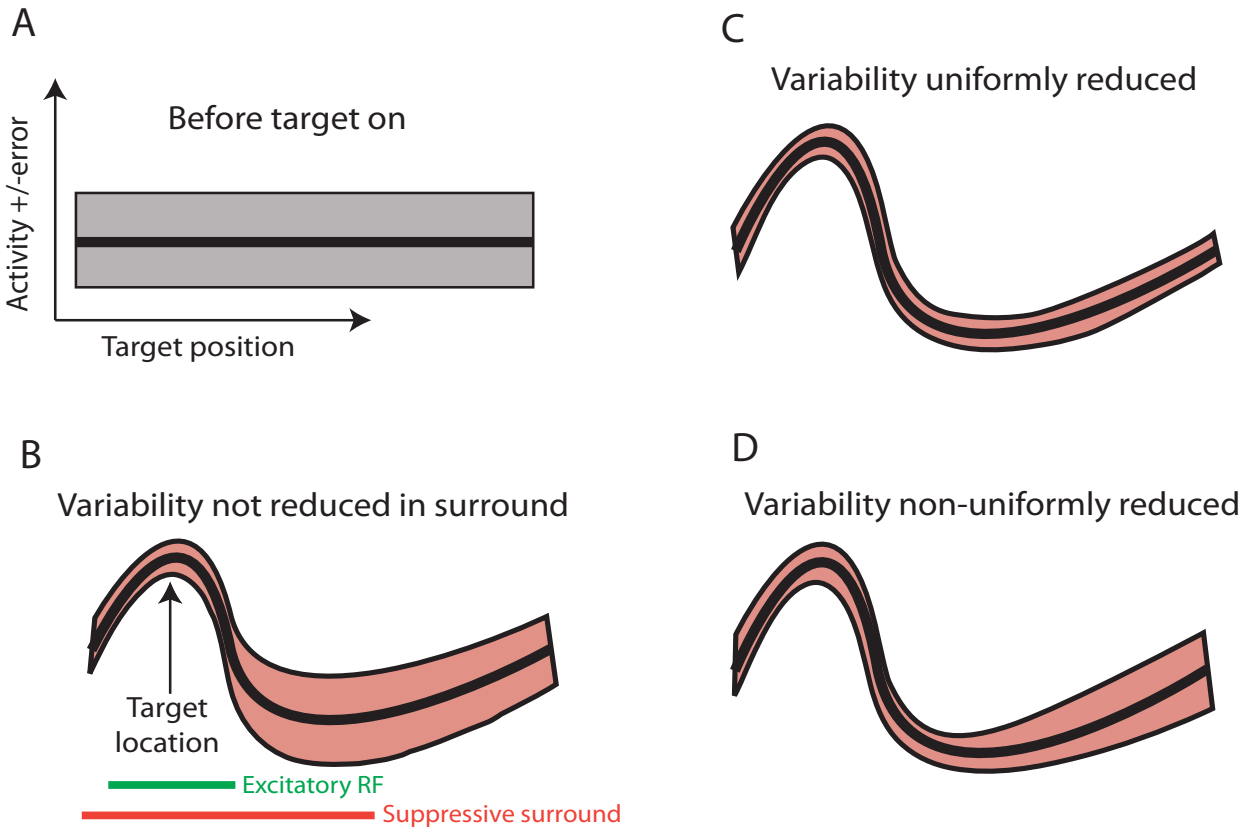

Figure 3.1 Across-trial variability predictions.
A-D) Schematic depicting changes in neural activity and variability as a function of target position. Prior to target onset, LIP has no changes in mean across space and a high amount of variability at each location. Black line represents mean activity and grey represent error bars around that mean (A). Target onset causes an increase in mean activity and decrease in variability at the location of the target and a decrease in mean in the surround (B-D). This could be associated with no change in variability in the surround (B), a uniform change in variability in the surround (C), or a change that is dependent on the distance from the target (D).

The effects of reducing neural variability can be conceptualized as the shrinking of an error bar around the mean response to repeated presentations of the same visual stimulus, for example, a saccade target (Figure 3.1). In this model, the onset of the saccade target is accompanied by strong suppressive surround responses that decrease the spontaneous activity at non-target locations. If the reduction of across trial variability is constrained only to the neurons encoding the location of the target, we should not see a change in across trial variability for neurons that encode spatial locations in the surround (Fig 3.1B). Alternatively, if variability

reduction is implemented by a non-spatial mechanism, we may see a uniform decrease in the Fano factor (a shrinking of the error bar around a mean response) irrespective of the location of the target, which would suggest that decreases in variability are a LIP map-wide phenomenon (Fig 3.1C). A third option is that we may observe a more complicated relationship between the spatial location of the target, the neural response, and the saccade target location (Fig 3.1D). This would strongly suggest the involvement of a mechanism that modulates LIP responses in a spatially dependent manner.

A further question is how LIP-wide changes in variability are related to the monkeys' behavior. The firing rates of distracting events at non-target spatial locations are correlated with the saccade latencies and error rates, how are changes in the variability related to behavioral differences in saccade latency and accuracy?

We explicitly tested the relationship between variability reduction and the spatial relationship of target and non-target locations by examining the across-trial variability of LIP neurons while varying the location of a saccade target with respect to a given spatial RF and having monkeys plan a delayed saccade to that target. We examined whether planning a saccade to a location outside the excitatory receptive field affects the variability of an LIP neuron encoding a non-target location, and whether this variability is correlated with the monkeys' saccadic behavior. We found that across trial variability is strongly modulated by the location of the target such that Fano factor is reduced when monkeys plan saccades to targets in the suppressive surround, the location where the spike rate is also the most reduced. The relationship between the spike rate and variability increases as the distance between the target and the RF center increases, suggesting that variability reduction is not uniform across spatial

locations. Surprisingly, the reduction in variability at non-target locations also correlates with several behaviors, including higher expected reward, decreased saccade latency, and increased saccade endpoint accuracy. The reduction in both mean firing rate and variability of neurons encoding the suppressive surround of a saccade target suggests the use of a duel strategy to improve the precision of LIP's spatial coding.

3.3 Materials and methods

Full methods for recording and surgical procedures are detailed in Falkner et al. (2010).

For detailed analysis of all tasks, see Methods chapter 2.

3.31 Neural variability analyses

All analyses were computed using Matlab (Natwick, MA). For the target into RF task, we calculated neural activity and across-trial variability in 100 ms bins stepped every 25 ms. Neural activity is shown either by the population average firing rate across each bin, or by the average spike count across each bin (number of spikes per 100 ms). Neural variability is calculated via the Fano factor, which is the spike count variance over the spike count mean calculated for each 100 ms bin independently. Significance tests across trials were done within trials by comparing spike rates and Fano factors in the spontaneous activity (100 ms prior to target onset) with spike counts and Fano factors at each bin independently with a paired t-test. Significance tests across trials were done using the non-parametric Wilcoxon signed-rank test, and were computed on appropriately paired epochs.

For the target-mapping task, we analyzed the variability by calculating the Fano factor (and spike count) independently for each spatial location as determined by target position on that trial. Measure of spike count and variability were subsequently averaged for target locations by the distance between the RF center and the target location (the "target-RF distance"). Across cells, the spike counts and Fano factors were grouped into bins according to the target-RF distance and significance was tested across bins using Wilcoxon signed rank test (for each bin separately). To ensure sufficient numbers of spikes for the population comparison, average spike count and Fano factor were extracted for the entire pre-distractor epoch (500ms prior to distractor onset). Comparisons between "near surround", ''far surround", and "in RF" bins were calculated across the population using a Wilcoxon signed rank test.

For the comparison of spike count to variability, spike count and Fano factor were again computed for each saccade target location across the entire pre-distractor epoch. The values for each cell were then placed into bins according to their spike count such that bins contained equal numbers of spatial locations. Bins then encoded spike rates with "high," "medium," and "low" spike counts. The corresponding Fano factors for those spatial locations were then averaged and plotted as a function of time. Significance comparisons between spike count determined bins were computed using a Wilcoxon signed rank test.

To determine the relationship between target-RF distance, spike count, and variability, we binned the values of spike counts and Fano factor by target-RF distance and regressed these values within each cell for each target-RF distance. We extracted the slopes of these regressions for each cell and averaged the slopes as a function of target-RF distance for each cell.

For the cued-reward task, we calculated spike counts and Fano factors for each cell at each reward condition (small reward vs. large reward expected). Spike counts and Fano factors were again calculated for each 100ms stepping each 25ms. To ensure significant number of spikes within the trials, significance tests were computed by taking the total number of spikes in the trial after target onset and compared using Wilcoxon signed rank test.

For analysis of memory-guided saccade behavior, trials were groups according to the median saccade latency so that they contained equal numbers of trials. For accuracy analysis, trials were considered accurate if their endpoint lay within 1.5 visual degrees of the location of the disappeared saccade target. Inaccurate saccades were correct saccades that were further than 1.5 degrees from target location. Since bins did not contain equal numbers of trials, significance between groups of accurate and inaccurate saccades was validated by recalculating spike counts and spike rates using resampling statistics (without replacement) so that each bin contained the same number of trials. These analyses did not qualitatively change our analyses.

3.4 Results

Monkeys performed several variants of the standard delayed saccade paradigm (see methods chapter 2). During the most basic variation of the task, monkeys were required to maintain fixation on a central red cue for a brief period of time, after which a saccade target would appear. After a delay of 1050 ms the fixation point disappeared and the monkey had to make a saccade to the target. During most trials, a distractor would be briefly flashed for <50ms at a time 500ms following the onset of the saccade target. The task timing is constant across task

variants, though the spatial locations of the target and distractor were modified between variations. We present here results separately from each task variant. The variable number of cells in each variant represents not a sub-selection of the data, but the fact that is some cases we were unable to hold each cell through all task variations.

3.41 Stimulus onset causes a drop in variability.

In the simple delayed saccade task (Figure 3.2A) the appearance of the target at the receptive field center evoked a statistically significant ($p < 0.05$ by Wilcoxon for each 100 ms bin after the stimulus onset as compared to the 100 ms bin before stimulus onset, n= 40 cells) visual response which continued until the monkey made the saccade (Figure 3.2B). We used these spike counts to compute the Fano factor in each bin and plotted it as a function of time aligned to the target onset and the saccade. In accordance with previous findings (Churchland et al., 2010), the onset of the target was also associated with a sharp decrease in the amount of variability across trials (Figure 3.2C). The Fano factor prior to the target onset was relatively high (2.40 ± 0.16 SEM), and was significantly quenched in each subsequent non-overlapping 100ms time bin following target onset ($p<0.05$ Wilcoxon signed-rank test, tested independently for each bin, n=40 cells). In the 100ms bin prior to the saccade, the Fano factor had dropped to 1.96 ± 0.18 SEM. Though we cannot rule out an effect of rising mean spike rate on the decrease in Fano factor, if this effect were due purely to changes in mean, the ratio of the spike rate over the course of the trial (spike counts in pre-saccadic epoch / spike count in pre-target epoch) should be equal to the ratio of the raw variance between the same 2 epochs but this is not the

case (Figure 3.2D). Instead, the increase in raw variance is less than would be expected if variance scaled directly with activity.

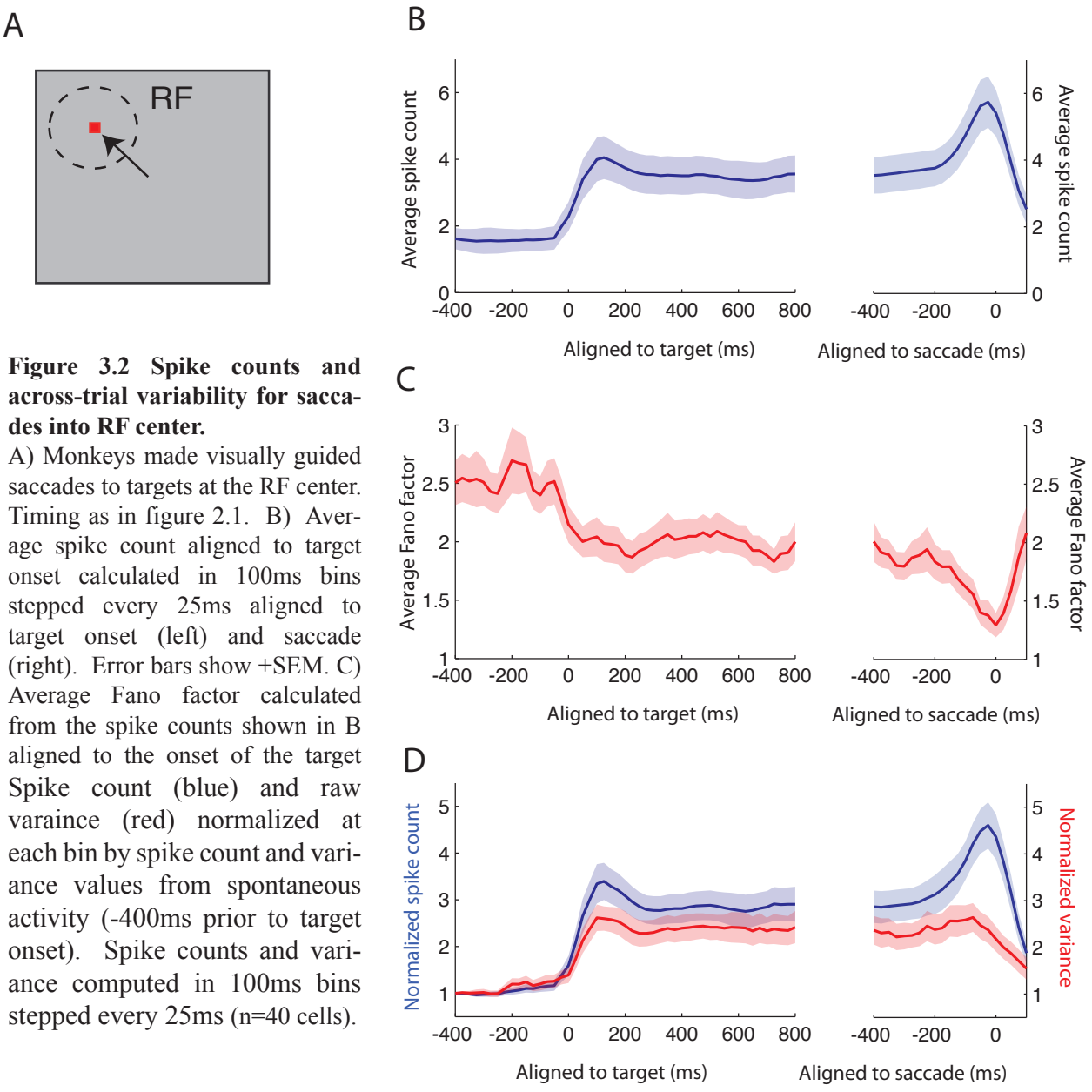

Figure 3.2 Spike counts and across-trial variability for saccades into RF center.
A) Monkeys made visually guided saccades to targets at the RF center. Timing as in figure 2.1. B) Average spike count aligned to target onset calculated in 100ms bins stepped every 25ms aligned to target onset (left) and saccade (right). Error bars show +SEM. C) Average Fano factor calculated from the spike counts shown in B aligned to the onset of the target Spike count (blue) and raw varaince (red) normalized at each bin by spike count and variance values from spontaneous activity (-400ms prior to target onset). Spike counts and variance computed in 100ms bins stepped every 25ms (n=40 cells).

3.42 Across trial variability is modulated by target location.

Previous studies have shown that the onset of a target in the RF causes a decrease in across trial variability when the target appears in the RF center, but is unclear whether this decrease in

variability extends to spatial locations beyond the excitatory receptive field in LIP. To test this we had the monkey make visually guided saccades to targets with randomly chosen locations (80 possible locations, on a grid with 5 degree spacing, see Figure 2.1C). In some cases, targets appeared in the excitatory receptive field, evoking an onset response, and in others, the target appeared outside the receptive field, evoking no excitatory response. When the target appeared in the neuron's suppressive surround, its onset was associated with a decrease in both "baseline" (pre-distractor) and distractor responses (Falkner et al., 2010). We probed how changes in the target location affected the across trial variability of these responses at non-target locations. As monkeys planned delayed saccades to various locations in the visual field, as expected, we observed a sharp decrease in Fano factor following the onset of the distractor (Figure 3.3B). Since this decrease could be caused by a rise in spike regularity generated primarily by refractoriness after fast volleys of spikes (Maimon and Assad, 2009), we have chosen to focus our analysis in the spatial domain on the pre-distractor period, where the effects can be attributed with the onset of the target (not the distractor).

We found systematic changes in the Fano factor depending upon the distance of the saccade target from the RF center and the mean firing-rate of the neuron. Although the saccade target caused the greatest decrease in Fano factor when it evoked an excitatory response (Figures 3.3B,C), the Fano factor in the pre-distractor epoch (470 ms before to 30 ms after distractor appearance) systematically increased with the distance of the saccade target from the RF center even when there was no systematic effect of the saccade target on the spike count (Figure 3.3C; p-value for all 3 pairwise comparisons of distances greater than 20 degrees > 0.28). For all target-RF distances, distractor onset at the RF center led to a marked reduction in

variability to a value close to 1, which is the expected variability for a Poisson process with no across-trial rate variability. This reduction in variability following distractor onset was transient and considerably reduced by the time of the saccade go-cue.

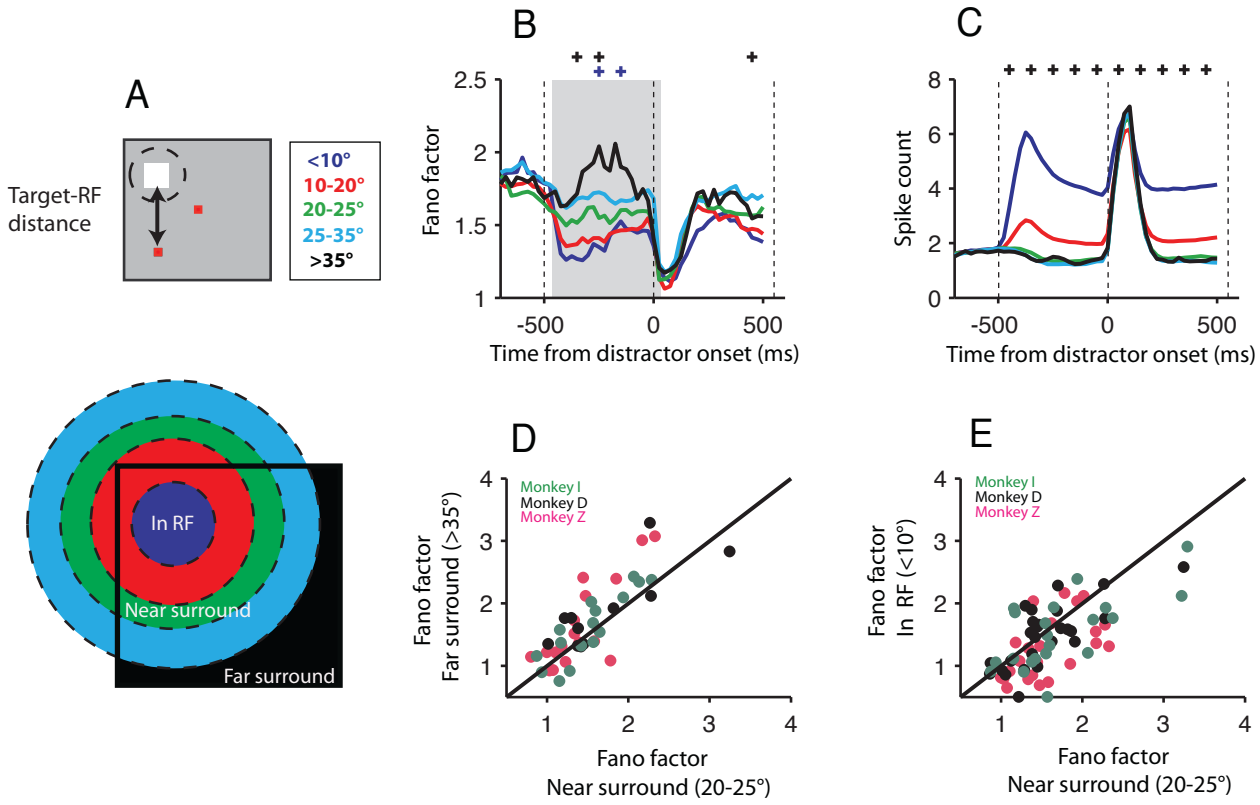

Figure 3.3 Fano factor increases with saccade target-RF distance.
A) Monkeys were required to make saccades to variable target locations and data was binned according to the visual distance between the variable saccade target location and the location of the RF center (top). Locations were sub-grouped into areas in the receptive field (inRF), in the "near" surround and the "far" surround (bottom). Colors correspond to plotted locations. B) Population average PSTH of the Fano factor (calculated in 100 ms bins, stepping every 25 ms) shows higher variability in the epoch between target and distractor appearance for higher target-RF distances (indicated in box to the right). Crosses mark centers of non-overlapping 100 ms time bins with a significant difference of the green PSTH compared to blue (blue cross) and black PSTHs (black cross) respectively (paired t-test, $p<0.05$, n=72 neurons for blue cross and 45 for black). C) Population average PSTHs of the corresponding mean spike-count for the PSTHs plotted in B. Black crosses as in B; none of the blue vs. green comparisons reached significance. D) Scatter plot of each neuron's Fano factor (5 non-overlapping 100ms bins, -470 to 30 ms relative to distractor onset, grey bar in B) during saccades to the near surround (abscissa) and the far surround (ordinate). Paired t-test: p=0.0093, n=45 neurons measured with targets in the far surround. E) Scatter plot of each neuron's Fano factor (same epoch as D) during saccades to the near surround (abscissa) and to the RF (ordinate). Paired t-test: p=0.0007, n=72 neurons.

Across the population in the pre-distractor epoch, the Fano factor for targets 20 to 25 degrees from the RF center (the "near" surround) was significantly lower than that for targets greater than 35 degrees from the RF center (the "far" surround; Figure 3.3D, mean decrease ± SEM = 0.22 ± 0.08 spikes/second, p=0.0093, n=45 neurons), even though the spike counts in these epochs were not significantly different. When the saccade goal was within 10 degrees of the RF center, the Fano factor was even lower than that in the near surround (Figure 3.3E, mean decrease ± SEM = 0.18 ± 0.05 spikes/second, p=0.0007, n=72 neurons).

3.43 The relationship of spike count and Fano factor

We next explored the relationship of the Fano factor to the mean spike count. If decreases in Fano factor are purely driven by increasing in the mean spike count of the neuon across the pre-distractor epoch, then the highest mean spike counts should be associated with the lowest Fano factors. Instead we found the opposite relationship was true: Fano factors affected by stimulation of the surround decreased with mean spike-count. We examined this by isolating locations with target-RF distances greater than 25 degrees and then dividing them equally into 3 classes based on their rank-ordered mean spike-count within the pre-distractor epoch (see methods). Instead, we found the opposite relationship was true. Within this epoch, locations with the lowest firing-rates (Figure 3.4B) were associated with the lowest across-trial variability (Figure 3.4A), and locations with the highest firing-rates with the highest across-trial variability. The average variability in the low-firing rate class was significantly lower than that in the middle-firing rate class (Figure 3.4C; mean decrease ± SEM = 0.240 ± 0.044, p<0.0001, n=72

neurons), which in turn was significantly lower than that in the high-firing rate class (Figure 3.4D; mean decrease ± SEM = 0.307 ± 0.068, p<0.0001, n=72 neurons).

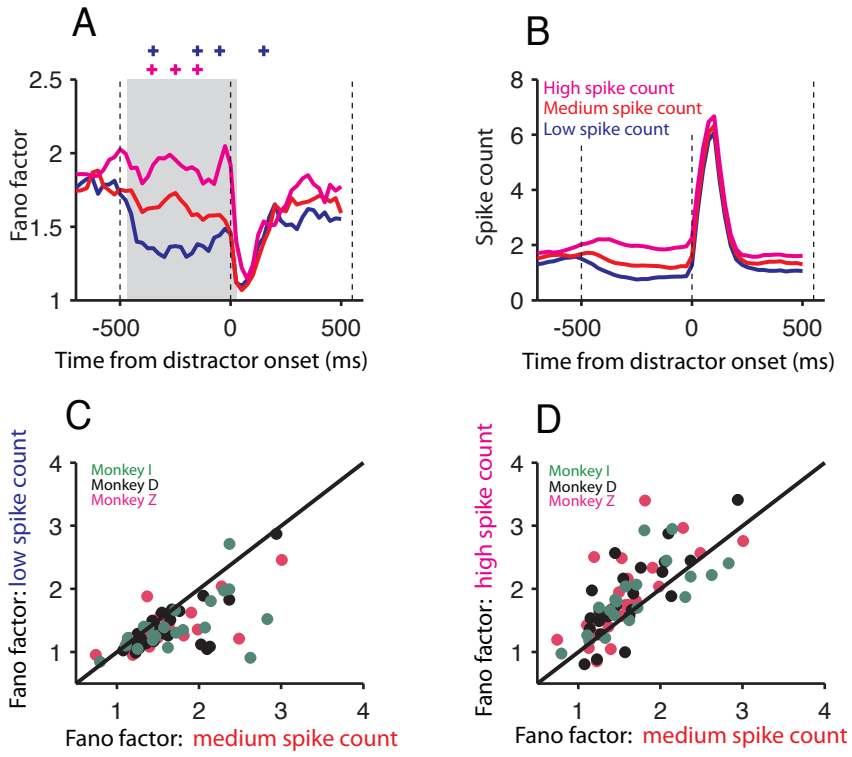

Figure 3.4. LIP neuronal Fano Factor increases with mean spike-count. A) Population average PSTH of the Fano factor (100 ms bins, stepping every 25 ms) shows higher variability in the epoch between target and distractor appearance for higher mean spike-counts. Target locations greater than 25 degrees from the RF center were rank-ordered and then split into three equal classes for each neuron prior to averaging. Lowest-third of spike-counts shown in blue, middle-third in red and highest-third in magenta PSTH. Colored crosses mark centers of non-overlapping 100 ms time bins with a significant difference for the corresponding PSTH compared to the red PSTH (paired t-test, p<0.05, n=72 neurons). B) Population average PSTHs of the corresponding mean spike-count for the PSTHs plotted in A. C) Scatter plot of each neuron's Fano factor (5 non-overlapping 100ms bins, -470 to 30 ms relative to distractor onset, grey bar in A) for saccades corresponding to the middle-third of spike-counts (abscissa) and lowest third of spike-counts (ordinate). Paired t-test: p<0.0001, n=72 neurons. D) Scatter plot of each neuron's Fano factor (same epoch as C) for saccades corresponding to the middle-third of spike-counts (abscissa) and highest-third of spike-counts (ordinate). Paired t-test: p<0.0001, n=72 neurons.

To explore the joint effect of target-RF distance and mean spike-count, we regressed the Fano factor computed for each saccade target location against the mean spike-count and the target-RF distance for that location (Figure 3.5). Across the population, the slopes relating variability to the mean spike-count (mean slope ± SEM = 0.20 ± 0.05, $p < 0.0001$, n=72 neurons) and to the target-RF distance (mean slope ± SEM = 0.018 ± 0.003, $p < 0.0001$, n=72 neurons) were both significantly greater than zero. To examine whether the spike-count vs. variability relationship varied with distance from the RF center, we repeated the multiple regression analysis for 10 degree target-RF distance windows centered 5 to 35 degrees from the RF center. The slope relating spike-count to variability systematically increased at higher target-RF distances (ANOVA, $F(6,466)=7.86$, $p<0.0001$). No such relationship was found for the slope relating target-RF distance to variability (ANOVA, $F(6,466)=0.82$, $p=0.5578$). Thus, on average, variability increases systematically with mean spike-count in LIP neurons and this effect is much stronger in the surround. The reduction of firing-rate by surround suppression in LIP is accompanied by reduced across-trial variability and potentially improved LIP map precision.

3.44 Across trial variability is modulated by the cognitive demands of the task.

The firing rates of LIP neurons are modulated by expected reward (Platt and Glimcher, 1999; Sugrue et al., 2004). Previously we have reported that the response to a distracting stimulus is oppositely modulated by increasing expected reward such that trials where the monkey made saccades to high reward targets are associated with an increased response to the target and a simultaneously decreased response to the distractor. However is it is unclear

whether across trial variability will also be modulated by changes in expected reward. To test this we required the monkeys to make visually guided saccades to targets appearing in the RF center or in a single location in the suppressive surround (for details on location selection see Falkner et al. 2010). Trials sorted by location were performed in blocks and the color of the saccade target instructed the monkey to expect a small reward or a large reward on that trial (Fig 3.6A).

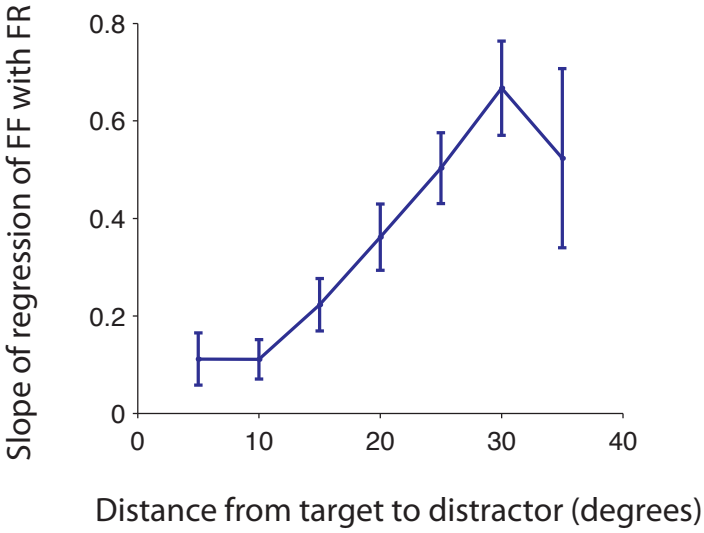

Figure 3.5 Results of regressing the Fano factor upon spike count and target RF distance. Computed for overlapping 10 degree target RF distance windows, centered at 5 degree intervals from 5 to 30 degrees away from the RF center. A final window included only locations greater than 35 degrees from the RF center. The slope relating mean spike count to the Fano factor increases with target-RF distance. Saccade target-RF distance on abscissa and the slope relating mean spike count to Fano factor on the ordinate. Error bars represent SEM. ANOVA, $F(6,466)=7.86$, $p<0.0001$. In individual neurons, regressing the slope relating Fano factor to spike count (in different target-RF distance windows) upon the target-RF distance and the mean spike count within that window yielded a significant effect for target-RF distance (mean slope $\pm$SEM$=0.04 \pm 0.008$, $p<0.0001$, $n=72$), but not for mean spike count.

As previously published, planning a saccade to a high reward target at the center of the response field evoked a greater visual response than the response to a low reward target, and planning a saccade to a high reward target located in the suppressive surround evoked more suppression than planning a saccade to a low reward target. We next examined the associated variability for these reward conditions by calculating the Fano factor for high and low reward trials.

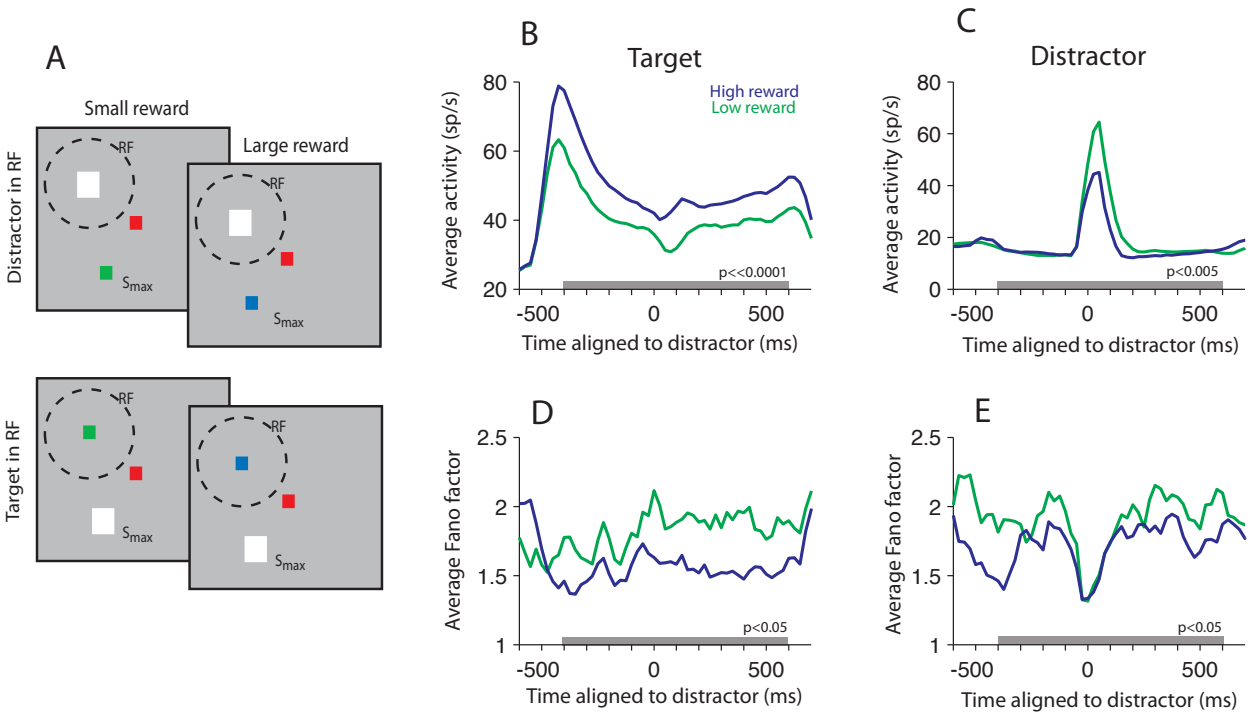

Figure 3.6 Increased reward expectation decreases across trial variability.
A) The monkey made saccades to targets in the RF or to targets in the suppressive surround. On each trial, the color of the saccade target indicated to the monkey to expect a small reward or a large reward. B) Average neural activity when the target was in the RF plotted in 100ms bins stepped every 25ms for trials where the target signaled a small reward (green) compared to trials where the target color signaled a large reward (blue). Neural activity was significantly larger for large reward trials ($p<<0.0001$, Wilcoxon signed-rank test, -400 to 500ms around distractor onset. n=38). C) Average neural activity when the target was in the surround and distractor was in the RF. Conventions as above. Neural activity was significantly reduced for large reward trials ($p<0.005$, Wilcoxon signed rank test, n=46). D) Fano factor for associated neural activity shown in B. Conventions as above. Variability was significantly reduced for large reward trials ($p<0.05$, Wilcoxon signed-rank test). E) Fano factor for associated neural activity shown in C. Conventions as above. ($p<0.05$, Wilcoxon signed-rank test).

Despite the fact that in one case (saccade to RF) average spike count increases, and in the other (saccade to surround) average spike count decreases across the trial, we see concurrent drops in the across trial variability at both the target and distractor location when he expects a large reward relative to when he expects a small reward. This effect is significant in a bin taken across the whole trial in each case (Figure 3.6B,D; $p<0.05$, Wilcoxon signed-rank test, n=38 for saccade to target in RF, n=46 for saccade to target in surround). This indicates that an increase in

reward expectation causes a drop in Fano factor not only at the target location, but at across distant locations on LIP's map (e.g. within the suppressive surround). Importantly, the difference in Fano factor between small reward trials and large reward trials is significant ($p=0.002$, Wilcoxon signed-rank test) in the bin prior to the distractor onset (-500 to 0ms before distractor), which indicates that is it the presence of the high reward target outside the RF, not the distractor response in the RF that is associated with the drop in variability.

3.45 Decreased across trial variability at non-saccade endpoint locations is associated with improved saccade accuracy.

If decreases in variability improve the precision of the representation of visual stimuli on LIP's map, a highly variable neural representation might be detrimental to the speed and accuracy of an intended saccade. Since visually guided saccades have more stereotyped saccade latencies and less scatter in endpoint, we used a standard memory-guided delayed saccade task to produce saccades with a broader scatter of both endpoints and latencies. In this task the target flashed for < 50 ms, and when the fixation point disappeared the monkey had to make his saccades to the spatial location of the vanished stimulus. The distractor appeared for 50 ms 500 ms after fixation began, just as in the visually-guided saccade task described above. We compared the responses in this task to those fixation control trials in which no saccade target appeared and the monkeys had to ignore the distractor and continue to fixate for the duration of the trial.

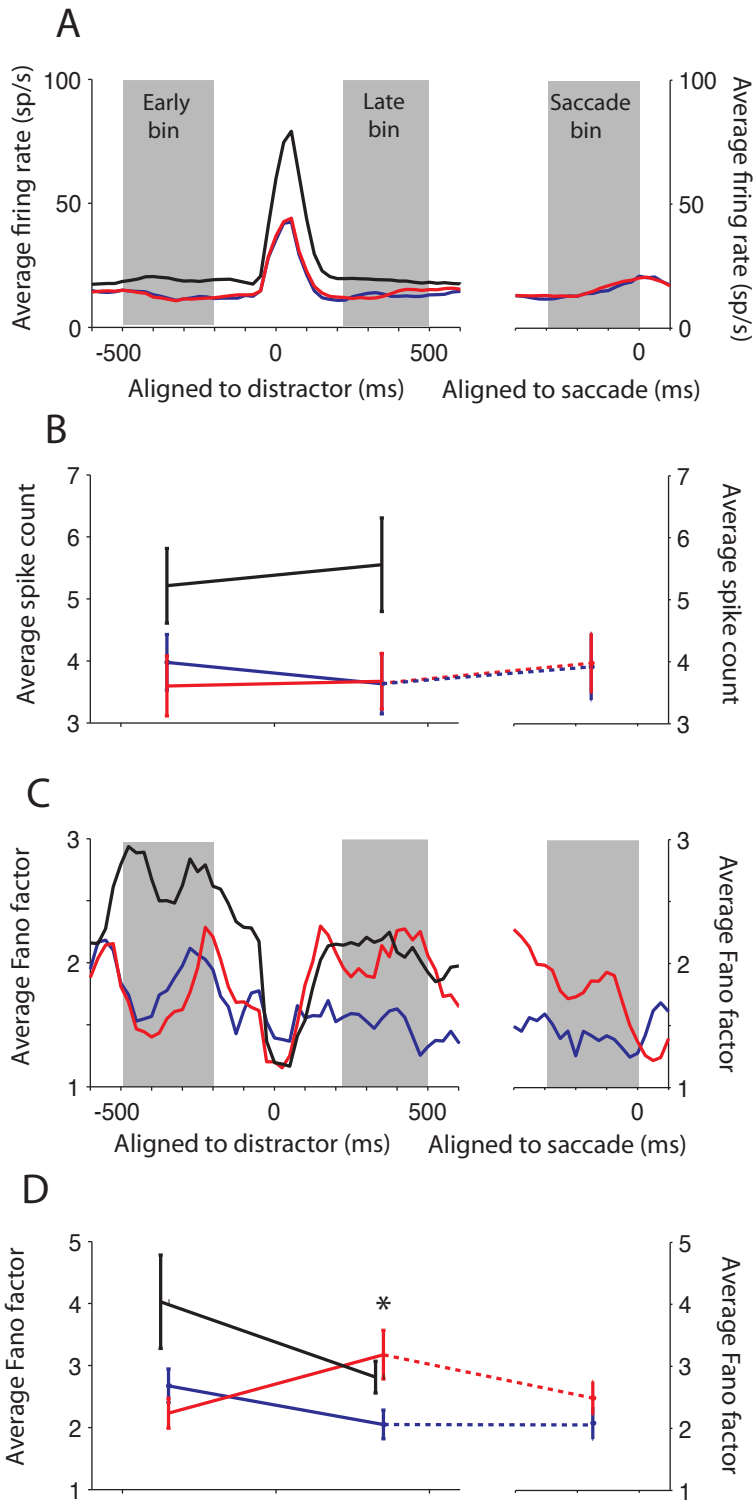

Figure 3.7 Decreased variability is associated with increased saccadic accuracy.
A) Average neural activity for the trials in which monkeys performed a memory guided saccade to a target in the suppressive surround split by saccade endpoint accuracy. Shown are accurate saccades (red), inaccurate saccades (blue), and responses to the no-target control (black). Activity is shown aligned to distractor onset (left panel) and saccade (right). Block control trials are not shown aligned to saccade since there are no saccades in these trials. B) Average Fano factor for trials show in A. C) Comparison of spike counts between early (300ms after target on), late (300ms prior to go-cue), and saccade (300ms prior to saccade) bins from the neural activity shown in A. Error bars shown are +SEM. No statistical differences were found between these epochs (p=0.12, accurate saccades, p=0.71, inaccurate saccades, p=0.16, no-target control trials, Wilcoxon signed-rank test, n=54) or between accurate and inaccurate saccades (p=. D) Comparison of associated Fano factors between late and early bins from the neural activity shown in C. Error bars shown are +SEM. Differences between accurate and inaccurate saccades are only significant in the late bin (p=0.06, accurate vs. inaccurate, early bin; p=0.0015, accurate vs. inaccurate, late bin, n=54).

If neural variability in the LIP map is related to the targeting accuracy of the saccade, we might expect to see a relationship between the Fano factor and the endpoint of the

saccade, even at locations that do not encode the remembered location of the target. To determine the relationship between neural variability at a non-target location and saccadic accuracy, monkeys made memory-guided saccades to a single location in the suppressive surround of each neuron. For each session of memory-guided saccade trials we first divided all correct trials based on the accuracy of the saccadic endpoint. We determined saccadic accuracy by an absolute measure of the error of the endpoint. Since saccades were not counted as "correct" unless they fell within a 5x5 degree window of the remembered target location, this placed an upper bound on this distribution of endpoint errors. Since distributions of endpoint depended critically on the distance of the saccade target from the fixation point, we adopted an absolute cutoff for "accurate" saccades. Correct saccades were considered "accurate" if their endpoints fell less than 1.5 degrees away from the location of the vanished stimulus. Saccades were considered "inaccurate" if they were correct, yet whose endpoints were greater than 1.5 degrees from the stimulus location.

We plotted the mean spike count and Fano factor for both accurate (blue) and inaccurate (red) saccades aligned to the distractor onset and the saccade. We also show the response to the distractor in those cells when monkeys planned no saccade (the "no-saccade control") and these responses are absent in the saccade-aligned panel since there was no eye movement in these trials.

We calculated the average spike count and Fano factor in 3 separate epochs during the trial: the early bin (300ms after target onset), the late bin (300ms prior to saccade go cue), and the saccade bin (300ms prior to eye movement) and plotted the average across neurons for each

epoch (Figure 3.7). As expected, we saw a suppression of the spike count in the late and early bins relative to the no-saccade control, since in these trials, a saccade target appeared in the suppressive surround of the neurons ($p=0.002$ for no-saccade control vs. accurate saccade, $p=0.0002$ for no-saccade control vs. inaccurate saccades, early bin, $p<<0.0001$ for both comparisons, late bin, Wilcoxon signed rank test). However there was no difference in the neural activity associated with the accurate and inaccurate saccades in either the early or the late bin ($p=0.14$ for early bin, $p=0.88$, late bin).

In contrast, the across-trial variability as measured by the Fano factor showed marked differences between the early and late bins. Across-trial variability was markedly reduced in both saccade conditions relative to the no-saccade control in the early bin, presumably due to the presence of the saccade target ($p<0.05$ for accurate, $p<<0.005$ for inaccurate) and variability between the accurate and inaccurate saccades was only slightly different ($p=0.06$, early bin, Wilcoxon signed rank test). Interestingly, in the period prior to the go-cue, the variability between the accurate and inaccurate saccade trials changed markedly, with the inaccurate saccade trials having significantly more across-trial variability ($p<0.0005$, late bin), a difference that occurred without a concurrent difference in spike count in this same epoch. This difference in variability disappeared prior to the saccade itself ($p=0.45$, inaccurate vs. accurate saccade Fano factor, saccade bin, Wilcoxon signed rank test), suggesting that the behavioral effects of increased variability are restricted to the time of the go-cue.

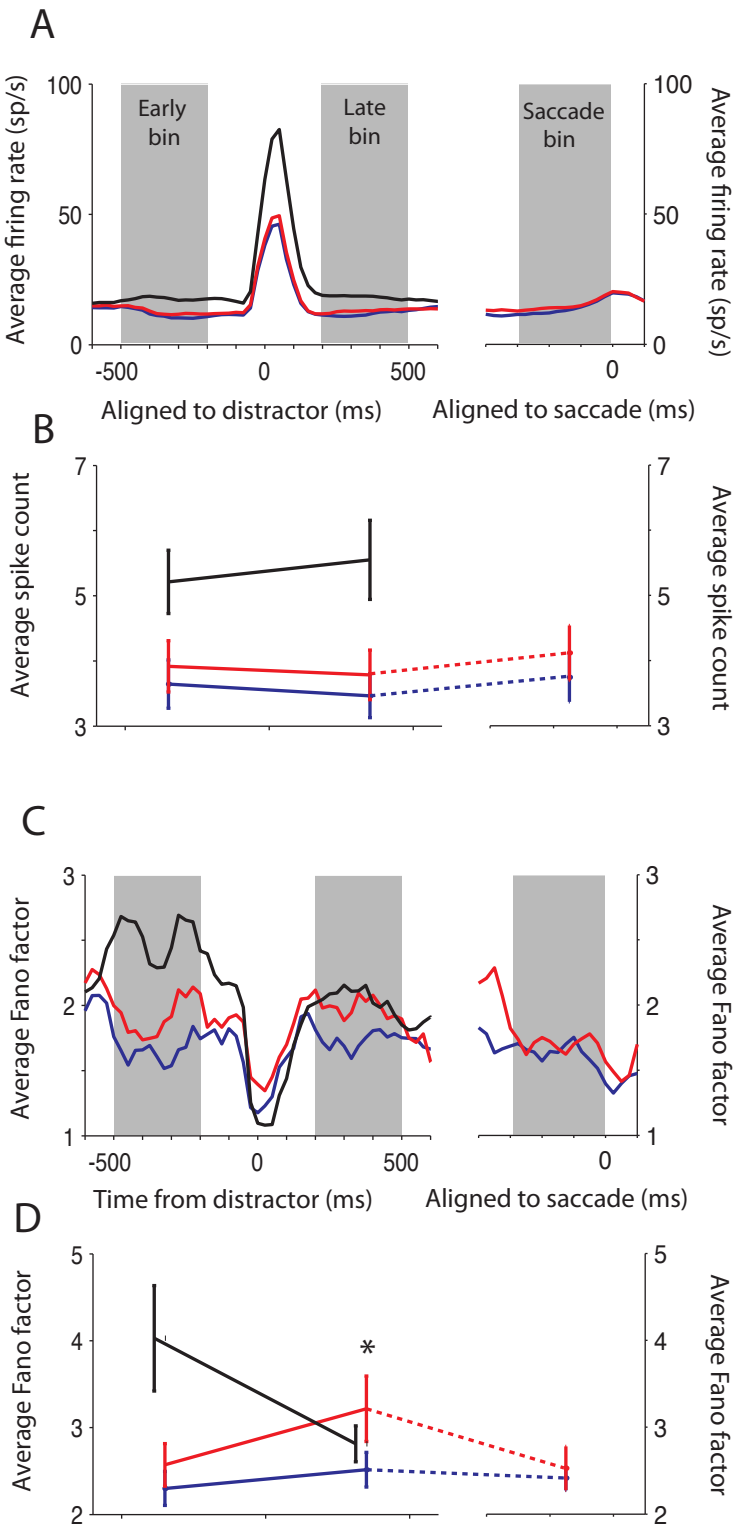

Figure 3.8. Decreased variability is associated with reduced saccadic latency.

A) Average neural activity for the trials in which monkeys performed a memory guided saccade to a target in the suppressive surround split by saccade saccade latency. Shown are fast saccades (red), slow saccades (blue), and responses to the no-target control (black). Plotting conventions as in figure 3.7. B) Average Fano factor for trials show in A. C) Comparison of spike counts between late and early bins from the neural activity shown in A. Error bars shown are +SEM. No statistical differences were found between these epochs (p=0.42, fast saccades, p=0.35, slow saccades, Wilcoxon signed-rank test, n=54) D) Comparison of associated Fano factors between late and early bins from the neural activity shown in C. Error bars shown are +SEM. Differences between fast and slow saccades are only significant in the late bin (p=0.33, fast vs. slow, early bin; p=0.044, fast vs. slow, late bin, n=54).

3.45 Decreased across trial variability at non-saccade endpoint locations is associated with long saccade latencies.

The Fano factor also predicted saccade latency. We divided the data from each cell into two equal populations, above and below the median saccade latency for all correct trials. The average spike counts were not significantly different between saccade trials where latencies were short compared to saccade trials where latencies were long at any epoch (Figure 3.8A,C see figure for corresponding p-values). In contrast, significant differences between the Fano factor during the late bin prior to the go-cue ($p = 0.04$, Wilcoxon signed rank test, n=54 neurons) but not in the early bin after the onset of the target ($p = 0.34$, $n = 54$ neurons) or in the presaccadic epoch ($p=0.73$). These results indicate that reduced variability in the pre-saccadic epoch even at spatial locations that do not represent the target location, and that this variability is associated with both shorter latency saccades and more accurate saccadic endpoints without corresponding changes in the spike count of the neurons.

3.5 Discussion

Lower neuronal variability can improve the precision of LIP's map representation (Paradiso, 1988) and a reduction in variability following stimulus onset at the RF center has been recently reported from multiple cortical areas (Mitchell et al., 2009; Churchland et al., 2010; Steinmetz and Moore, 2010). Our data show that LIP neuronal variability drops systematically both when the neuronal firing-rate decreases and when the saccade target gets closer to the RF, and the effect of firing-rate on variability is greater in the surround. The reduced firing-rates

produced by surround stimulation are thus also accompanied by a reduction in across-trial variability. This decrease could result from a true reduction in the input variability across trials to these neurons when a saccade is planned to the surround.

It is important to note that though firing-rate is known to influence response variability via the refractory period (Mitchell et al., 2009) this effect leads to an *increase* in response variability for lower firing-rates, the opposite of the effect we describe. This result can emerge from a simple Poisson process model whose firing-rate varies across trials (a Cox process, (Lansky and Vaillant, 2000): if the across-trial variance of the firing-rate remains constant, then decreasing the mean firing-rate will increase the Fano factor. Therefore the relationship that we observe between mean spike-count and variability is not the result of these previously known relationships. Finally, the reduction in variability when saccade target-RF distance increases, even when the mean firing-rate is constant, indicates that neuronal firing can be affected by saccade plans to the surround even when mean firing-rate is not. The sharp drop in Fano factor following the onset of the distractor in the RF center may be the result of a sharp rise in mean firing rate, or result from that fact that at high firing rates, the mean interspike interval approaches the short timescale of a refractory period, such that the variability appears to become more regular (Softky and Koch, 1993).

We suggest that decreasing the across trial variability represents a second mechanism that acts, along with decreasing mean spiking through surround suppression, by which neurons in LIP can reliably improve discrimination between signals related to spatial accuracy. LIP neurons are statistically noisy relative to other parietal regions such as area 5 (though more regular that

areas MT/MST;(Maimon and Assad, 2009) and this extra jitter could mean the difference between a target location encoded in one region of space, and one that is slightly mislocalized. Signals are least variable when target stimuli are in the RF center and most variable when they are furthest from the RF. A spatially tuned surround suppressive mechanism that stretches beyond the bounds of the "classic" excitatory RF could mediate such an effect, reducing variability both in the RF and at intermediate distances outside the excitatory RF bound. Such an idea is consistent with models of cortical normalization that include both a "stimulus drive" and a "suppressive drive" that act simultaneously on neural responses although these models do not explicitly predict any changes in the neural variability after normalization (Reynolds and Heeger, 2009).

Surround suppression in other visual areas has been shown to act via shunting inhibition, a mechanism that reduces neural activity by clamping down on noisy inputs to a brain area (Ayaz and Chance, 2009). Along with reducing the mean neural response, such a mechanism could also do double duty, decreasing the across-trial variability by increasing the threshold necessary to evoke spikes in those same neurons. In several visual areas including V1 and MT, neural variability has been shown to increase with age, an effect that has been attributed to synaptic degradation over time (Yang et al., 2009).

The degree of variability reduction also correlates with several cognitive and behavioral variables, including increased reward expectation, faster saccade latencies, and increased saccade endpoint accuracy. It is important to note that with both benefits in saccadic behavior, the benefit arises not with the reduction of the variability over time (in the case of the short latency and

more accurate saccades), but with the increase in across-trial variability of the slower, less accurate saccades. This suggests that the state of the neural variability at the time of the go-cue, not the epoch just prior to the saccade itself, is associated with the speed and accuracy of the eye movement. This is consistent with results from motor and pre-motor cortices, in which the variability of neurons associated with reach have been found to converge on a specific mean with maximally reduced variability (the "optimal subspace") prior to movement initiation (Churchland et al., 2006a; Churchland et al., 2006b). Though the dynamics of saccade initiation differ from reaching, the increased saccade latencies for neurons with increased variability may indicate that variability even at non-target locations must reach a particular subspace before an eye movement can be initiated.

Additionally, although it has been demonstrated that variability is reduced by the presence of the stimulus both in the cortex of anesthetized as well as awake, we have demonstrated that cognitive and behavioral factors can influence variability, a result that is unlikely to arise from external factors alone. It is likely that both stimulus onset and "top-down" factors tap into the same mechanism, and recent theoretical work has suggested that large networks with recurrent connectivity have reduced variability with increased input, regardless of the source of that input (Rajan et al., 2010).

Taken together, these data demand a refinement of the hypothesis that reduced neural variability represents a cortex-wide phenomenon. Instead, there is a tight relationship between the amount of variability reduction and the spike rate at those locations such that locations are not uniformly affected by these changes. Many areas shown to have this property, including V1, MT, and V4, have extensive suppressive surround mechanisms that have been shown to

modulate activity across spatial locations (Angelucci and Bressloff, 2006; Alitto and Usrey, 2008; Ozeki et al., 2009; Sundberg et al., 2009). Further study needs to be done to establish the links between surround suppression and the spatial extent of variability reduction in these areas.

Chapter 4: Changes in correlation reflect competition between visual stimuli in LIP.

4.1 Abstract

Activity in the monkey lateral intraparietal area (LIP) encodes the relative salience of locations in visual space. When multiple stimuli compete for attentional priority, a single winner must emerge on this map to be used as the upcoming saccade target or the locus of visual attention, though it is unclear how the "winning" process is functionally implemented or whether cognitive demands can influence the competition. One model of competition suggests that peaks of activity in LIP could rise and fall independently and a winner could emerge as one peak hits a designated threshold. Alternatively, activity between peaks could be non-independent, exhibiting correlations across trials. These correlations could be static across the duration of the trial or fluctuate with the changing demands of the task and behavioral state. We tested this by recording from LIP during a free choice task where monkeys were required to chose between 2 targets with a saccade under varying reward probability. We recorded from the locations of both targets simultaneously using 2 independent electrodes and looked at correlated noise during the spontaneous activity and during the pre-saccadic "decision" period for a given saccadic choice. We found that even from cells with separated receptive fields that do not share stimulus-evoked activity, activity from competing spatial locations is not independent. Neural noise was positively correlated before the saccade targets appeared and decreased in correlation during the decision, with a subpopulation of cells exhibiting negative correlations prior to the saccade. Since

correlated noise can indicate the presence of either a common input or mutual connectivity, changes in correlation suggest a change in functional connectivity between neurons during competitive visual decisions. A measure of the monkey's reward history was negatively correlated with saccade latency for a given choice. Noise correlations between neurons but not the firing rates of individual neurons encoded the monkey's history of rewards, indicating that more trial-to-trial variability may be shared during periods of indecision.

4.2 Introduction

In our neural representation of the physical world, spatial locations compete with each other for saccadic and attentional priority. Choices must be made with our eyes on a moment-to-moment basis about which spatial locations contain the most information and which locations might be associated with likely rewards. Since saccadic eye movements are ballistic, all or none events, a single winner must emerge every time an eye movement is to be made, such that competition between possible saccadic endpoint locations must be resolved prior to the eye movement.

Several areas of the brain including the macaque lateral intraparietal area (LIP) encode the relative salience of spatial locations and its activity can be used to signal attentional priority and program saccades if saccades are appropriate (Bisley and Goldberg, 2003a; Ipata et al., 2006a). Many previous studies have demonstrated how increases in spike rate in this area signal increased priority at the associated spatial location and more recently, surround suppressive interactions have been shown to dampen responses at competing locations (Falkner et al., 2010).

These interactions in LIP suggest that active competition is occurring between neural representations of potential saccade targets, though the mechanisms of these interactions are unknown. Peaks on LIP's salience map may rise and fall independently, eliciting a saccade when they cross a particular threshold, or the activity of a particular peak could be dependent on the activity of a competing peak.

Competition between the representations of visual stimuli may also be implemented by a change in the functional connectivity between relevant neurons. This change in functional connectivity can be assessed by examining changes in the non-stimulus evoked activity: the so-called noise correlation between multiple neurons. This noise is a measure of the shared variability between neurons. LIP neurons whose response fields (RFs) overlap would be expected to share variability due to the noise inherent in stimulus presentation (since the neurons would share a time-locked response to the same visual input). However it is less clear whether neurons that do not share stimulus input will also share variability. Uncorrelated neuronal noise between 2 LIP neurons is evidence for an independent race-to-threshold model where neurons associated with spatial locations generate eye movements when the responses arrive at a particular threshold, irrespective of what is happening at competing spatial locations. In contrast, positive correlations indicate fluctuations that simultaneously affect competing peaks, while negative correlations are evidence for suppressive interactions, a possible mechanism to resolve spatial competition.

Changes in noise correlation are also a neural signature of top-down cognitive involvement. Several recent studies have shown that activity in other macaque visual areas exhibit low levels of correlation between simultaneously recorded neurons that can be modulated by the monkey's

behavior. In V4, positive correlations decreased when spatial attention was deployed to the location of one of the cells' RFs during a covert tracking task, suggesting that the correlations between neural activity may provide an independent channel of information about the state of attention at a given time (Mitchell et al., 2009). Moreover, modulations in noise correlation in area V4 account for the majority of attentional improvement in a measure of population sensitivity, and that measurements of spike rates alone provide an incomplete description of the monkey's cognitive state (Cohen and Maunsell, 2009). Since shared noise between visually responsive neurons has also been shown to limit cortical information processing capability (Zohary et al., 1994), this suggests that a reduction of any shared noise might be a necessary precursor to an ongoing decision process, though this has not been explicitly tested.

Monkeys' behavior during choice tasks has been shown to be sensitive to previous rewards (Platt and Glimcher, 1999; Sugrue et al., 2004; Corrado et al., 2005; Lau and Glimcher, 2005), and many studies have shown that saccade latencies reflect the monkeys' motivation state at the time of the eye movement (Lauwereyns et al., 2002; Takikawa et al., 2002; Hikosaka et al., 2006). LIP, in addition to other priority map areas, encodes information about attention and reward and these signals can affect the relative peaks on LIP's priority map, though it is unknown whether these factors can influence competitive neural mechanisms or the dynamics of changing noise correlations between neurons. To disambiguate between models of saccadic competition in LIP, we performed simultaneous paired recordings of 2 LIP neurons that were explicitly selected so that they did not share excitatory stimulus evoke activity. We examined changes in the neural noise during the decision process while monkeys chose between pairs of saccade targets located in the receptive fields of each neuron. This approach allowed us to study

neural interactions that were not generated by external stimuli. By varying the relative reward ratio between the 2 targets, we modulated the monkey's internal motivation to chose a particular target and examined the contributions of varying cognitive demands on noise correlations in LIP.

4.3 Materials and Methods

We used two male rhesus monkeys (Macaca mulatta) weighing 8–12 kg in this experiment. All experimental protocols were approved by the Animal Care and Use Committees at Columbia University and the New York State Psychiatric Institute, and complied with the guidelines established by the Public Health Service Guide for the Care and Use of Laboratory Animals. We located the intraparietal sulcus in each monkey using a T1 volume scan obtained on a GE Signa 1.5 T magnet. Using standard sterile surgical techniques and endotracheal isofluorane general anesthesia we made a 2 cm trephine hole over the intraparietal sulcus and implanted 12-16 titanium screws in the monkey's skull and used them to anchor an acrylic cap in which we placed a head holding device, the recording chamber, and the plug for subconjunctival search coils for eye position recording.

4.31 Data collection

We used the REX/MEX/VEX system developed at the National Eye Institute's Laboratory for Sensorimotor Research for behavioral control, visual stimulus display and data collection using Dell Optiplex PC's running QNX (REX and MEX) and Windows 2000 (VEX). The monkeys sat in a dimly illuminated room with their head fixed and viewed a screen that

stood 75 cm away. Visual stimuli were back-projected onto the screen using a LCD projector (Hitachi CP-X275) with a refresh rate of 75 Hz. We used a photodiode to register the actual times for stimulus onsets and offsets. Fixation point and saccade target stimuli were 0.3 degree wide colored squares. Fixation points were red and saccades targets were blue and green. We introduced the 2 separate electrodes per recording session into the same grid separated by a minimum of 2 mm through a separate guide tubes positioned in a 1 mm grid (Crist Instruments). We recorded single units from each electrode from area LIP with glass-insulated tungsten electrodes (Alpha Omega Engineering, Nazareth, Israel) while the monkeys performed a passive fixation task as white spots flashed sequentially at different locations in the visual field. We amplified, filtered and discriminated action potentials using an amplitude window discriminator (MEX software). Only well-isolated single neurons with highly discriminable waveforms were studied.

4.32 Neuron inclusion criteria

We considered neurons to be in LIP if they showed consistent visual, delay-period and saccade related response during the memory-guided saccade task.

For each neuron we isolated, we identified the center of the RF using flashed spots at 400ms intervals (4 per trial, located on a 40 x 40 degree grid with 5 degree spacing, less than 50 ms duration) during passive fixation. We defined the center of the RF as the spatial location of the flashed spot that elicited the maximum activity. Once 2 neurons were independently isolated, we tested each the response of each neuron using memory guided saccade task. We recorded the response to both neurons simultaneously while monkeys made memory guided saccades to a

single saccade target. In one block of trials (~50 trials), the target was placed in the response field of the first neuron (RF1) and in the second block of trials in RF2. For each block of trials we compared the activity during the delay period to the activity during prior to target onset. Neurons were considered to have sufficient delay period activity if activity was greater during the delay period (t-test, one-tailed $p<0.05$).

Cells pairs were included in the choice task analysis and determined not to share stimulus evoked activity if during the memory guided saccade task, one cell had significant activity 30-300ms after target onset compared to an equivalent bin during the pre-target fixation period, and the other cell did not have an increase (one tailed t-test $p>0.05$). Un-stimulated cells could have a significant decrease in activity that would not be considered for exclusion by this test. Once it was determined that cell pairs had non-overlapping RF centers, that could be used for the choice task.

4.33 Task details

Once LIP cells were isolated on each electrode, the monkey was required to perform the free choice foraging task. For each trial in this task, the monkey fixated central red spot for 500 ms, at which point 2 saccade targets appeared simultaneously, one in the RF of each isolated cell. Either target (green or blue) could appear randomly in either RF. The targets were present for 750-1050 ms, at which point the fixation spot disappeared which was the cue for the monkey to choose one target. Monkeys had 400 ms after the go-cue to make a saccade to a 4.5x4.5 degree window around the saccade target. If the monkey's eye was in the window for 100 ms from 400 ms to 500 ms after the go-cue, a beep indicated whether the monkey would receive a reward: a

long beep signaled reward while a short beep indicated no reward. Rewards were determined using a changing relative probability schedule that was changed pseudo-randomly approximately every 200 trials. Reward magnitudes were fixed for the duration of each session. The range of reward probabilities tested included 3:1,2:1,1:1,1:2,1:3, though not all relative probabilities were tested each session, depending on the number of trials and the monkeys' satiety. Each target was re-baited (using a random flip of an independent coin for each target) each time that color target was chosen but uncollected rewards carried over across trials so that monkeys could harvest rewards maximally by visiting each target color with the same proportion at which it is rewarded relative to the other color. We did not use a changeover delay. Though monkeys did not always perform this task optimally, they did change their choice strategy when reward probabilities changed during a session, indicating that they had learned that the target reward probabilities had changed. The monkeys' behavior was quantified by comparing the relative reward ratio ($Reward_{Green}$ / ($Reward_{Green}$+$Reward_{Blue}$)) to the monkeys' choice ratio ($Choice_{Green}$ / ($Choice_{Blue}$ +$Choice_{Green}$)). For the monkeys's instantaneous choice ratio, the choice ratio was averaged over blocks of 10 trials. Saccade latencies for variable reward trials were normalized by the average saccade latency across all trial types for each saccade direction.

For a subset of cell pairs (n=33 cell pairs), we also recorded data for the "empty" RF task. The empty RF task is identical to the free choice task in every respect, except that the locations of the choice targets were changed so that a target appeared in RF1 and the second target appeared diametrically opposite RF1 such that it did not excite either RF1 or RF2. RF2 thus became the "empty" RF and was then no longer a choice option associated with a reward.

4.34 Data analysis

All data analysis programs were written in MATLAB (Mathworks Inc, Natick, MA). For the foraging task we examined the relationship between the spike count of each neuron during the choice separately for each saccade direction (saccade into RF1 and saccade into RF2) and reward probability. We used a sliding bin of 300 ms stepped every 25 ms and calculated the spike counts from each cell across the trial. Spike counts were normalized by subtracting the mean spike count from each trial type from the absolute spike count of each trial. We used a sliding average from the surrounding 10 trials of the same saccade trial type to eliminate slower fluctuations in rate that could be caused by slow changes in the monkeys' alertness. Calculating the Pearson coefficient without this sliding average made no qualitative difference in the results. We also calculated the Pearson coefficient on the z-score of the spike counts rather than the raw spike counts themselves (Kohn and Smith, 2005; Smith and Kohn, 2008) and again this made no qualitative difference in our findings.

We calculated the Pearson correlation of each pair of spike counts separately for each bin across the duration of the trial. The Pearson correlation was computed separately for each saccade direction within a given pair of cells, NOT pooled across saccade directions, which can produce spurious negative correlations that are uninformative about functional connectivity. For single cells, error bars were calculated using Jackknife methods leaving out individual trials (iterated 1000 times). For populations of cells, error bars were calculated using standard error of the mean for population averages at each timestep. Significant correlations were assessed using a t-test on the distribution of correlation coefficients for each selected bin independently, while pairwise significance testing was done using Wilcoxon signed rank tests ($p<0.05$) at each time-

step correcting for multiple comparisons. Cell pairs were excluded from analysis if individual decisions did not have a minimum of 20 trials in order to ensure an minimally appropriate estimate of the correlation.

We validated that 300 ms was an appropriate bin to use (Bair et al., 2001; Smith and Kohn, 2008; Mitchell et al., 2009) by calculating the Pearson correlation using different sized bins slid along the baseline period (500 ms prior to target onset) in the choice task. Bin sizes used were 5 10 25 50 100 150 250 300 400 and 500 ms stepped through the duration of the baseline period at 50ms increments. For example, a binsize of 400ms would be calculated 3 times in during the 500ms (starting at -500, -450, and -400).

We calculated synchrony between neurons by taking the spike trains from the pre-target and pre-saccadic epoch and computed a cross average cross correlogram across trials for each pair. For each pair of neurons, we then recomputed the cross correlogram after shuffling trial order and iterated this process 1000 times. From these shuffled correlograms we extracted 95% confidence bounds. We considered a neuron to have significant synchronous spiking if the value of the spike coincidence was greater than the upper 95% bound for a 3ms window across the 0 time lag.

For the reward history model, we extracted a measure of the reward history by computing a vector of previous rewards where positively rewarded trials were labeled with a 1 and negatively rewarded trials with correct saccades were labeled with a 0. Trials were the monkeys' saccades were overly inaccurate or exceeded the time limit were excluded. This reward vector was then convolved with an exponential with a variable time constant tau. For each behavioral session, we determined the best-fit tau by regressing the saccade latency for each

trial with the reward history term and minimizing the squared residuals minus a tau^2 term, which prevents the model from over fitting. We performed this analysis for the total reward stream over all choices and also for choices only to each particular color target as controls. The coefficient of regression between latency and reward history was computed using the best-fit tau for each session. Distributions of coefficients were compared to a predicted mean of 0 using a t-test.

To determine the relationship between correlation and reward history, we binned the trials from each session into 5 equal bins using the best-fit tau for each session and recalculated the noise correlations and average spike counts across trials in each of the bins. Regressions were computed using standard techniques and linear fits were done using least-squares.

4.4 Results

4.41 Choice Behavior

To get the monkeys to make free saccadic choices into the receptive fields of the recorded cells, we used a dynamic foraging task (Sugrue et al., 2004; Lau and Glimcher, 2005) where monkeys were required to saccade to one of 2 possible targets (green or blue) after a variable delay (Figure 4.1A). The relative reward ratio between the different targets was changed pseudo-randomly every 200-300 trials (see methods), while absolute reward magnitude was fixed throughout the duration of each session.

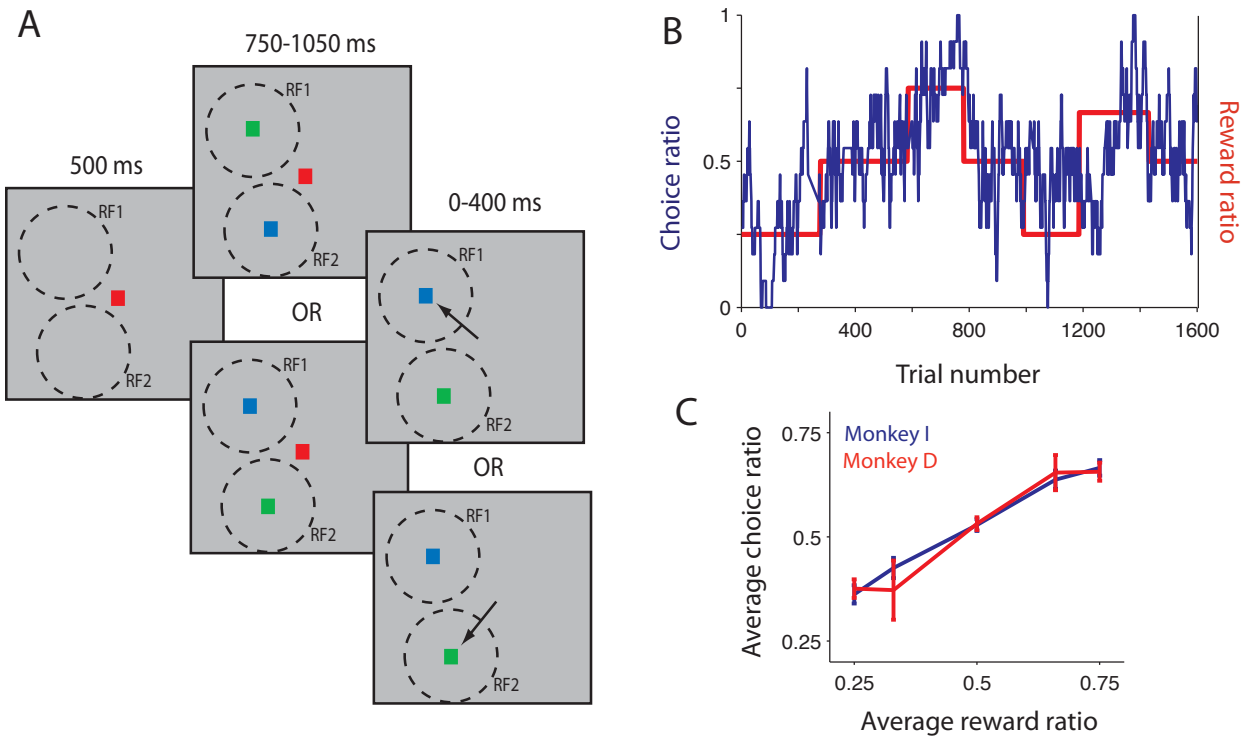

Figure 4.1 Choice task behavior.
A) Monkeys performed choice task after 2 LIP cells had been isolated and their RF's mapped (see methods). Monkeys fixated on a central red spot for 500 ms, then 2 targets appeared (green and blue), one in the center of each RF. 750-1050 ms later, the fixation point disappeared, at which point the monkey had up to 400 ms to make a saccade to either target. Targets colors were assigned either a reward or no reward based on a fixed reward ratio that was changed approximately every 200 trials. Targets were re-baited with rewards every time the target color was chosen. B) Choice behavior during an example session. Red line shows the relative reward ratio as a function of trial number. The blue line shows the monkey's instantaneous choice ratio averaged over bins of 10 trials. C) Monkeys' choice behavior averaged over all sessions across all reward ratios. Error bars are +SEM (Monkey D, n=71 sessions, Monkey I, n=33 sessions). All reward ratios significant from reward ratio 0.5 (ANOVA $p<0.05$).

In theory, monkeys could optimize reward collection by choosing each colored target with the same relative frequency as its relative reward ratio (Hernstein, 1961), so it benefited the monkey to adjust his choice allocation frequency accordingly. In practice, monkeys did not behave optimally, but showed a clear bias demonstrating that they were aware of the changing reward structure of the task (Figure 4.1B). Though the monkey's behavior is clearly not optimal, changes in his average choice probability track changes in the relative reward ratio across the

duration of the session. Across all sessions, both monkeys consistently under-matched (Fig 4.1C), though on average clearly tracked changes in the relative reward ratio through his instantaneous choice behavior. For the purposes of this study, we were not concerned with whether the monkeys' behavior was optimal, only that the session-by-session behavior of the monkeys reflected the changing reward probabilities. All average choice frequencies of relative reward ratios other than 0.5 were determined to be significantly different from the monkey's behavior when the reward ratio was 0.5 (1-way ANOVA $p<0.05$ for each comparison).

We recorded the activity of 134 LIP neurons (n=67 pairs of neurons) in 2 monkeys. To eliminate the possibility of stimulus-evoked correlation we recorded only from pairs of neurons with spatially distinct RF centers such that a stimulus in the center of one cell's RF did not excite the other cell (see methods for inclusion criteria). We recorded the neural activity associated with these targets while monkeys chose to saccade to one target or the other.

4.42 Noise correlations decrease over the course of the saccadic decision

Each trial consisted of 2 possible choices: saccade to the target RF1 and saccade to the target RF2. Since we made no assumptions about mutual or symmetric connectivity between neurons, we treated each choice as a separate decision and did not pool across possible decisions. However we did pool across colors for a given target position and reward ratio: response differences between targets of different colors were indistinguishable and were averaged together for each saccadic decision ($p>0.05$, paired t-test at each time bin).

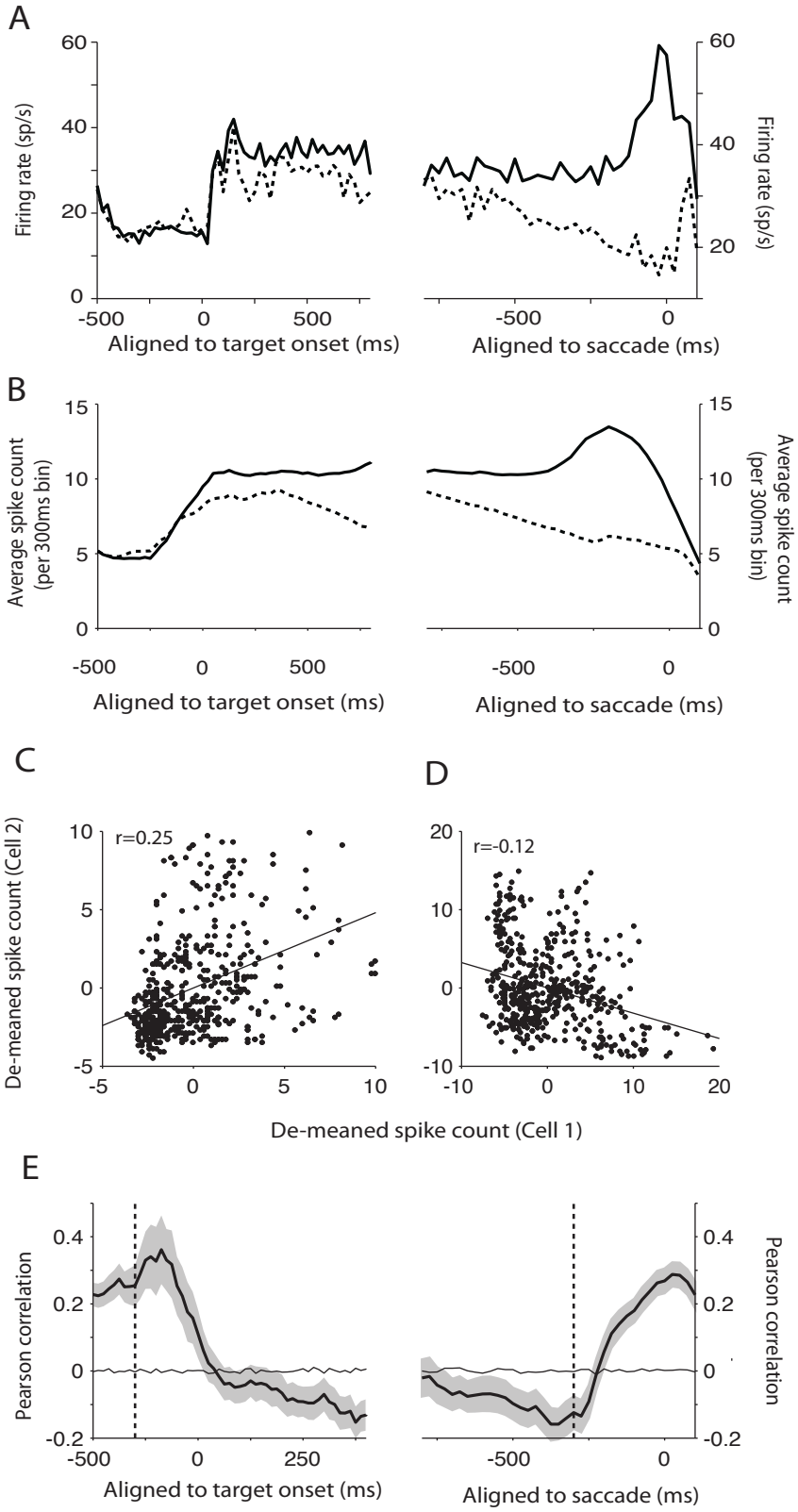

Figure 4.2 Activity and correlation in example neuron pair. A) PSTH of activity for choices to target in RF1 shown aligned to target onset (left) and saccade onset (right) for neuron 1 (solid line) and neuron 2 (dotted line) of example simultaneously recorded pair. PSTH bin is 20ms. B) Activity of example pair shown in spike counts. Spike counts shown are from 300 ms bins stepped every 25 ms and are aligned to the beginning of the bin. Conventions as above. C) Scatter plot of de-meaned spike counts (the "noise) from the 300 ms bin preceding target onset ("pre-target" epoch) for neuron 1 and neuron 2. Sold line is least-squares fit. Pearson correlation coefficient (r) is 0.25 ($p<000.1$). D) Scatter plot of de-meaned spike counts from 300 ms preceding saccade ("pre-saccadic" epoch). Conventions as above. Pearson correlation coefficient (r) is -0.12 ($p<0.001$). E) Noise correlations computed from spike counts shown in B as a function of trial time (thick black line) with Jackknife error bars. Thin black line is noise correlation computed after shuffling trials.

For each choice, activity consisted of the simultaneously recorded responses to the chosen target and the rejected target. As expected, activity corresponding to the chosen target was greater than the activity evoked by the rejected target (Figure 4.2A). For each cell, we smoothed the spike rates into a running average of spike counts by computing the spike counts in each bin of 300 ms (stepped every 25 ms) for each cell's response to the chosen and the rejected targets (Figure 4.2B). We used a bin size large enough to contain sufficient spikes in order to capture "slow" correlations resulting from shared variability, but small enough to capture the temporal resolution of the emerging decision. The spike count traces appear to rise prior to the onset of the target stimuli (Figure 4.2B, left) because they are aligned to the beginning of the bin such that the response aligned to -250 ms actually contain 50 ms of the target onset response.

We next computed the Pearson correlation (r), a measure of correlation that is equivalent to the covariance of the cells' spike counts divided by the product of their respective standard deviations, across each set of spike counts, taking each decision (saccade to RF1 vs. saccade to RF2) separately. To calculate the noise correlation we extracted the Pearson correlation coefficient from the spike counts after subtracting the mean for each bin for each of the decisions shown in 4.2A (Figure 4.2C,D). The correlation was calculated separately for each time step and error bars were computed by using jackknife methods leaving out individual trials. The Pearson correlation coefficient calculated on the same spike counts after shuffling trial order was not significantly different from 0 at any individual time bin.

For this example pair of cells, the Pearson correlation of the de-meaned spike counts changed dynamically over the course of the decision. For the 300 ms prior to target (the pre-target epoch), the correlation coefficient was significantly positive ($r=0.25$, Figure 4.2C). In

contrast, for the 300ms prior to the saccade (the "pre-saccadic" epoch) the correlation was significantly negative (r=-0.12, Figure 4.2D), indicating that there is negative trial-to-trial variability across the spike count for this epoch of the decision making process.

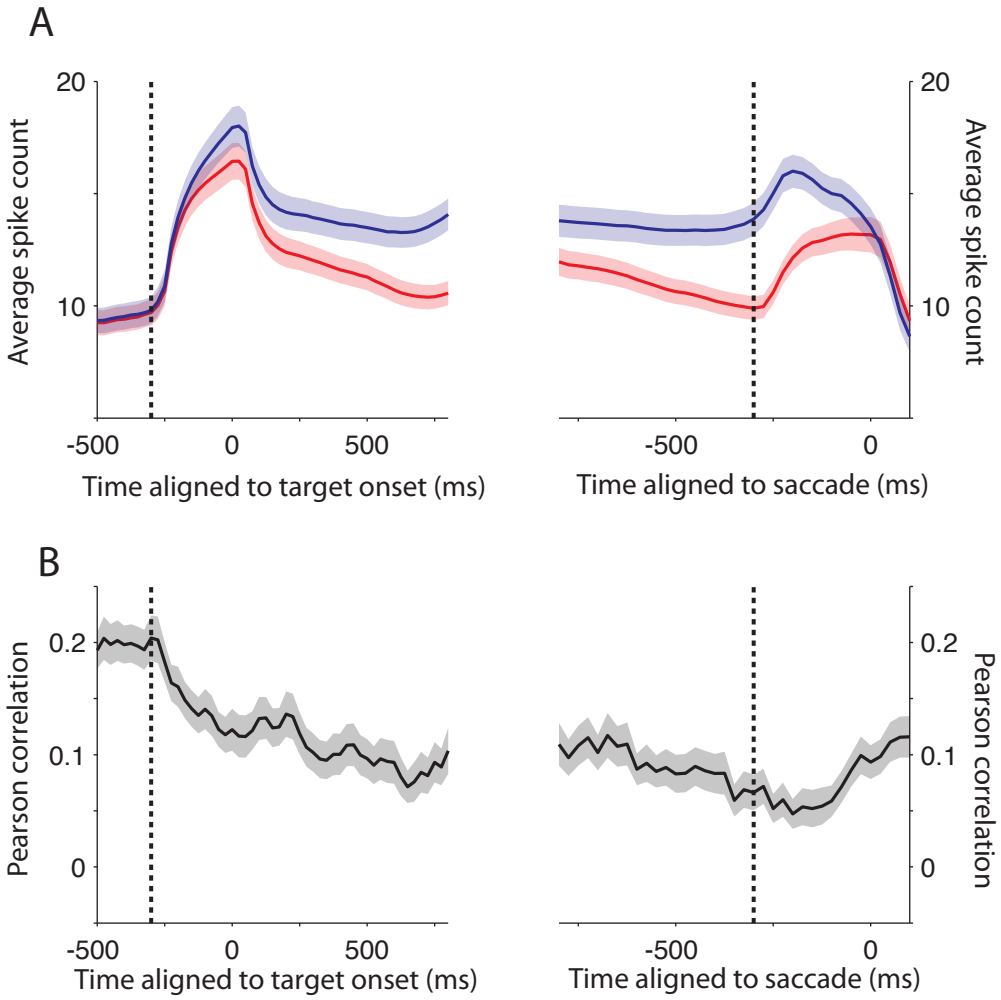

Figure 4.3 Neurons decorrelate across a decision
A) Average spike counts across the population of cells shown for all choices to targets into each cell's RF (blue) and saccades away from each cell's RF (red). Spike counts are shown aligned to the target onset (left) and the saccade (right). (n=108 choices, n=54 cell pairs). B) Average Pearson correlation coefficient for the population as a function of time using bin size of 300ms. Dotted black lines represent time point of pre-target epoch (left) and pre-saccadic epoch (right).

The transition from positive to negative correlation occurred smoothly throughout the trial: in the period prior to the target onset the correlation was significantly positive (Figure

4.2E), indicating that there was positive trial-to-trial variability, but after the targets appeared in the receptive field of each cell the magnitude of the correlation steeply declined until in this pair it eventually changed sign and became a significantly negative correlation prior to the saccade. The correlation coefficient returned to positive after the eye moved (Figure 4.2E, right).

We calculated the noise correlation for each choice in each pair of cells. Across the population of cells pairs we observed similar changes in spike count (Figure 4.3A) and correlation trajectory (Figure 4.3B) over the course of the decision. In this population average, the correlation was significantly positive in the pre-target epoch (students t-test $p<<0.001$), and taken individually 58% of cell pairs had significantly positive correlations in this epoch. No cell pairs had significantly negative correlations in this epoch.

Correlations were significantly reduced prior to the saccade. For almost every individual choice, correlations in the 300 ms before the target appearance were significantly higher than the correlations were 300ms before the saccade (Figure 4.4A, $p<<0.0001$, Wilcoxon signed rank test).

Correlations can trivially increase as spike rates increase (Zeitler et al., 2006; de la Rocha et al., 2007). To ensure that the decrease in Pearson correlation observed over the course of the saccadic decision is not due simply to decreases in spike rate over the course of the trial we plotted the average spike count from the baseline vs. the spike count from the decision period (Figure 4.4B). As expected, the spike counts for the decisions where saccades were executed into the RF were significantly enhanced in the pre-saccadic decision bin in comparison with the baseline bin (Figure 4.4B, blue, Wilcoxon signed rank test $p<<0.001$). The average spike counts for the cells where saccades were made opposite the cells' RF had largely declined to the level of

the pre-target epoch (Figure 4.4B, red, Wilcoxon signed rank test p=0.72). Since the spike counts were actually increased for one set of choices and were unchanged for the other, these changes cannot account for the change in correlation observed between the 2 epochs.

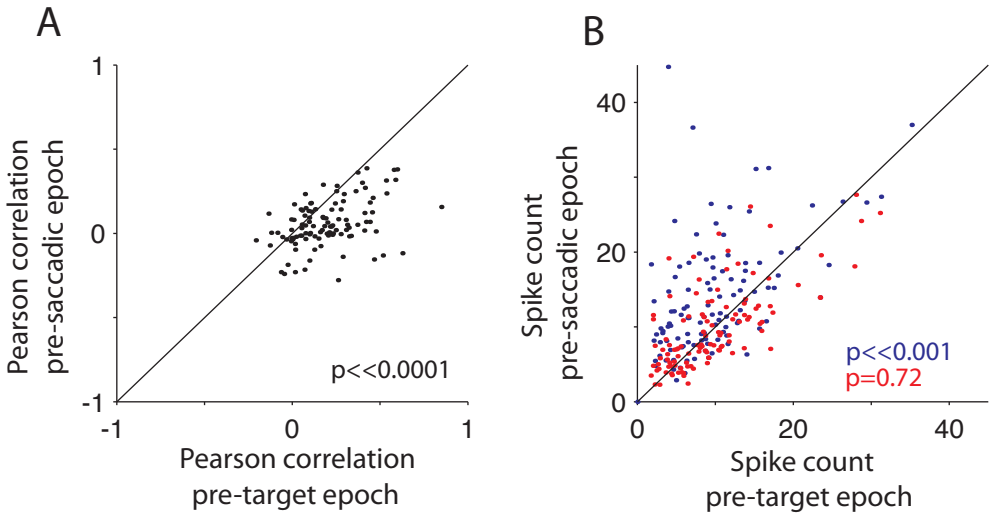

Figure 4.4 Comparison of pre-target and pre-saccadic epoch
A) Comparison of correlation coefficient from pre-target (ordinate) and pre-saccadic (abscissa) epochs for each choice. Pre-target correlations are significantly higher than pre-saccadic correlations across the population ($p<<0.001$, Wilcoxon signed rank test). B) Comparison of spike counts between the pre-target and pre-saccadic epochs across the population. For choices to target in each cell's RF saccades (blue), spike counts were higher for the pre-saccadic period ($p<<0.001$, Wilcoxon signed rank test). Spike counts for the response to the rejected target were not significantly different from pre-target activity ($p=0.716$, Wilcoxon signed rank test).

The change in noise correlation between these 2 epochs is also not due to an overall change in independent variability of the spike counts. The raw variance for the 2 epochs (pre-target vs. pre-saccadic) is not significantly different for neurons encoding the rejected target (spike count for saccades out of RF, $p=0.55$) and trends closely to significance for neurons encoding the chosen target ($p=0.06$, Wilcoxon signed rank test), though the direction of this difference is an increase, the opposite direction predicted if a change in Pearson correlation were due strictly to a change in the independent variance of the neurons.

To examine the dynamics of cell pairs with different correlations, we computed the Pearson correlation across the entire decision period (750ms prior to saccade) for each cell pair for each decision when the reward ratio was 0.5. From this, we created an index of significantly negatively correlated pairs (n=14) and positively correlated pairs (n=32). We re-plotted the correlation coefficient calculated from the sliding 300ms bin from these positive and negative (Figure 4.5) subpopulations to compare the coefficients from the pre-target and pre-saccadic epochs. Both subpopulations show a decrease in noise correlation from the pre-target to the pre-saccadic epoch, regardless of the sign of the correlation.

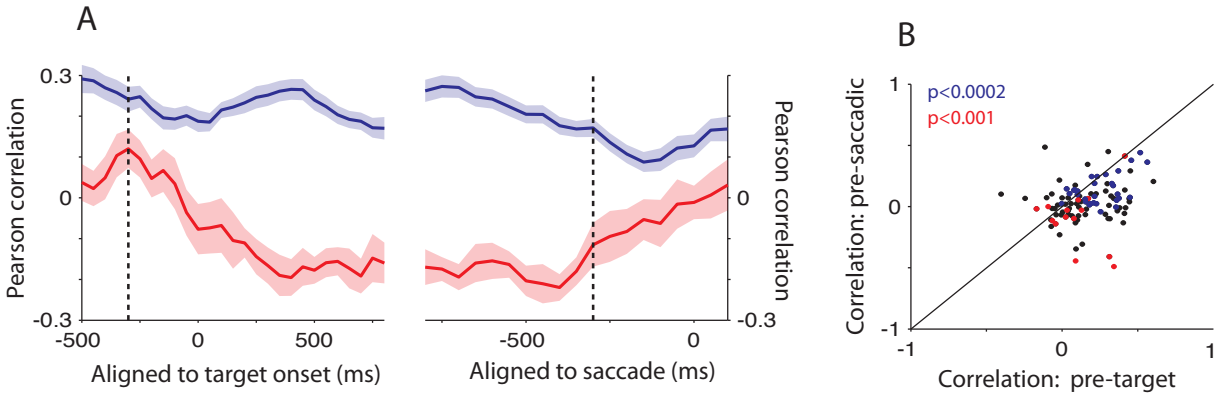

Figure 4.5 Both positive and negatively correlated cells decorrelate during a decision.
A) Subpopulations of cell pair choices that showed significantly positive correlations (blue, 28%) and significantly negative correlations (red, 12%) across the entire target epoch (750ms prior to saccade) were extracted. Correlations for both subpopulations decrease over prior to the saccade. B) Comparison of correlation coefficients between the pre-target (300 ms prior to target) and the pre-saccadic (300 ms prior to saccade) epochs. Comparisons for both positive (blue) and negative (red) subpopulations were significant ($p<0.0002$ and $p<0.001$ respectively, Wilcoxon signed rank test). Black points show cell pairs that fall into neither subpopulation.

4.43 Decorrelation abolishes synchrony

We validated our use of bin size by repeatedly calculating the correlation coefficient for multiple bin sizes, then averaging over all correlations within a particular neuron pair (Figure 4.6). We used bin sizes of ascending size (5, 10, 25, 50, 100, 200, 300, 400, 500ms) stepped

every 50ms through a 500ms epoch prior to target onset and a 500ms bin prior to saccade. For both epochs, correlations are weakest when binsize is smallest and in both cases, the correlations increase with increasing binsize. The magnitude of the correlation plateaus at a binsizes >300ms, indicating that this bin size captures shared variability during trial-to-trial fluctuations, but can be examined dynamically over a trial that exceeds 1s.

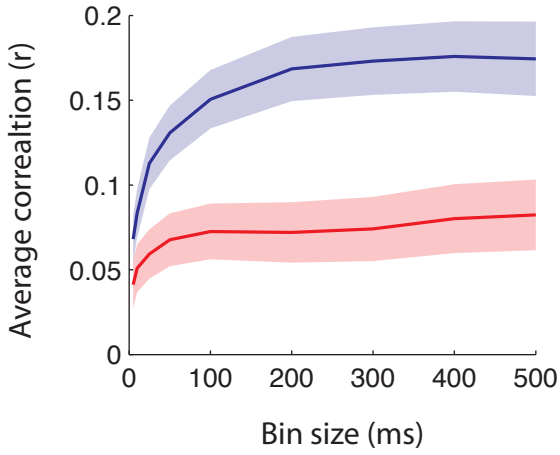

Figure 4.6 Timescale of correlations. Average Pearson correlation as a function of bin size for 500 ms pre-target epoch (blue) and 500 ms pre-saccadic epoch (red). Correlations averaged for each pair after stepping through epoch with varying bin sizes. Error bars represent SEM across population of pairs (n=108 choices). Bin sizes used are 5, 10, 25, 50, 100, 200, 300, 400, and 500 ms.

Although we found that correlations are maximal for binsizes >300ms, suggesting that these correlations emerge on a slow timescale, this does not preclude a contribution from synchronously occurring spikes. We calculated the incidence of synchronously occurring spikes by computing the cross correlation for each pair of cells during the pre-target and pre-saccadic epoch. For each epoch, we recalculated the cross correlation after shuffling trials and iterated this calculation 1000 times to extract estimates of the 95% confidence bounds for each pair of cells. Individually, 17/67 pairs of cells (25%) had significantly higher incidence of synchronous spikes than would be expected by chance in the pre-target epoch (Figure 4.7A). During the pre-saccadic epoch, despite the fact that there are more spikes evoked, only one pair of cells (1%) had significantly higher incidence of coincident spikes (Figure 4.7B).

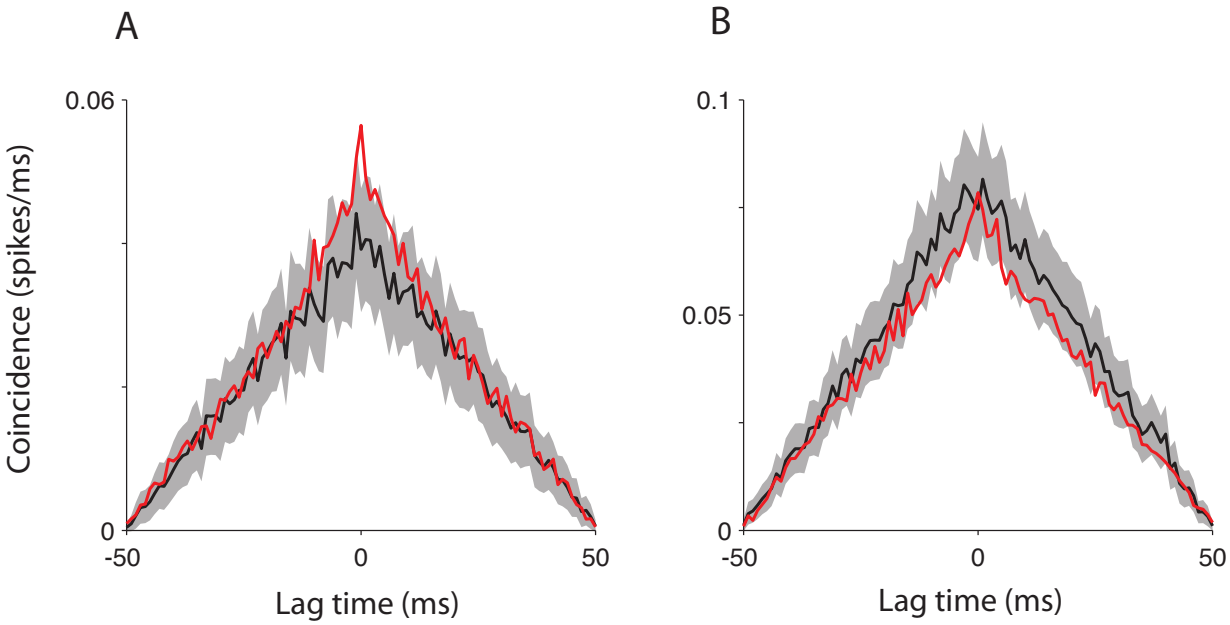

Figure 4.7 Incidence of synchronous spikes in the A) pre-target epoch and B) pre-saccadic epoch. Red line shows the average coincidence of synchronous spikes at varying time lags. Black line shows the average coincidence of synchronous spikes after shuffling trials. 95% confidence bounds were calculated after iterating shuffled coincidence 1000x (n=67 pairs of cells).

4.44 Correlations encode information about reward history

To perform the choice task well, monkeys must learn the value of the relative reward of each target and use this information to allocate his choices between the two targets. Increasing his harvesting efficiency across this task requires that the monkey retain information about previous rewards. Monkeys have been found to use this information to generate upcoming choices, but it may influence other behavioral measures, including his saccade latency to a particular choice target.

To test this, we first divided the trials into "rewarded" and "unrewarded" trials based on whether the monkey had successfully harvested a reward on the previous trial and examined whether the monkeys' saccade latencies were different between these 2 groups. We found a

highly significant difference in average saccade latency for each choice (Figure 4.8D, $p<<0.0001$, blue, $p<0.005$ for choices to RF1 and RF2 respectively). This effect was true whether choices to targets with all relative rewards were included, or whether the analysis was restricted to choices when the relative reward was equivalent (relative reward=0.5). This effect was also significant regardless of which choice the monkey made previously ($p<<0.0001$ for previous green or blue choices respectively), his upcoming choice ($p<<0.0001$ for upcoming green or blue choices respectively) or which RF he chose on the previous trial ($p<<0.0001$ for RF1 choices, p for RF2 choices, Wilcoxon signed rank test). Thus the monkeys' saccade latency is not a function of the properties of the choice and instead reflects an overall state variable related to his history of rewards.

We next looked at the spike rates and correlation between neurons when monkeys made choices after a successful and unsuccessful previous trial. Between these 2 groups of trials (previous trial rewarded vs. previous trial unrewarded), the average spike counts showed no significant difference across the trial (Figure 4.8A). In contrast, the average correlation coefficient was significantly different for the unrewarded trials compared to the rewarded trials (Figure 4.8B). When monkeys failed to receive a reward on the previous trial, the amount of correlated noise between the neurons encoding the choices options was significantly higher than if he was successful. This effect begins in the spontaneous activity prior to the target onset and is exhibited several hundred ms into the trial. For the pre-target epoch (300ms prior to target onset), this effect is highly significant (Figure 4.8C, $p<<0.0001$ Wilcoxon signed rank test). The average values of the correlation converge when aligned to the saccade onset, both exhibiting the stereotyped decrease over the trial described above. These data suggest that in the pre-target

epoch, correlations, though not spike counts, encode information about the previous reward and that missed previous rewards are associated with slower saccades on the next trial.

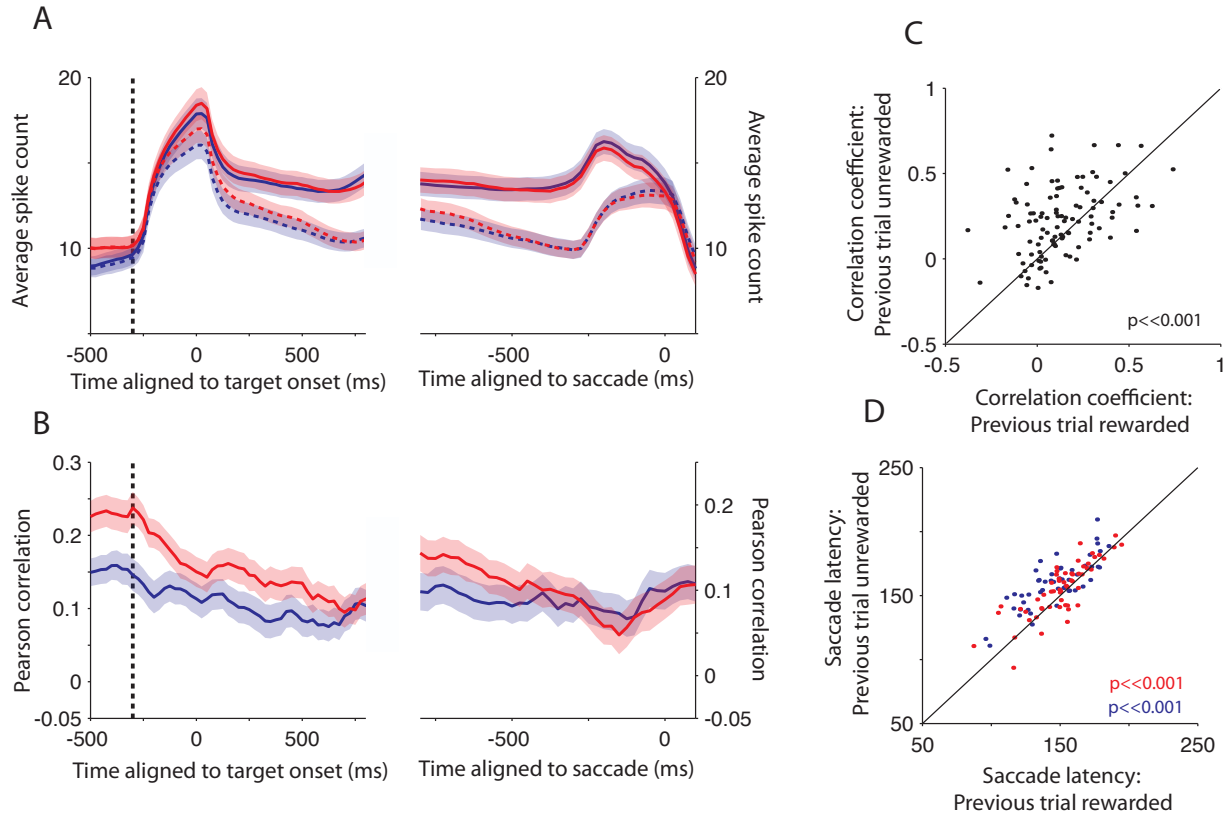

Figure 4.8 Correlations are influenced by previous rewards.
A) Average spike counts for the population of cells shown for saccades into the RF (solid) and saccades away from the RF (dotted) split between trials where the previous saccade did result in a reward (blue) and trials where the previous saccade trial was unrewarded (red). Spike counts between these trials were not significantly different (paired t-test). Error bars are standard errors. Average spike counts are shown aligned to the target onset (left) and the saccade (right). n=67 pairs of cells. B) Average Pearson correlation coefficient for the spike counts shown in A. Trials where the previous saccade was unrewarded had higher correlation coefficients than trials where the previous saccade was rewarded. (n=114 individual saccade directions, n=67 pairs of cells.) C) Scatter plot comparing the correlation coefficient across the population in the baseline period (300 ms prior to target onset) between rewarded and unrewarded previous trials. ($p<<0.001$, Wilcoxon signed rank test). D) Scatter plot comparing the saccade latencies between trials where the previous trial was rewarded to the trials where the previous trial was unrewarded. Saccades to RF1 are shown in blue, and saccades to RF2 are shown in red. (n=114 individual saccade directions). ($p<<0.0001$, blue, $p<0.005$, red, Wilcoxon signed rank test).

We examined this relationship more rigorously by extending this analysis to rewards further back in time: if monkeys' saccade behavior is sensitive to rewards on the previous trial, it may be sensitive to a string of missed rewards. We determined a measure of reward history for

each trial by convolving the stream of rewards on previous trials (a vector where 1's represent obtained rewards and 0's represent missed rewards) with an exponential with a particular time constant tau. We regressed the latency of the saccades in a particular behavioral session with the reward history terms and extracted a best-fit time constant (Figure 4.9A). A short time constant would indicate that the monkeys' behavior is determined primarily by very recent rewards, and a longer time constant would suggest that he also takes into account rewards farther back in time.

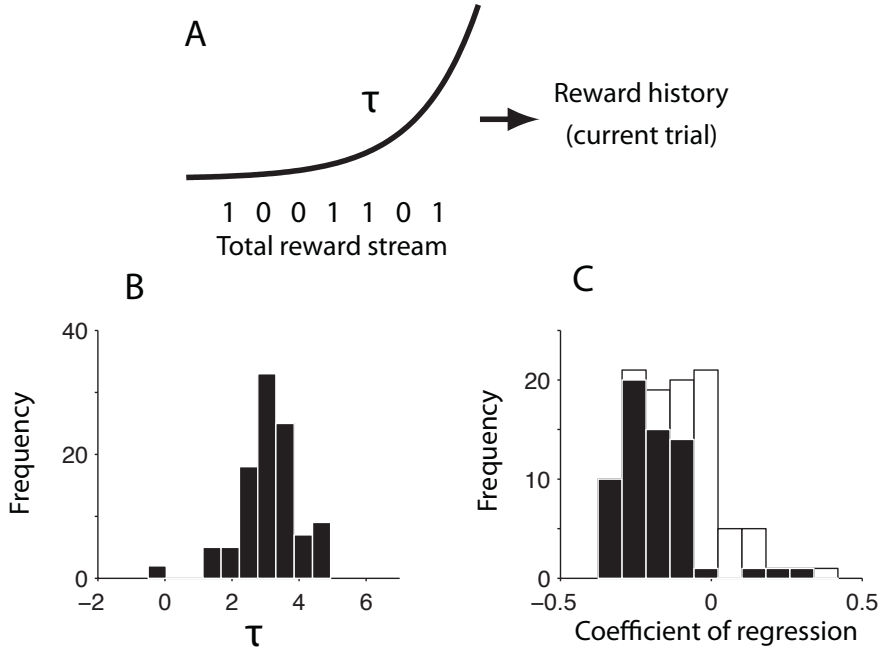

Figure 4.9 Reward history predicts saccadic latency.
A) For each day, the monkey's history of past rewards, represented by a vector of 1's (reward received) and 0's (reward not received), was convolved with an exponential and fit with a time constant tau by regressing the reward history term with the saccade latency. B) Histogram of best-fit taus for each session by regressing reward history with saccade latency for each behavioral session. Mean tau=3.08+0.08 SEM. (n=104 behavioral sessions). C) Histogram of coefficients of regression of saccade latency with reward history. Mean slope=-0.12+0.01SEM. 63 of sessions (61%) had significant regressions ($p<0.05$, n=104 behavioral sessions). Distribution is significantly different from 0 ($p<<0.0001$, student's t-test).

We extracted the time constants (Figure 4.9B) and the slopes of the regression for each session (Figure 4.9C). Monkeys had an average time constant (tau) of 3.08$\pm$0.08 SEM and an average

regression slope of -0.12±0.01 SEM. This indicated that across all sessions (n=104 behavioral sessions), saccade latencies were negatively correlated with the reward history for that particular trial: when reward on a particular trial was high, the saccade on the next trial was faster.

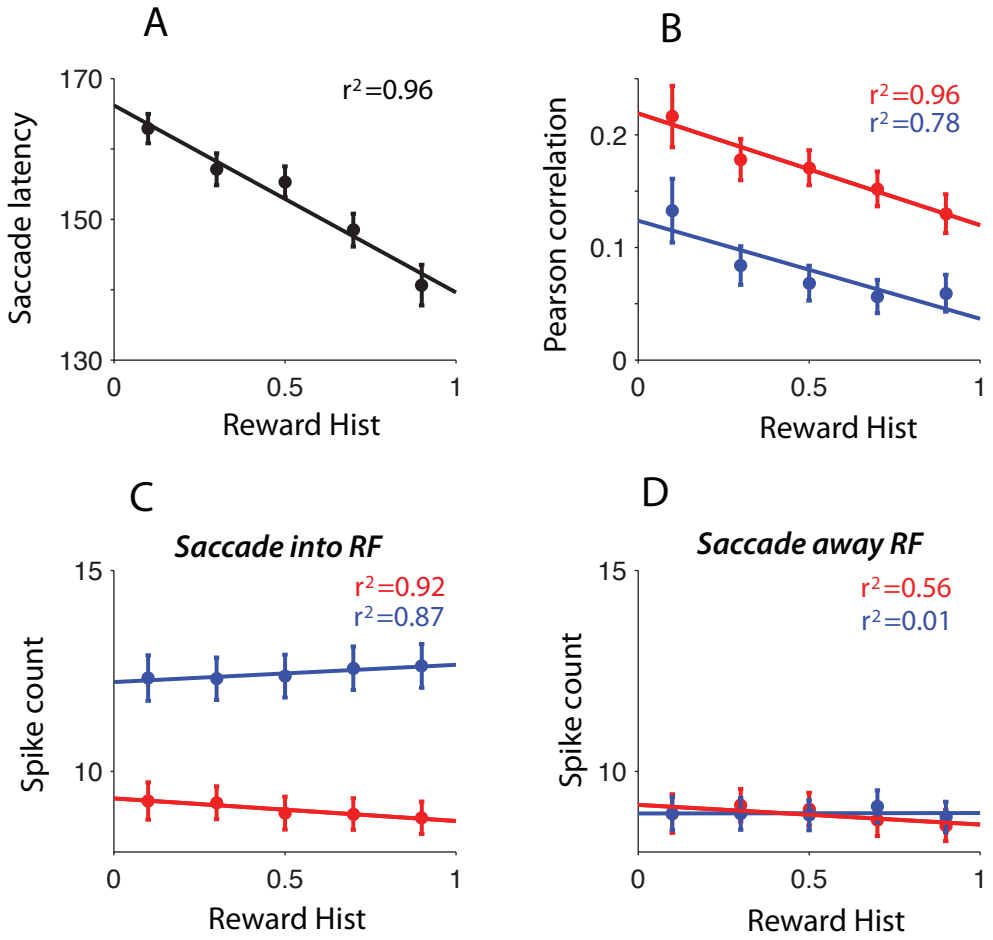

Figure 4.10 Noise correlations vary with reward history.
A) Saccade latency is negatively correlated with reward history across sessions. Each data point is the average saccade latency for across sessions for trials binned by reward history (error bars are +SEM) and solid line is best-fit least square regression (r-square=0.96, p<<0.001, n=104 choices). B) Noise correlations of trials binned by the trials' reward histories. Conventions as above. Correlations regress significantly with reward history across choices in both pre-target epoch (red, rsquare=0.96, p<<0.0001) and the pre-saccadic epoch (blue, r-square=0.78, p<<0.001, n=108 choices). C,D) Correlation of the spike count with reward history across choices for the pre-target and pre-saccadic epochs (red and blue respectively) for responses to the chosen target (C) and the rejected target (D).

Since correlations between neurons cannot be computed for individual trials and require a sufficient number of trials to achieve an accurate estimate of the coefficient, we next binned the trials during each session according to the reward history computed with the best-fit tau (see methods). The reward history term is bounded between 0 and 1, so trials were binned into 5 equally spaced bins. We extracted the spike counts associated with both the pre-target epoch and the pre-saccadic epoch and computed the correlations for each bin and averaged across sessions. We plotted the average saccade latency across sessions for each of the bins (Figure 4.10A). As expected from the negative regression slopes, there was significant negative correlation between the average reward history and the average saccade latency that was fit extremely well using linear least-squares regression (r^2=0.96). We also found that the average correlation coefficients also significantly varied across reward history, with high reward history values being associated with the lowest correlations. This was true for both the pre-target epoch (Figure 4.10B, red) and the pre-saccadic epoch (Figure 4.10B, blue).

Surprisingly we found that the average spike counts varied little across differing values of reward history for both epochs (Figure 4.10C,D), and average spike counts between the highest and lowest reward history bins were not significantly different (all comparisons across reward history $p>0.05$, Wilcoxon signed rank test).

To test whether saccade latencies on current trials were sensitive to information about the rewards associated with a particular saccadic choice, we recomputed the reward history for each trial, but included only choices to a given target (i.e. choices to green targets or choices to blue targets only). We computed the reward history as above, by convolving the new single choice reward vectors with an exponential and regressing the saccade latencies of the upcoming choices

with the new reward history term (Figure 4.11). For both green and blue choices, distributions of correlation coefficients were not significantly different from 0 (p=0.15 and p=0.48 respectively, t-test), indicating that overall, saccade latencies are more associated with a measure of the total reward stream than rewards to a particular choice. This suggests that rather than use this measure to inform upcoming choices, the monkey may be deriving his overall motivational state from his aggregated rewards.

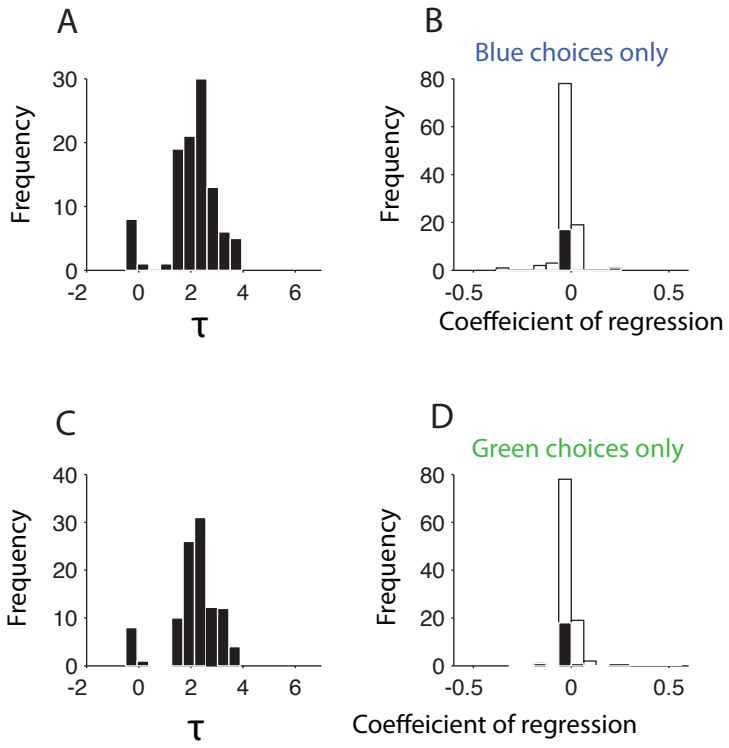

Figure 4.11 Reward history for a particular choice is not correlated saccade latency.
A) Best fit taus for each behavioral session where reward history is computed for choices to green targets only. B) Histogram of regression coefficients for reward history (green choices) with saccade latencies (choices to greens) for each session. Black shows significant regressions ($p<0.05$). Distribution is not significantly different from 0 ($p=0.15$ student's t-test). C) Best fit taus for blue choices. Conventions as in A. C) Histogram of regression coefficients for blue choices. Conventions as in B. Distribution is not significantly different from 0 ($p=0.48$ student's t-test).

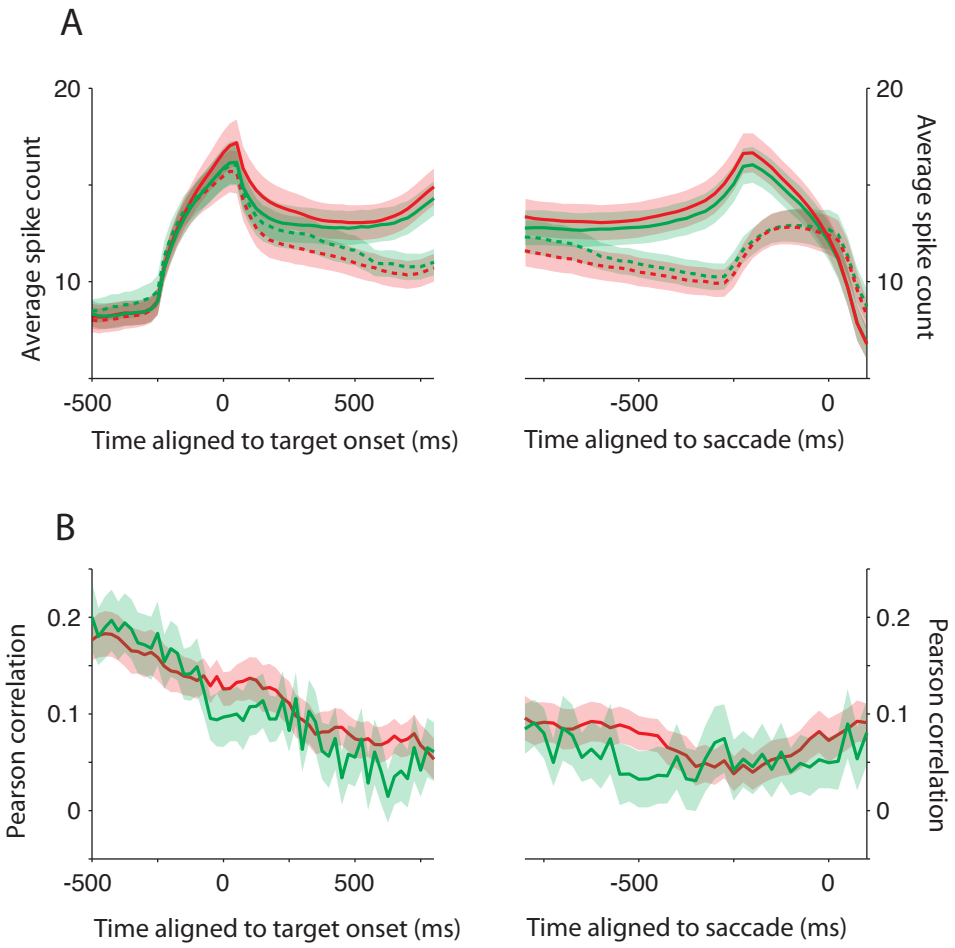

Figure 4.12 Correlations do not encode relative reward.
Trials were divided into saccades to high relative reward targets (red, relative reward ratio>0.5) and saccades to low relative reward targets (green, relative reward<0.5). A) Average spike counts for responses to the chosen (solid) and rejected (dotted) targets aligned to target onset (left) and saccade (right). Conventions as above. Responses to low and high relative reward targets were not significantly different at any time point ($p>0.05$ Wilcoxon signed rank test at each bin). B) Average Pearson correlation of spike counts shown in A. Correlations for choices to high and low relative reward targets were not significantly different from each other ($p>0.05$ Wilcoxon signed rank test).

4.45 Correlations do not encode reward of chosen target

While correlations encode information about the monkeys' total history of rewards, do they also encode information about the relative reward of the chosen target? We compared the spike counts and correlations of trials when monkeys made choices to reward "high" targets

(relative reward ratio>0.5) and choices to reward "low" targets (relative reward ratio<0.5). We found no significant difference between either the spike counts or the correlations across the different choice conditions ($p>0.05$ at each time epoch, Wilcoxon signed rank test) between the high (Figure 4.12A,B red) and low (green) choices. This demonstrates that while correlations encode information about previous rewards, they are insensitive to the absolute relative reward of the chosen target.

4.46 Target representations compete with non-target spatial locations.

During a saccadic decision, potential targets compete with each other for attentional priority, though it is unknown whether potential targets also compete with spatial locations that do not encode the locations of legitimate choice options. For example, a winning peak on LIPs map may compete with other target locations, and also locations that do not encode potential targets, resulting in changes in the noise correlation across the trial. However, spatial locations that are not in direct competition may exhibit different dynamics in their noise correlation across the same set of choices. To test this, we varied the spatial design of the task such that one of the choice targets lay inside a cell's RF, and the other lay diametrically opposed to it such that the second target did not excite either cell's RF. This orientation allowed for 2 possible competitive scenarios for the recorded cells: 1) if the monkey chooses the in RF target, that target is not only competing with the target diametrically opposed, but the other cell which is encoding only empty space, and 2) if the monkey chooses the target encoded by neither RF, the 2 cells being recorded from are no longer in competition. If targets only compete with each other, we might expect the correlation between the 2 cells in this to be identical, regardless of the monkeys' choice.

However, if an individual target competes with the whole map, then we might see difference in the time course of the correlation.

We tested this in a subpopulation of cell pairs (n=33 pairs) with each recorded pair divided into choices to the in RF target and choices to the out or RF target (Figure 4.13A). For simplicity during experimentation, we restricted task design to include only trials where the reward ratio was equal to 0.5. As expected, there were deviations in the spike count between the these 2 choices (Figure 4.13B, solid lines) for the responses to the cell encoding target 1, with choices to that target having a higher spike count prior to the saccadic decision. However there were no significant differences in the spike count for the cell that encoded a patch of empty space, regardless of which target the monkey chose.

When we calculated the average Pearson correlation for each of the saccadic decisions for each cell pair we found striking differences in the magnitude of the correlation in the epoch prior to the saccade (Figure 4.13C). Both choices (saccade to inRF target and saccade to noRF target) had highly positive correlations during the baseline epoch and following the target onset, both groups begin to decorrelate, but 500ms after the onset of the targets, the correlations begin to deviate from each other (Figure 4.13C, left). When aligned to the saccade (Figure 4.13C, right), choices to the inRF target are significantly lower than choices to the out of RF saccade. Though differences in the spike count could potentially account for differences in the correlations, the differences in spike count observed in this experiment go the opposite direction of that prediction: spike counts are higher for the in RF choices, though Pearson correlation coefficients are lower.

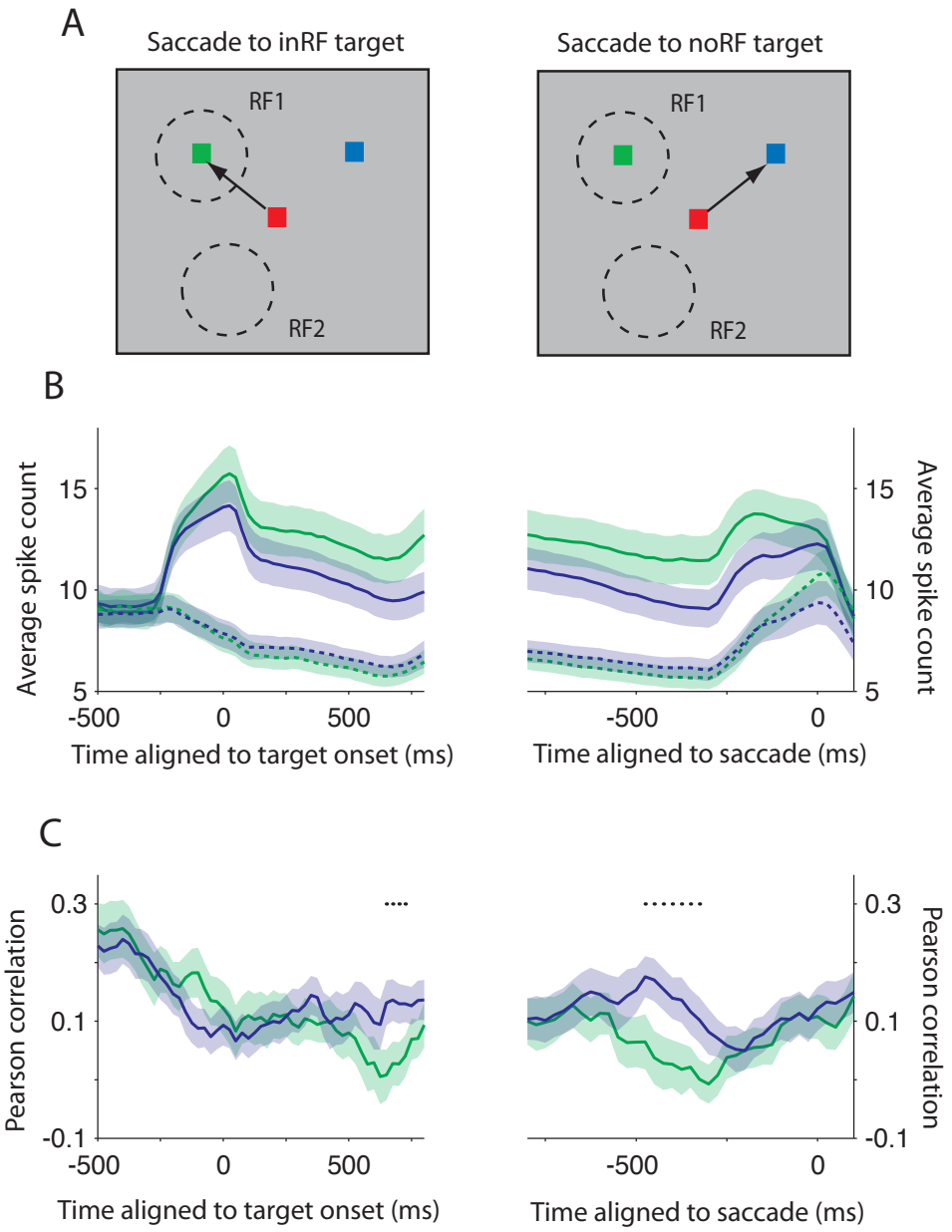

Figure 4.13 Targets compete with non-target locations.
A) "Empty" RF task: configuration of stimuli. Target 1 was placed inside RF1, but Target 2 was placed diametrically opposite target in RF1. RF2, the "empty" RF was not excited by either Target 1 or Target 2. If monkey chooses T1, RF 1 may compete with all spatial locations, including empty RF (left), but if monkey chooses T2, RF1 and RF2 are not in competition (right). B) Average spike counts for a sub-population of cell pairs (n=33 cell pairs) used in the paradigm shown in A. Responses show activity in RF1 (solid lines) when monkey choose T1 (green) and T2 (blue). Activity in RF2 (dotted lines), where there is no stimulus, is shown for the same choices. Spike counts are for 300 ms bins and are shown aligned to the target onset (left) and to the saccade (right). C) Average Pearson correlation coefficients for the spike counts shown in B for choices to T1 (green) and choices to T2 (blue). Correlations are lower earlier for choices to targets in RF1. Dots show significant bins ($p<0.05$ Wilcoxon signed rank test).

These results indicate that the timing and amount of decorrelation during a saccadic decision depends on the distinct spatial configuration of the choice being made. When response fields represent spatial locations that are in direct competition, this is reflected in the reduced correlation across the trial.

4.5 Discussion

We demonstrate that pairs of cells with non-overlapping RFs have correlated spontaneous activity while monkeys are passively fixating on a central target. While monkeys chose between 2 saccade targets, this correlated activity decreases over the course of the trial. A key finding is that the degree of correlation encodes information about the history of rewards and is reflected in the latency of upcoming saccades, suggesting that noise correlation between neurons are influenced by top-down mechanisms and represent the motivational state of the monkey. The amount of decorrelation between LIP neurons is also decreased between neurons that are not in direct competition with each other, indicating that there is a spatial specificity to these changes during a choice.

Few previous studies have looked at interneuronal correlations in the parietal cortex and none to date have isolated the contributions of "noise" from variability associated with a particular stimulus or behavioral outcome. In areas 2 and 5 of the parietal cortex, neurons recorded simultaneously on the same electrode were found to have a consistent relationship between the amount of stimulus evoked noise (signal correlation) and the amount of correlated

noise in the spontaneous activity though this effect was abolished at neuronal distances greater than 1.5mm (Lee et al., 1998). In contrast, the electrode tips in the current study were separated a minimum of 2mm in cortex, and significant correlations were observed in the spontaneous activity in almost all pairs.

4.51 Possible mechanisms of correlation and decorrelation

Since noise correlations cannot arise de novo and by definition cannot arise purely from intrinsic independent noise within each cell, they are indicative of either a common input or reciprocal connectivity between cells in LIP

During the choice task, LIP neurons are likely receiving input from a number of different areas. They receive spatially specific visual input about the locations and properties of visual stimuli in the world from areas V4 and V1. Along with the frontal eye fields and the superior colliculus, they can encode a signal related to the decision process or spatial attention. LIP neurons also receive a number of ascending non-spatial signals from the brainstem (Baizer et al., 1993). The correlated activity between widely separated neurons in the pre-target epoch likely arises from a non-spatial signal and these inputs are likely candidates that would act to synchronize the LIP map on each trial.

The dynamics of the reduction in correlation suggests a change in the functional connectivity between cells representing competing options over the course of the decision. Several previous studies have found changes in noise correlations that depend on the parameters of the task. In MT correlations between neurons were increased when the information encoded by individual neurons could be pooled to solve the task (Cohen and Newsome, 2008). In FEF,

the degree of correlation between neurons during a visual search task depended on the location of the search target, showing greater competition and reduced correlations when the target was restricted to a location that excited a single neuron (Cohen et al., 2010). In both cases, the authors suggest that mutual inhibition between cortical neurons can serve to taper the amount of shared variability, so that information can be pooled in cases of large amount of shared variability, and separated during competitive interactions.

In this study, we have taken this further by excluding any component of shared variability due to the visual stimulus and we have tailored the task and stimuli to explore the specific relationship between cells that represent spatial locations that should be in direct competition. Our results show that sources of shared variability are reduced over the duration of the trial. This could occur mechanistically in two distinct ways. First, sources of shared variability may simply decrease during the decision. Second, mutual inhibition between competing neurons could actively change the amount of shared variability between cells.

Of course these hypotheses are not mutually exclusive, but several lines of evidence lend support to the latter. First, a quarter of cell pairs (far more than predicted by chance) change from a positive correlation in the pre-target epoch to a negative correlation in the pre-saccadic epoch. But more importantly, shared variability is decreased in a spatially specific manner during the course of the decision, as evidenced by the empty RF task. If synchronous inputs to the whole LIP map cause trial-to-trial fluctuations, decreases in this input would be apparent regardless of which spatial location was encoded by the cells' RF. Instead, this spatially specific decrease suggests that mutual suppressive interactions are only engaged between competing alternatives (even if one of the alternatives signals only a *potential* saccade target, not an *actual*

saccade target) and not when spatial locations are not in competition. LIP, which has been previously shown to reflect "push-pull" interactions using surround suppressive mechanisms, may implement competition using surround suppressive mechanisms (Falkner et al., 2010).

A failure to detect a negative correlation coefficient in a majority of cases is not, on its face, counter evidence for mutual inhibition. One caveat of using large bin sizes is that subtle circuit dynamics that occur on a shorter timescale (i.e. 10's of ms as opposed to 100's of ms) are effectively washed away when spike counts computed using the large bins. This is, however, necessary computationally, since very small bin sizes contain far fewer spikes and will violate assumptions of normality implicit in calculating the noise correlation. A reduced but non-zero correlation coefficient during the pre-saccadic epoch is not counter evidence for mutual inhibition, and could reflect an incomplete suppression of shared variability from an common input.

The magnitude of the correlations observed in the pre-target epoch is on the order of correlations observed in other previous studies of noise correlations in cortex. In V1 the amount of correlation shared between 2 neurons was found to vary with distance between the physical distance between the electrodes such that correlations had varying spatial extents (Smith and Kohn, 2008). In the motor cortex and macaque parietal areas 2 and 5, shared neuronal noise varied only for small inter-electrode distances (Lee et al., 1998). Though we did not systematically vary this parameter in this study (the distance between the neurons was constrained by where we could isolate individual neurons with non-overlapping RFs) we did not find any evidence that the amount of positive correlation in the pre-stimulus epoch varied with the distance between the RFs. This finding is in line with the difference in local anatomy

between V1 and LIP. V1 architecture has cortical columns that represent a fine topological representation with extensive local connectivity, while LIP neurons have been shown to much more broadly connected with very little topography (Baizer et al., 1991; Ben Hamed et al., 2001). This interconnectivity would make it possible for LIP neurons to share information across larger spatial distances than the more constrained V1.

Several studies have suggested that cortical neurons may share variability by gamma synchronization across large spatial extents and across brain areas (Fries et al., 2001). We found that a quarter of neuron pairs had an increased incidence of coincident spikes, and that this coincidence disappeared in the epoch prior to the saccade in all but one neuron pair. These data would be consistent with a hypothesis in which a distributed form of arousal encompasses both RFs in the pre-target epoch, in some cases synchronizing the activity of the cells. This coincident spiking disappears and neurons de-synchronize when spatial attention is focused on one of the RFs.

4.52 Correlations and behavioral significance

We found that the monkeys' saccade latency during this choice task explicitly reflected information about the monkeys' history of reward. A trial-to-trial measure of the accumulated previous rewards was negatively correlated with the latency of the upcoming saccade: when more rewards were obtained recently, saccades to choice targets were faster. This metric demonstrated to us that the monkeys' reward history was an indicator of the motivational or attentional state of the monkey on that particular trial, and his latency was an appropriate behavioral readout. When trials were grouped according to similar reward histories, we found

that the correlation within each of these groups encoded information about this behavioral state of the monkey. These changes in motivational/attentional state modulated the amount of shared variability far more than the actual spike count, which differed the highest and lowest reward history groups only by about ~0.5 spikes.

This is consistent with several previous studies that show that spatial attention in V4 is accompanied by a decrease in interneuronal correlations (Cohen and Maunsell, 2009; Mitchell et al., 2009). Though we are not measuring attention per se in this task, we would argue that our free choice task accesses a mechanism that is common to both decision processes and to spatial attention. In both cases, the decorrelation could represent attention being allocated to a particular choice target and arguably monkeys are attending more when they are doing well (i.e. in this case harvesting many rewards by allocating his choices appropriately). We believe what we have demonstrated reveals a general mechanism that may be employed across many cortical areas during tasks that require visuo-spatial selection.

Previous studies have attempted to quantify the relationship of past rewards to the monkeys choice behavior and have produced generative models which make predictions about upcoming decisions (Corrado et al., 2005; Lau and Glimcher, 2005). In this study we took a different approach and merely using the total stream of incoming rewards as a prediction of the state of the monkey. This approach is validated by the fact that the total stream of rewards is a much better predictor of the upcoming saccade latency that an estimate of rewards to a particular target.

Previous studies have also found that firing rates in LIP vary with the expected reward of the visual stimulus (Platt and Glimcher, 1999). We found weak though non-specific modulation

of firing rate as a function of the absolute relative reward of the acquired target, though this is possibly due to differences in the task design. By using a foraging task where targets remained baited until chosen, the actual reward probability of a given target increases as it is left unchosen. This suggests that in our task, when the monkey selected targets that had low relative rewards at a lower rate, each choice had a higher probability of being rewarded.

4.53 Functional implications of correlations for priority maps

Changes in the mean spike rate can affect the relative salience of peaks on LIP's priority map and the ease with which a winner can be selected. In addition to changes in the means, the precision of LIP's representation can potentially be improved by reducing the variability of LIP neuronal responses (Paradiso, 1988; Vogels, 1990). Attentional processes decrease the amount of neural variability, which results in higher reliability of spiking at the attended receptive field, allowing higher discriminiability by enhancing the signal to noise ratio. The results of this study suggest that decreasing the amount of shared variability is associated with changes in the relative salience of competing neural representations.

During an ongoing decision, competing neurons move from having shared noise, to having relatively independent noise. Since long saccade latencies accompanied trials where neurons share more variability, this noise may act as a hindrance to the decision process. This result is in line with several studies that show that positive correlations can limit the amount of information processed by a network. In V1, positive correlations between cells have been shown to reduce the amount of Fisher Information about the encoded stimulus (Kohn and Smith, 2005), and in MT, even small amount of correlations between cells have been shown to limit the

psychophysical benefits of pooling across cell populations (Zohary et al., 1994; Bair et al., 2001). These results indicate that populations of cells with reduced shared variability can more reliably signal stimulus information. This has direct implications for LIP, a brain area that signals the location of an upcoming saccade. Shared variability across neurons that represent competing saccade locations could potentially result in less reliable or slower saccades, since it may take longer for a "winning" location to emerge.

Models of visual attention and saccadic selection routinely invoke mutually suppressive interactions between competing alternatives to resolve competition. Our data is consistent with such a model, and suggests that motivation or attentional allocation can be implemented by adjusting the gain on this mutual suppression in a competitive-cooperative circuit. This would have the dual effect of reducing spike rates and reducing the amount of variability to a particular stimulus. These data also suggest that decision-making models that propose that neurons with independent variability race to a threshold are an incomplete description of the processes occurring during saccadic choice. Instead, non-independent noise is actively reduced until the amount of shared variability approaches 0 prior to the behavioral readout of the choice.

Chapter 5: Conclusions

5.1 Summary

When multiple stimuli in the visual world compete for your limited attentional resources there are winners and losers. The winners become the loci of attention and possibly the target of the next saccade while the losers are ignored. In the brain, neural representations of events in the real world are locked in a constant struggle, an invisible fight of ever changing players. This body of work describes several mechanisms at work during these competitive processes and explores the dynamics of how attention is allocated to a winning spatial location and a saccade is initiated. We have examined the responses of neurons in monkey LIP during a series of saccadic tasks where monkeys were required to prioritize certain spatial locations and make timed eye movements to them. LIP neurons encode the priority of spatial locations, combining incoming sensory information with cognitive signals that carry information about the nature of the stimulus in the receptive field, reward and the motivational state of the monkey. In each set of tasks, we modulated the monkeys' motivation by changing the expected reward or probability of reward and looked for corresponding changes in saccadic behavior.

We first probed competitive processes in LIP by asking a very simple question: How do we ignore distracting events? We recorded the responses to distractors in LIP and required the monkey to make a series of planned eye movements to saccade targets at various spatial locations. We discovered that neurons have large, spatially tuned suppressive surrounds such that when monkeys plan saccades to particular regions of space, the response to the distracting stimulus is maximally reduced. This suppression can occur even when the monkey is planning a

saccade to a remembered location, suggesting that the genesis of this suppression is from a brain area that is active during this memory period. Suppression of the distractor can be evoked by the target stimulus, but concurrent suppression of the target response can be evoked by the flash of the distractor, suggesting that these interactions are implemented by a mutually suppressive mechanism.

We modulated the monkeys' motivation in this task by cueing him to expect a large reward on some trials and a small reward on others. When monkeys expect a large reward, target representations in LIP are enhanced and distractor representations are reduced. The opposite is true for small reward trials, which are associated with low target responses and high distractor responses. The monkeys' saccadic behavior also mirrored these changes. On small reward trials, monkeys made more errors, and had much slower saccade latencies. Saccade latencies have positive trial-to-trial correlations with the neural activity at the distractor, which suggests that a high distractor response is directly related to the monkeys' behavior on that particular trial. These experiments demonstrate that modulations in firing rate, specifically suppression of task irrelevant visual stimuli in LIP have a direct relationship with saccade behavior and task performance. Increases in firing rates at attended locations are coupled with decreases in firing rates at ignored locations, allowing a winner to emerge easily on LIPs priority map.

Competitive processes can also be stymied by unreliable signals. Increasing the fidelity of neural signals can increase the discriminability between competing visual stimuli and allow for ease of target selection. We next explored whether neurons in LIP reflect changes in the variability of neural signals during a saccade task. We found that surround suppression in LIP, in addition to reducing spike rates at unattended locations, can also increase the reliability of

signals by decreasing the amount of across-trial variability of the neural response. Neural variability decreases at the location of the saccade target following the onset of the visual stimulus, but non-target locations also show decreases in neural variability. The amount of variability reduction at a spatial location is strongly modulated its distance from the target location such that farther locations have greater amounts of reduction. There is a strong relationship between the spike counts and the variability: high spike counts are associated with high amount of variability, demonstrating that these effects are not driven by changes in firing rate alone. This suggests a common mechanism such as surround suppression might drive both changes in firing rate and changes in the variability.

Decreases in across-trial variability are observed in both the representation of the target and the distractor when expected reward is high, which suggests that the whole LIP map may be more reliable when the monkeys' motivation is strong to complete the task. Changes in variability also have important behavioral consequences for the monkey. During a memory guided saccade task, reduced variability around the time of the go cue is associated with faster and more accurate saccades, without concurrent changes in firing rates. These differences disappear prior to the saccade itself, suggesting that it is the reliability of the signal at the time of the cue that most significantly affects behavior.

Neurons in LIP may change their functional connectivity as a result of competitive decision processes. This can be assessed by looking at the amount of shared variability or neural noise between multiple neurons. Neurons in LIP that are widely separated in cortex and do not share stimulus-evoked activity are correlated in the epoch prior to the appearance of the saccade targets. In a task where monkeys were required to make a free saccadic choice between two

saccade targets that appeared in the receptive field center of each neuron and did not drive the activity of the competing neuron, the amount of noise correlation between neurons decreased over the course of the trial, reaching its nadir in the epoch prior to the saccade.

The motivational and attentional state of the monkey also affects the competitive processes occurring in LIP. During the choice task, the targets were associated with different probabilities of reward, and monkeys allocated their choices accordingly. Saccade latency in this, a primary indicator of motivation, was significantly affected by the monkeys' history of previous rewards: when monkeys had gotten many previous rewards, saccade latencies were faster than if he had gotten few rewards on the previous trials. When sorted by a measure of total history of previous rewards on each trial, the correlation between neurons was greater when monkeys had gotten few previous rewards. Correlations, but not spike rates, encoded information about the monkeys' motivational state, suggesting that correlations provide an extra channel of information and that studies of single cells in LIP provide an incomplete description of the dynamics that occur during saccadic choice. Moreover, these data are evidence against models of saccadic choice that suggest that neurons compete via an independent race-to-threshold mechanism. Instead, noise is correlated between competing pools of neurons when targets appear and the level of independence is modulated by the cognitive state of the monkey.

The take-home message from these studies is that changes in firing rates, across-trial variability, and shared variability occur during saccadic choices, and these changes can have important implications for behavior. During this time, faster saccades are accompanied with increased firing rates at target locations and decreased firing rates at non-target locations. To our surprise, these changes are also accompanied by increases in the reliability of the neural signal,

and decreased shared variability. These changes allow peaks on LIP's priority map to become more separated and provide a mechanism for ease of target selection.

A note about the tricky relationship between firing rates, variability, and noise correlation

During the same trial, LIP neurons can undergo changes in firing rates, independent variability, and shared variability. Sometimes these changes co-occur within the same epoch, and during other epochs, a change can occur within one variable without a concurrent change in another, suggesting that they can be modulated in an independent manner. For example, changes in the independent variability of a neuron accompany, but do not account for changes in the shared variability during a saccadic choice. Additionally, changes in firing rate accompany, but do not account for a drop in Fano factor.

Instead, it suggests a more complex relationship between firing rates and variability than previously appreciated. In truth there are few good ways to assess changes in variability when firing rates are also changing. Fano factor does a particularly poor job of this, since this measure can change directly even when there is no change in variability. Our best estimates of the contribution of variability reduction can be made over epochs where the firing rate changes very little or not at all. Correlations, which are a direct measurement of the co-variation between multiple neurons are also difficult to disentangle from changes in independent variability. The Pearson correlation, our chosen measure of the shared variability between neurons is not insensitive to changes in the independent variance of each neuron since it is scaled by the standard deviation of each distribution of the underlying spike counts. This normalization

implies that increases in these variances will result in a decrease in the Pearson correlation if the amount of shared variability is constant.

5.2 A proposed model

What kinds of circuits could mediate these types of competitive interactions? A serious limitation of experimenting using single and multiple electrode recording techniques is that it allows you to conclude very little about circuitry. Even in the case of the paired cell recordings, it is highly unlikely that by randomly inserting our electrodes into several square millimeters of cortex that we will be recording from two cells that are physically connected. When we observe correlations (and especially negative correlations) on these time scales (i.e. several hundred ms), we do not mean to suggest that these cells are physically mutually connected. Rather, they are part of a population of cells that is jointly encoding the location of a salient event and over repeated trials, responses co-vary with a secondary population of cells that is encoding a second spatial location.

Let us take each of the results in turn. Chapter 2 demonstrates that the responses to a distracting stimulus during the baseline and the on response are suppressed when a target appears outside the excitatory RF of a given neuron. These results are consistent with a circuit that includes long-range excitation and shorter-range mutual suppression between competing spatial locations. Several lines of evidence suggest this particular circuitry. First, the effects of surround suppression in LIP are spatially tuned. Though LIP does not have a strict topography, there is clustering of cells representing distinct spatial locations. This would suggest that neurons in LIP do not have random connectivity and instead have an architecture that would

support more spatially selective connections. The fact that the suppressive effects are patchy and unsystematic within single cells lends further support to this. Second, increased target responses are coupled with decreased distractor responses. This is suggestive of a mutual inhibitory circuitry because the increased target response would activate inhibitory cells and generate the suppression necessary to make the representations of spatial events more discriminable on LIP's priority map (Figure 5.1).

An alternative hypothesis that could account for much of this data would be that it is generated by an attentional mechanism with a single "enhancement" feature. In this model, spatial attention (or something akin to it) could alight on a spatial location and turn up the gain of responses at that particular location, resulting in a *relative* suppression of the responses to stimuli at competing spatial locations. While this could certainly account for the increased response at the target location, this would be insufficient to explain the distinct spatial tuning observed at both the single cell level and across the population.

We also found that across-trial variability is reduced at spatial locations that are widely separated from the target. Close spatial locations are associated with the most variability reduction and far spatial locations have the most variable responses. This is also consistent with a circuitry of spatially tuned mutual suppression. Since the lowest firing rates in the surround of LIP are also the least variable, we propose that inhibitory circuits activated by the target response affects the across-trial variability of the target response by raising the threshold necessary to evoke spikes at competing spatial locations. This would in effect reduce average firing rates and trim spikes from the most variable, noisy responses, resulting in a decreased Fano factor.

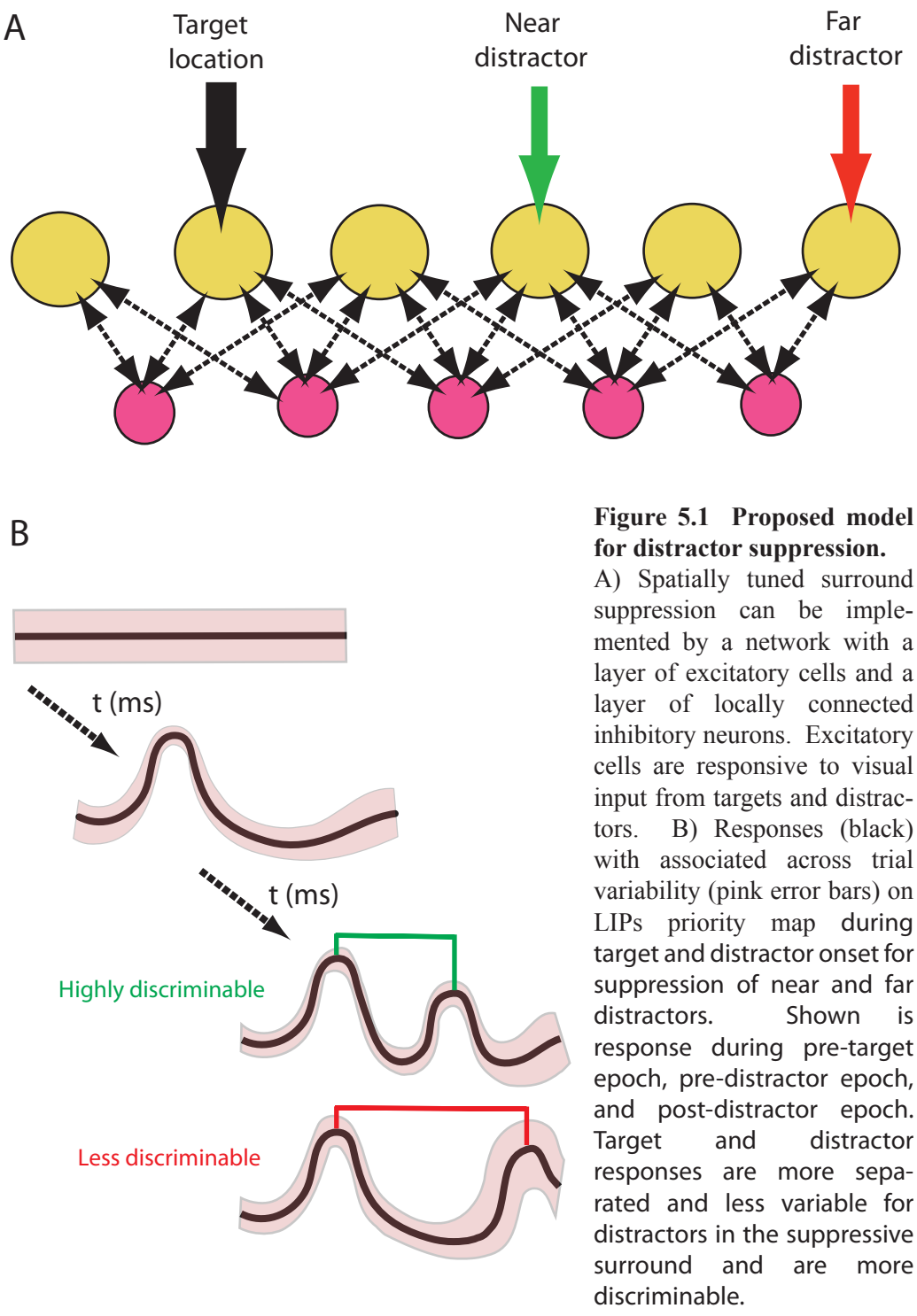

Figure 5.1 Proposed model for distractor suppression. A) Spatially tuned surround suppression can be implemented by a network with a layer of excitatory cells and a layer of locally connected inhibitory neurons. Excitatory cells are responsive to visual input from targets and distractors. B) Responses (black) with associated across trial variability (pink error bars) on LIPs priority map during target and distractor onset for suppression of near and far distractors. Shown is response during pre-target epoch, pre-distractor epoch, and post-distractor epoch. Target and distractor responses are more separated and less variable for distractors in the suppressive surround and are more discriminable.

Using paired recording techniques, we also found that the responses of multiple neurons reduced the amount of shared variability (as assessed by noise correlations) prior to the saccadic choice.

Pairs of neurons have significantly positive correlations in the spontaneous activity prior to the target onset and this noise is decreased over the duration of the choice, reaching its nadir in the epoch directly prior to the eye movement. It is likely that this initial correlation arises from a shared, non-spatial input, since the correlation is not restricted to pairs of cells that encode potential saccade targets. Instead, even neurons that respond to blank portions of the screen (see the "empty RF" task) are correlated with target encoding neurons. Additionally, this correlation is likely derived from a non-spatial input because it is significant regardless of what the upcoming choice will be. This correlation carries information about the reward history of the monkey and is directly related to the upcoming saccade latency, a measure of the monkeys' motivational state.

This pre-target correlation quantifies the amount to which this shared non-spatial input can synchronize the cells in the LIP map. The changes in shared variability in this epoch could be implemented by inhibitory neurons that act to stabilize the network. They cannot be directly mediated by a change in the shared input itself, since that would modulate the firing rates of the neurons in addition to the correlations. Instead, mutual inhibition could modulate the *state of the network* during a given trial, depending on cognitive variables such as reward history. Reduced correlation during this epoch places the network in a state of readiness and allows for faster saccades since the correlation is decreased at an earlier timepoint relative to the go-cue. The onset of the targets further stabilizes the network, moving the neurons from a regime where their noise is correlated to where their noise is largely independent. Simply adding variability to a single neuron (via a spatial attention signal or visual input signal) cannot in itself, account for the changes in noise correlation in the pre-target epoch. The Pearson correlation measures how

much activity between neurons co-varies and is scaled by the standard deviations of the single neurons. An increase in independent noise at one (or both) location(s) would result in a decrease in Pearson correlation in the pre-target epoch. In the pre-saccadic epoch, the decrease in correlation could, in principle, be due to an increase in independent noise in one of the recorded neurons. However, what is observed in LIP is an overall decrease in neural variability over the course of the trial, reaching its nadir prior to the movement.

Previous work has demonstrated that stimulus onset is associated with both a drop in the shared variability and the independent variability in several cortical areas, including LIP. Our data suggests that this occurs by the de-synchronization of the network from a non-spatial input that contains relevant information about previous rewards. These data are consistent with computational descriptions of competitive networks that use a single parameter (the gain of inhibition) to modulate the state of the network at a given time (Moldakarimov et al., 2005).

5.3 Broader implications

5.31 Is this happening within LIP?

A valid question is whether these processes are occurring within LIP. The current data do not allow us to definitively assess this, and since LIP shares many of the same properties with other areas in the attentional-oculomotor network, such as the SC and the FEF, it is possible that these interactions (including mutual inhibitory interactions) are a phenomenon of the larger network. Many of these properties (specifically ones that are mediated by a present visual stimulus) may also be computed at other levels of visual processes such that they are “inherited”

from their inputs. Other processes, such as suppression evoked by the memory of a stimulus, must emerge from areas, such as LIP, that maintain a focalized bump of activity during a working memory oculomotor task. However it is important to remember that to date, *no property* described in LIP has been shown to occur exclusively within LIP, and instead, we believe that these interactions could represent more general phenomena that occur in cortical networks when competitive decisions are made and are not specific to LIP.

5.32 A word about attention

LIP neurons encode information about the locus of attention, and the results in this thesis can also be framed in this light. For example, the response increase at the target locations and concurrent response decrease at the distractor location can be described as attention deployed to the location of the target and removed from the location of the distractor. The decorrelation observed during the decision process could concurrently be described as an allocation of spatial attention to one target location.

While these explanations provide an excellent psychophysical description of the processes occurring during these experiments, what is needed is a complete description of how attentional processes are implemented. We propose that the changes observed in these studies (changes in firing rate, variability, and noise correlation) provide the actual mechanism by which attention is deployed and a winner is chosen on LIP's map.

5.4 Future directions

From this body of work, a number of testable predictions can be generated that will further increase our understanding of attention, saccade selection, and competitive decision-making. I will outline several experiments that could serve as "next steps" to further validate the hypotheses in this body of work.

Psychophysics

The nature of LIP's spatially tuned suppressive surround suggests several immediate psychophysical questions. Are we more distracted by visual stimuli at the edge of the surround, where responses are higher and more variable? Our data did not have a sufficient number of error trials to test this, but a modified task with fewer assayed locations could probe this question in more depth. What is the relationship between surround suppression and perception? Is there a spatial "blind spot" created by surround suppression? This can be probed using a task that varies the spatial relationship between an attended stimulus and a subthreshold stimulus to be discriminated that occasionally appears in the suppressive surround of the attended stimulus.

Physiology

What is the relationship between neural variability and perception? Is there an "optimal subspace" for attention or choice? Previous research has suggested that motor preparatory activity has reduced variability prior to the movement and converges upon an optimal mean for a

particular movement. An interesting question would be to look more closely at the reliability of neural signals that encode spatial attention.

Pharmacology

A further step would be to employ pharmacology loss of function experiments to test the prediction that inhibition within LIP is involved in distractor suppression and saccadic decision-making. A testable hypothesis would be to inject Bicuculline (a $GABA_A$ antagonist) into LIP during the choice task. If inhibition is involved in stabilizing the network during the spontaneous activity, we may see the saccade latency effect with previous reward abolished. Alternatively, if we pharmacologically enhance the amount of inhibition in LIP with muscimol, we may see deficits in choice behavior that reflect an inability to decide between the competing options.

5.5 General conclusions

We have demonstrated that neurons in the lateral intraparietal area employ surround suppressive mechanisms to reduce the firing rates and the neural variability of the representations of competing spatial locations. Furthermore, we demonstrate that shared variability between competing options is modulated as a function of the cognitive state of the monkey. We believe these data shed light on the mechanisms the brain uses during attention, saccade selection, and free choice between competing options.

References

Abbott LF, Dayan P (1999) The effect of correlated variability on the accuracy of a population code. Neural Comput 11:91-101.

Adair JC, Barrett AM (2008) Spatial neglect: clinical and neuroscience review: a wealth of information on the poverty of spatial attention. Ann N Y Acad Sci 1142:21-43.

Alitto HJ, Usrey WM (2008) Origin and dynamics of extraclassical suppression in the lateral geniculate nucleus of the macaque monkey. Neuron 57:135-146.

Allman J, Miezin F, McGuinness E (1985a) Stimulus specific responses from beyond the classical receptive field: neurophysiological mechanisms for local-global comparisons in visual neurons. Annu Rev Neurosci 8:407-430.

Allman J, Miezin F, McGuinness E (1985b) Direction- and velocity-specific responses from beyond the classical receptive field in the middle temporal visual area (MT). Perception 14:105-126.

Andersen RA (1997) Multimodal integration for the representation of space in the posterior parietal cortex. Philos Trans R Soc Lond B Biol Sci 352:1421-1428.

Andersen RA, Asanuma C, Cowan WM (1985) Callosal and prefrontal associational projecting cell populations in area 7A of the macaque monkey: a study using retrogradely transported fluorescent dyes. J Comp Neurol 232:443-455.

Andersen RA, Bracewell RM, Barash S, Gnadt JW, Fogassi L (1990) Eye position effects on visual, memory, and saccade-related activity in areas LIP and 7a of macaque. J Neurosci 10:1176-1196.

Andersen RA, Snyder LH, Batista AP, Buneo CA, Cohen YE (1998) Posterior parietal areas specialized for eye movements (LIP) and reach (PRR) using a common coordinate frame. Novartis Found Symp 218:109-122; discussion 122-108, 171-105.

Angelucci A, Bressloff PC (2006) Contribution of feedforward, lateral and feedback connections to the classical receptive field center and extra-classical receptive field surround of primate V1 neurons. Prog Brain Res 154:93-120.

Arieli A, Sterkin A, Grinvald A, Aertsen A (1996) Dynamics of ongoing activity: explanation of the large variability in evoked cortical responses. Science 273:1868-1871.

Armstrong KM, Chang MH, Moore T (2009) Selection and maintenance of spatial information by frontal eye field neurons. J Neurosci 29:15621-15629.

Asanuma C, Andersen RA, Cowan WM (1985) The thalamic relations of the caudal inferior parietal lobule and the lateral prefrontal cortex in monkeys: divergent cortical projections from cell clusters in the medial pulvinar nucleus. J Comp Neurol 241:357-381.

Assad JA (2003) Neural coding of behavioral relevance in parietal cortex. Curr Opin Neurobiol 13:194-197.

Averbeck BB, Latham PE, Pouget A (2006) Neural correlations, population coding and computation. Nat Rev Neurosci 7:358-366.

Avillac M, Deneve S, Olivier E, Pouget A, Duhamel JR (2005) Reference frames for representing visual and tactile locations in parietal cortex. Nat Neurosci 8:941-949.

Ayaz A, Chance FS (2009) Gain modulation of neuronal responses by subtractive and divisive mechanisms of inhibition. J Neurophysiol 101:958-968.

Bair W, Zohary E, Newsome WT (2001) Correlated firing in macaque visual area MT: time scales and relationship to behavior. J Neurosci 21:1676-1697.

Baizer JS, Ungerleider LG, Desimone R (1991) Organization of visual inputs to the inferior temporal and posterior parietal cortex in macaques. J Neurosci 11:168-190.

Balan PF, Gottlieb J (2006) Integration of exogenous input into a dynamic salience map revealed by perturbing attention. J Neurosci 26:9239-9249.

Balan PF, Oristaglio J, Schneider DM, Gottlieb J (2008) Neuronal correlates of the set-size effect in monkey lateral intraparietal area. PLoS Biol 6:e158.

Ben Hamed S, Duhamel JR, Bremmer F, Graf W (2001) Representation of the visual field in the lateral intraparietal area of macaque monkeys: a quantitative receptive field analysis. Exp Brain Res 140:127-144.

Bisley JW, Goldberg ME (2003a) Neuronal activity in the lateral intraparietal area and spatial attention. Science 299:81-86.

Bisley JW, Goldberg ME (2003b) The role of the parietal cortex in the neural processing of saccadic eye movements. Adv Neurol 93:141-157.

Bisley JW, Goldberg ME (2006) Neural correlates of attention and distractibility in the lateral intraparietal area. J Neurophysiol 95:1696-1717.

Bisley JW, Krishna BS, Goldberg ME (2004) A rapid and precise on-response in posterior parietal cortex. J Neurosci 24:1833-1838.

Blatt GJ, Andersen RA, Stoner GR (1990) Visual receptive field organization and cortico-cortical connections of the lateral intraparietal area (area LIP) in the macaque. J Comp Neurol 299:421-445.

Bremmer F, Duhamel JR, Ben Hamed S, Graf W (2002) Heading encoding in the macaque ventral intraparietal area (VIP). Eur J Neurosci 16:1554-1568.

Bruce CJ, Goldberg ME, Bushnell MC, Stanton GB (1985) Primate frontal eye fields. II. Physiological and anatomical correlates of electrically evoked eye movements. J Neurophysiol 54:714-734.

Brunel N (2003) Dynamics and plasticity of stimulus-selective persistent activity in cortical network models. Cereb Cortex 13:1151-1161.

Bushnell MC, Goldberg ME, Robinson DL (1981) Behavioral enhancement of visual responses in monkey cerebral cortex. I. Modulation in posterior parietal cortex related to selective visual attention. J Neurophysiol 46:755-772.

Caputo G, Guerra S (1998) Attentional selection by distractor suppression. Vision Res 38:669-689.

Carpenter RH, Williams ML (1995) Neural computation of log likelihood in control of saccadic eye movements. Nature 377:59-62.

Chen Y, Martinez-Conde S, Macknik SL, Bereshpolova Y, Swadlow HA, Alonso JM (2008) Task difficulty modulates the activity of specific neuronal populations in primary visual cortex. Nat Neurosci 11:974-982.

Churchland AK, Kiani R, Shadlen MN (2008) Decision-making with multiple alternatives. Nat Neurosci 11:693-702.

Churchland AK, Kiani R, Chaudhuri R, Wang XJ, Pouget A, Shadlen MN (2011) Variance as a signature of neural computations during decision making. Neuron 69:818-831.

Churchland MM, Santhanam G, Shenoy KV (2006a) Preparatory activity in premotor and motor cortex reflects the speed of the upcoming reach. J Neurophysiol 96:3130-3146.

Churchland MM, Yu BM, Ryu SI, Santhanam G, Shenoy KV (2006b) Neural variability in premotor cortex provides a signature of motor preparation. J Neurosci 26:3697-3712.

Churchland MM et al. (2010) Stimulus onset quenches neural variability: a widespread cortical phenomenon. Nat Neurosci 13:369-378.

Cohen JY, Crowder EA, Heitz RP, Subraveti CR, Thompson KG, Woodman GF, Schall JD (2010) Cooperation and competition among frontal eye field neurons during visual target selection. J Neurosci 30:3227-3238.

Cohen MR, Newsome WT (2008) Context-dependent changes in functional circuitry in visual area MT. Neuron 60:162-173.

Cohen MR, Maunsell JH (2009) Attention improves performance primarily by reducing interneuronal correlations. Nat Neurosci 12:1594-1600.

Colby CL, Goldberg ME (1999) Space and attention in parietal cortex. Annu Rev Neurosci 22:319-349.

Colby CL, Duhamel JR, Goldberg ME (1996) Visual, presaccadic, and cognitive activation of single neurons in monkey lateral intraparietal area. J Neurophysiol 76:2841-2852.

Constantin AG, Wang H, Martinez-Trujillo JC, Crawford JD (2007) Frames of reference for gaze saccades evoked during stimulation of lateral intraparietal cortex. J Neurophysiol 98:696-709.

Constantin AG, Wang H, Monteon JA, Martinez-Trujillo JC, Crawford JD (2009) 3-Dimensional eye-head coordination in gaze shifts evoked during stimulation of the lateral intraparietal cortex. Neuroscience 164:1284-1302.

Constantinidis C, Wang XJ (2004) A neural circuit basis for spatial working memory. Neuroscientist 10:553-565.

Constantinidis C, Williams GV, Goldman-Rakic PS (2002) A role for inhibition in shaping the temporal flow of information in prefrontal cortex. Nat Neurosci 5:175-180.

Cook EP, Maunsell JH (2004) Attentional modulation of motion integration of individual neurons in the middle temporal visual area. J Neurosci 24:7964-7977.

Corbetta M, Akbudak E, Conturo TE, Snyder AZ, Ollinger JM, Drury HA, Linenweber MR, Petersen SE, Raichle ME, Van Essen DC, Shulman GL (1998) A common network of functional areas for attention and eye movements. Neuron 21:761-773.

Corrado GS, Sugrue LP, Seung HS, Newsome WT (2005) Linear-Nonlinear-Poisson models of primate choice dynamics. J Exp Anal Behav 84:581-617.

de la Rocha J, Doiron B, Shea-Brown E, Josic K, Reyes A (2007) Correlation between neural spike trains increases with firing rate. Nature 448:802-806.

Deco G, Pollatos O, Zihl J (2002) The time course of selective visual attention: theory and experiments. Vision Res 42:2925-2945.

Desimone R, Schein SJ, Moran J, Ungerleider LG (1985) Contour, color and shape analysis beyond the striate cortex. Vision Res 25:441-452.

Desimone R, Moran J, Schein SJ, Mishkin M (1993) A role for the corpus callosum in visual area V4 of the macaque. Vis Neurosci 10:159-171.

DeSouza JF, Everling S (2004) Focused attention modulates visual responses in the primate prefrontal cortex. J Neurophysiol 91:855-862.

DeWeese MR, Hromadka T, Zador AM (2005) Reliability and representational bandwidth in the auditory cortex. Neuron 48:479-488.

Dias EC, Segraves MA (1999) Muscimol-induced inactivation of monkey frontal eye field: effects on visually and memory-guided saccades. J Neurophysiol 81:2191-2214.

Dorris MC, Glimcher PW (2004) Activity in posterior parietal cortex is correlated with the relative subjective desirability of action. Neuron 44:365-378.

Dorris MC, Olivier E, Munoz DP (2007) Competitive integration of visual and preparatory signals in the superior colliculus during saccadic programming. J Neurosci 27:5053-5062.

Duhamel JR, Colby CL, Goldberg ME (1998) Ventral intraparietal area of the macaque: congruent visual and somatic response properties. J Neurophysiol 79:126-136.

Egeth HE, Yantis S (1997) Visual attention: control, representation, and time course. Annu Rev Psychol 48:269-297.

Eifuku S, Wurtz RH (1998) Response to motion in extrastriate area MSTl: center-surround interactions. J Neurophysiol 80:282-296.

Eriksen CW, St James JD (1986) Visual attention within and around the field of focal attention: a zoom lens model. Percept Psychophys 40:225-240.

Falkner AL, Krishna BS, Goldberg ME (2010) Surround suppression sharpens the priority map in the lateral intraparietal area. J Neurosci 30:12787-12797.

Fecteau JH, Munoz DP (2006) Salience, relevance, and firing: a priority map for target selection. Trends Cogn Sci 10:382-390.

Freedman DJ, Assad JA (2006) Experience-dependent representation of visual categories in parietal cortex. Nature 443:85-88.

Friedman-Hill SR, Robertson LC, Desimone R, Ungerleider LG (2003) Posterior parietal cortex and the filtering of distractors. Proc Natl Acad Sci U S A 100:4263-4268.

Fries P, Reynolds JH, Rorie AE, Desimone R (2001) Modulation of oscillatory neuronal synchronization by selective visual attention. Science 291:1560-1563.

Gandhi NJ, Katnani HA (2010) Motor Functions of the Superior Colliculus. Annu Rev Neurosci.

Gnadt JW, Andersen RA (1988) Memory related motor planning activity in posterior parietal cortex of macaque. Exp Brain Res 70:216-220.

Gold JI, Shadlen MN (2000) Representation of a perceptual decision in developing oculomotor commands. Nature 404:390-394.

Gold JI, Shadlen MN (2007) The neural basis of decision making. Annu Rev Neurosci 30:535-574.

Goldberg ME, Wurtz RH (1972) Activity of superior colliculus in behaving monkey. II. Effect of attention on neuronal responses. J Neurophysiol 35:560-574.

Goldberg ME, Bisley JW, Powell KD, Gottlieb J (2006) Saccades, salience and attention: the role of the lateral intraparietal area in visual behavior. Prog Brain Res 155:157-175.

Gottlieb J, Goldberg ME (1999) Activity of neurons in the lateral intraparietal area of the monkey during an antisaccade task. Nat Neurosci 2:906-912.

Gottlieb J, Balan P (2010) Attention as a decision in information space. Trends Cogn Sci 14:240-248.

Gottlieb JP, Kusunoki M, Goldberg ME (1998) The representation of visual salience in monkey parietal cortex. Nature 391:481-484.

Graham NV (2011) Beyond multiple pattern analyzers modeled as linear filters (as classical V1 simple cells): Useful additions of the last 25 years. Vision Res.

Green, D.M., Swets J.A. (1966) *Signal Detection Theory and Psychophysics*. New York: Wiley.

Grefkes C, Fink GR (2005) The functional organization of the intraparietal sulcus in humans and monkeys. J Anat 207:3-17.

Hanes DP, Schall JD (1996) Neural control of voluntary movement initiation. Science 274:427-430.

Hanks TD, Ditterich J, Shadlen MN (2006) Microstimulation of macaque area LIP affects decision-making in a motion discrimination task. Nat Neurosci 9:682-689.

Herrnstein, R.J. (1961). Relative and absolute strength of responses as a function of frequency of reinforcement. *Journal of the Experimental Analysis of Behaviour*, 4, 267–272.

Hikosaka O, Wurtz RH (1983) Visual and oculomotor functions of monkey substantia nigra pars reticulata. III. Memory-contingent visual and saccade responses. J Neurophysiol 49:1268-1284.

Hikosaka O, Nakamura K, Nakahara H (2006) Basal ganglia orient eyes to reward. J Neurophysiol 95:567-584.

Huk AC, Shadlen MN (2005) Neural activity in macaque parietal cortex reflects temporal integration of visual motion signals during perceptual decision making. J Neurosci 25:10420-10436.

Ignashchenkova A, Dicke PW, Haarmeier T, Thier P (2004) Neuron-specific contribution of the superior colliculus to overt and covert shifts of attention. Nat Neurosci 7:56-64.

Ikeda T, Hikosaka O (2003) Reward-dependent gain and bias of visual responses in primate superior colliculus. Neuron 39:693-700.

Ipata AE, Gee AL, Goldberg ME, Bisley JW (2006a) Activity in the lateral intraparietal area predicts the goal and latency of saccades in a free-viewing visual search task. J Neurosci 26:3656-3661.

Ipata AE, Gee AL, Gottlieb J, Bisley JW, Goldberg ME (2006b) LIP responses to a popout stimulus are reduced if it is overtly ignored. Nat Neurosci 9:1071-1076.

Itti L, Koch C (2000) A saliency-based search mechanism for overt and covert shifts of visual attention. Vision Res 40:1489-1506.

Itti L, Koch C (2001) Computational modelling of visual attention. Nat Rev Neurosci 2:194-203.

Janssen P, Shadlen MN (2005) A representation of the hazard rate of elapsed time in macaque area LIP. Nat Neurosci 8:234-241.

Jones HE, Grieve KL, Wang W, Sillito AM (2001) Surround suppression in primate V1. J Neurophysiol 86:2011-2028.

Kastner S, Ungerleider LG (2000) Mechanisms of visual attention in the human cortex. Annu Rev Neurosci 23:315-341.

Keller EL, McPeek RM (2002) Neural discharge in the superior colliculus during target search paradigms. Ann N Y Acad Sci 956:130-142.

Kenet T, Bibitchkov D, Tsodyks M, Grinvald A, Arieli A (2003) Spontaneously emerging cortical representations of visual attributes. Nature 425:954-956.

Koch C, Ullman S (1985) Shifts in selective visual attention: towards the underlying neural circuitry. Hum Neurobiol 4:219-227.

Kohn A, Smith MA (2005) Stimulus dependence of neuronal correlation in primary visual cortex of the macaque. J Neurosci 25:3661-3673.

Kohn A, Zandvakili A, Smith MA (2009) Correlations and brain states: from electrophysiology to functional imaging. Curr Opin Neurobiol 19:434-438.

Kuffler SW (1953) Discharge patterns and functional organization of mammalian retina. J Neurophysiol 16:37-68.

Kustov AA, Robinson DL (1996) Shared neural control of attentional shifts and eye movements. Nature 384:74-77.

Kusunoki M, Goldberg ME (2003) The time course of perisaccadic receptive field shifts in the lateral intraparietal area of the monkey. J Neurophysiol 89:1519-1527.

Lansky P, Vaillant J (2000) Stochastic model of the overdispersion in the place cell discharge. Biosystems 58:27-32.

Lau B, Glimcher PW (2005) Dynamic response-by-response models of matching behavior in rhesus monkeys. J Exp Anal Behav 84:555-579.

Lauwereyns J, Watanabe K, Coe B, Hikosaka O (2002) A neural correlate of response bias in monkey caudate nucleus. Nature 418:413-417.

Lee D, Port NL, Kruse W, Georgopoulos AP (1998) Variability and correlated noise in the discharge of neurons in motor and parietal areas of the primate cortex. J Neurosci 18:1161-1170.

Lee P, Hall WC (2006) An in vitro study of horizontal connections in the intermediate layer of the superior colliculus. J Neurosci 26:4763-4768.

Lewis JW, Van Essen DC (2000) Corticocortical connections of visual, sensorimotor, and multimodal processing areas in the parietal lobe of the macaque monkey. J Comp Neurol 428:112-137.

Lynch JC, Graybiel AM, Lobeck LJ (1985) The differential projection of two cytoarchitectonic subregions of the inferior parietal lobule of macaque upon the deep layers of the superior colliculus. J Comp Neurol 235:241-254.

Lytton WW, Sejnowski TJ (1991) Simulations of cortical pyramidal neurons synchronized by inhibitory interneurons. J Neurophysiol 66:1059-1079.

Maimon G, Assad JA (2009) Beyond Poisson: increased spike-time regularity across primate parietal cortex. Neuron 62:426-440.

Mao ZH, Massaquoi SG (2007) Dynamics of winner-take-all competition in recurrent neural networks with lateral inhibition. IEEE Trans Neural Netw 18:55-69.

Maunsell JH (2004) Neuronal representations of cognitive state: reward or attention? Trends Cogn Sci 8:261-265.

Mazurek ME, Roitman JD, Ditterich J, Shadlen MN (2003) A role for neural integrators in perceptual decision making. Cereb Cortex 13:1257-1269.

McAdams CJ, Maunsell JH (1999) Effects of attention on orientation-tuning functions of single neurons in macaque cortical area V4. J Neurosci 19:431-441.

McAdams CJ, Reid RC (2005) Attention modulates the responses of simple cells in monkey primary visual cortex. J Neurosci 25:11023-11033.

McCoy AN, Platt ML (2005) Expectations and outcomes: decision-making in the primate brain. J Comp Physiol A Neuroethol Sens Neural Behav Physiol 191:201-211.

McPeek RM, Keller EL (2002) Saccade target selection in the superior colliculus during a visual search task. J Neurophysiol 88:2019-2034.

Mitchell JF, Sundberg KA, Reynolds JH (2007) Differential attention-dependent response modulation across cell classes in macaque visual area V4. Neuron 55:131-141.

Mitchell JF, Sundberg KA, Reynolds JH (2009) Spatial attention decorrelates intrinsic activity fluctuations in macaque area V4. Neuron 63:879-888.

Moldakarimov S, Rollenhagen JE, Olson CR, Chow CC (2005) Competitive dynamics in cortical responses to visual stimuli. J Neurophysiol 94:3388-3396.

Moore GP, Segundo JP, Perkel DH, Levitan H (1970) Statistical signs of synaptic interaction in neurons. Biophys J 10:876-900.

Moore T, Fallah M (2001) Control of eye movements and spatial attention. Proc Natl Acad Sci U S A 98:1273-1276.

Moran J, Desimone R (1985) Selective attention gates visual processing in the extrastriate cortex. Science 229:782-784.

Morris JS, Friston KJ, Dolan RJ (1997) Neural responses to salient visual stimuli. Proc Biol Sci 264:769-775.

Muller NG, Mollenhauer M, Rosler A, Kleinschmidt A (2005) The attentional field has a Mexican hat distribution. Vision Res 45:1129-1137.

Orban GA (2008) Higher order visual processing in macaque extrastriate cortex. Physiol Rev 88:59-89.

Oristaglio J, Schneider DM, Balan PF, Gottlieb J (2006) Integration of visuospatial and effector information during symbolically cued limb movements in monkey lateral intraparietal area. J Neurosci 26:8310-8319.

Ozeki H, Finn IM, Schaffer ES, Miller KD, Ferster D (2009) Inhibitory stabilization of the cortical network underlies visual surround suppression. Neuron 62:578-592.

Palmer J, Huk AC, Shadlen MN (2005) The effect of stimulus strength on the speed and accuracy of a perceptual decision. J Vis 5:376-404.

Paradiso MA (1988) A theory for the use of visual orientation information which exploits the columnar structure of striate cortex. Biol Cybern 58:35-49.

Peck CJ, Jangraw DC, Suzuki M, Efem R, Gottlieb J (2009) Reward Modulates Attention Independently of Action Value in Posterior Parietal Cortex. Journal of Neuroscience 29:11182-11191.

Platt ML, Glimcher PW (1999) Neural correlates of decision variables in parietal cortex. Nature 400:233-238.

Posner MI, Cohen Y, Rafal RD (1982) Neural systems control of spatial orienting. Philos Trans R Soc Lond B Biol Sci 298:187-198.

Powell KD, Goldberg ME (2000) Response of neurons in the lateral intraparietal area to a distractor flashed during the delay period of a memory-guided saccade. J Neurophysiol 84:301-310.

Rajan K, Abbott LF, Sompolinsky H (2010) Stimulus-dependent suppression of chaos in recurrent neural networks. Phys Rev E Stat Nonlin Soft Matter Phys 82:011903.

Ratcliff R, Rouder JN (2000) A diffusion model account of masking in two-choice letter identification. J Exp Psychol Hum Percept Perform 26:127-140.

Ratcliff R, McKoon G (2008) The diffusion decision model: theory and data for two-choice decision tasks. Neural Comput 20:873-922.

Reynolds JH, Heeger DJ (2009) The normalization model of attention. Neuron 61:168-185.

Reynolds JH, Pasternak T, Desimone R (2000) Attention increases sensitivity of V4 neurons. Neuron 26:703-714.

Robinson DA (1972) Eye movements evoked by collicular stimulation in the alert monkey. Vision Res 12:1795-1808.

Robinson DA, Fuchs AF (1969) Eye movements evoked by stimulation of frontal eye fields. J Neurophysiol 32:637-648.

Robinson DL, Goldberg ME (1978) Sensory and behavioral properties of neurons in posterior parietal cortex of the awake, trained monkey. Fed Proc 37:2258-2261.

Roesch MR, Olson CR (2003) Impact of expected reward on neuronal activity in prefrontal cortex, frontal and supplementary eye fields and premotor cortex. J Neurophysiol 90:1766-1789.

Roitman JD, Shadlen MN (2002) Response of neurons in the lateral intraparietal area during a combined visual discrimination reaction time task. J Neurosci 22:9475-9489.

Salzman CD, Belova MA, Paton JJ (2005) Beetles, boxes and brain cells: neural mechanisms underlying valuation and learning. Curr Opin Neurobiol 15:721-729.

Schall JD (1995) Neural basis of saccade target selection. Rev Neurosci 6:63-85.

Schall JD, Hanes DP, Thompson KG, King DJ (1995) Saccade target selection in frontal eye field of macaque. I. Visual and premovement activation. J Neurosci 15:6905-6918.

Schall JD, Sato TR, Thompson KG, Vaughn AA, Juan CH (2004) Effects of search efficiency on surround suppression during visual selection in frontal eye field. J Neurophysiol 91:2765-2769.

Schiller PH, Tehovnik EJ (2003) Cortical inhibitory circuits in eye-movement generation. Eur J Neurosci 18:3127-3133.

Schiller PH, Tehovnik EJ (2005) Neural mechanisms underlying target selection with saccadic eye movements. Prog Brain Res 149:157-171.

Schlack A, Hoffmann KP, Bremmer F (2002) Interaction of linear vestibular and visual stimulation in the macaque ventral intraparietal area (VIP). Eur J Neurosci 16:1877-1886.

Schwartz ML, Goldman-Rakic PS (1984) Callosal and intrahemispheric connectivity of the prefrontal association cortex in rhesus monkey: relation between intraparietal and principal sulcal cortex. J Comp Neurol 226:403-420.

Scobey RP, Gabor AJ (1989) Orientation discrimination sensitivity of single units in cat primary visual cortex. Exp Brain Res 77:398-406.

Serences JT, Yantis S (2007) Spatially selective representations of voluntary and stimulus-driven attentional priority in human occipital, parietal, and frontal cortex. Cereb Cortex 17:284-293.

Sereno AB, Maunsell JH (1998) Shape selectivity in primate lateral intraparietal cortex. Nature 395:500-503.

Sereno AB, Amador SC (2006) Attention and memory-related responses of neurons in the lateral intraparietal area during spatial and shape-delayed match-to-sample tasks. J Neurophysiol 95:1078-1098.

Seung HS, Lee DD, Reis BY, Tank DW (2000) Stability of the memory of eye position in a recurrent network of conductance-based model neurons. Neuron 26:259-271.

Shadlen MN, Newsome WT (1996) Motion perception: seeing and deciding. Proc Natl Acad Sci U S A 93:628-633.

Shadlen MN, Newsome WT (1998) The variable discharge of cortical neurons: implications for connectivity, computation, and information coding. J Neurosci 18:3870-3896.

Shadlen MN, Newsome WT (2001) Neural basis of a perceptual decision in the parietal cortex (area LIP) of the rhesus monkey. J Neurophysiol 86:1916-1936.

Simmons JM, Ravel S, Shidara M, Richmond BJ (2007) A comparison of reward-contingent neuronal activity in monkey orbitofrontal cortex and ventral striatum: guiding actions toward rewards. Ann N Y Acad Sci 1121:376-394.

Smith MA, Kohn A (2008) Spatial and temporal scales of neuronal correlation in primary visual cortex. J Neurosci 28:12591-12603.

Smith PL, Ratcliff R (2004) Psychology and neurobiology of simple decisions. Trends Neurosci 27:161-168.

Snyder LH, Batista AP, Andersen RA (1997) Coding of intention in the posterior parietal cortex. Nature 386:167-170.

Softky WR, Koch C (1993) The highly irregular firing of cortical cells is inconsistent with temporal integration of random EPSPs. J Neurosci 13:334-350.

Sommer MA, Wurtz RH (2006) Influence of the thalamus on spatial visual processing in frontal cortex. Nature 444:374-377.

Spitzer H, Desimone R, Moran J (1988) Increased attention enhances both behavioral and neuronal performance. Science 240:338-340.

Steinman BA, Steinman SB, Lehmkuhle S (1995) Visual attention mechanisms show a center-surround organization. Vision Res 35:1859-1869.

Steinmetz NA, Moore T (2010) Changes in the response rate and response variability of area V4 neurons during the preparation of saccadic eye movements. J Neurophysiol 103:1171-1178.

Sugrue LP, Corrado GS, Newsome WT (2004) Matching behavior and the representation of value in the parietal cortex. Science 304:1782-1787.

Sundberg KA, Mitchell JF, Reynolds JH (2009) Spatial attention modulates center-surround interactions in macaque visual area v4. Neuron 61:952-963.

Takikawa Y, Kawagoe R, Itoh H, Nakahara H, Hikosaka O (2002) Modulation of saccadic eye movements by predicted reward outcome. Exp Brain Res 142:284-291.

Thier P, Andersen RA (1998) Electrical microstimulation distinguishes distinct saccade-related areas in the posterior parietal cortex. J Neurophysiol 80:1713-1735.

Thompson KG, Bichot NP (2005) A visual salience map in the primate frontal eye field. Prog Brain Res 147:251-262.

Treue S, Maunsell JH (1999) Effects of attention on the processing of motion in macaque middle temporal and medial superior temporal visual cortical areas. J Neurosci 19:7591-7602.

Usher M, McClelland JL (2001) The time course of perceptual choice: the leaky, competing accumulator model. Psychol Rev 108:550-592.

Van Essen DC (2005) Corticocortical and thalamocortical information flow in the primate visual system. Prog Brain Res 149:173-185.

Vogels R (1990) Population coding of stimulus orientation by striate cortical cells. Biol Cybern 64:25-31.

Wang DL (1999) Object selection based on oscillatory correlation. Neural Netw 12:579-592.

Wang XJ (2001) Synaptic reverberation underlying mnemonic persistent activity. Trends Neurosci 24:455-463.

Wardak C, Olivier E, Duhamel JR (2002) Saccadic target selection deficits after lateral intraparietal area inactivation in monkeys. J Neurosci 22:9877-9884.

Wardak C, Olivier E, Duhamel JR (2004) A deficit in covert attention after parietal cortex inactivation in the monkey. Neuron 42:501-508.

Wardak C, Ibos G, Duhamel JR, Olivier E (2006) Contribution of the monkey frontal eye field to covert visual attention. J Neurosci 26:4228-4235.

Watanabe K, Lauwereyns J, Hikosaka O (2003a) Neural correlates of rewarded and unrewarded eye movements in the primate caudate nucleus. J Neurosci 23:10052-10057.

Watanabe K, Lauwereyns J, Hikosaka O (2003b) Effects of motivational conflicts on visually elicited saccades in monkeys. Exp Brain Res 152:361-367.

Watanabe M (2007) Role of anticipated reward in cognitive behavioral control. Curr Opin Neurobiol 17:213-219.

Wong KF, Huk AC, Shadlen MN, Wang XJ (2007) Neural circuit dynamics underlying accumulation of time-varying evidence during perceptual decision making. Front Comput Neurosci 1:6.

Xie X, Hahnloser RH, Seung HS (2002) Selectively grouping neurons in recurrent networks of lateral inhibition. Neural Comput 14:2627-2646.

Xing J, Andersen RA (2000) Memory activity of LIP neurons for sequential eye movements simulated with neural networks. J Neurophysiol 84:651-665.

Yang Y, Liang Z, Li G, Wang Y, Zhou Y (2009) Aging affects response variability of V1 and MT neurons in rhesus monkeys. Brain Res 1274:21-27.

Zeitler M, Fries P, Gielen S (2006) Assessing neuronal coherence with single-unit, multi-unit, and local field potentials. Neural Comput 18:2256-2281.

Zohary E, Shadlen MN, Newsome WT (1994) Correlated neuronal discharge rate and its implications for psychophysical performance. Nature 370:140-143.